2010

ANALYTICAL APPLICATIONS OF SURFACE-MODIFIED FUSED SILICA CAPILLARIES

Jesse James Stine
The University of Montana

ANALYTICAL APPLICATIONS OF SURFACE-MODIFIED FUSED SILICA CAPILLAREIS

By

Jesse James Stine

B.S. Chemistry, Eastern Illinois University, Charleston, IL, 2002

Dissertation

Presented in partial fulfillment of the requirements
for the degree of

Doctor of Philosophy in Chemistry

The University of Montana
Missoula, MT

December 2009

Approved by:

Perry Brown, Associate Provost for Graduate Education
Graduate School

Dr. Christopher Palmer, Chair
Chemistry and Biochemistry

Dr. Mike DeGrandpre,
Chemistry and Biochemistry

Dr. Edward Rosenberg,
Chemistry and Biochemistry

Dr. Sandy Ross
Chemistry and Biochemistry

Dr. Steven Lodmell
Biological Sciences

Stine, Jesse, Ph.D., Autumn 2009 Chemistry

Analytical Applications of Surface-Modified Fused Silica Capillaries

Chairperson: Christopher P. Palmer

Fused silica capillaries have become a major tool for many applications in analytical chemistry. These capillaries are physically robust, permit gasses or solutions to be introduced and pumped through with relative ease, and due to their small dimensions allow fast mass transfer to and from the capillary walls as well as miniaturization of analytical systems. This dissertation describes two projects that utilize modification of fused silica capillary surfaces for specific analytical applications.

The first project is to reverse the charge on the capillary surface by immobilization of cationic polymers, thus creating a very stable coating for application to CE separations. The chemistry proposed by Rosenberg *et al.* for the covalent attachment of amine polymers to silica is adapted to the modification of fused silica capillaries for CE applications. PEI and PAA were covalently bonded to the interior surface of fused silica capillaries utilizing 3-chloro- propyltrichlorosilane (CPTCS) or 3-glycidoxypropyl-trimethoxysilane (GPTMS) to anchor the polymers to the surface. The surface-bound polymers were subsequently quaternized using methyl iodide (MeI). The resulting modified capillaries were studied using CE, and were shown to provide reproducible, stable, and robust anodic EOF throughout the pH range of 2 – 10. Surface modifications utilizing CPTCS could be rinsed with up to 6 M HCl or 1 M NaOH without significant loss of surface modifier. The utility of the modified capillaries for the separation of simple anions and cations was demonstrated.

The second project involves modifying a fiber optic capillary to detect nerve agents by immobilizing fluorescent labeled acetylcholinesterase (AChE) to the surface and using evanescent waves to monitor the enzyme activity. The hypotheses for the chemical sensor are that the improved enzyme activity of a recombinant AChE, along with the improved sensing capabilities of the fiber optic capillaries, will improve detection limits and sensor robustness. The capillary based sensor is shown to work for the detection of warfare agent surrogates by following changes in fluorescein absorbance, but background emission from the capillary prevented potentially more sensitive detection by following changes in fluorescein fluorescence.

Acknowledgements

First and foremost I would like to thank Chris Palmer for his support, guidance and most importantly his seemingly endless amount of patience. Dr. Palmer put an enormous amount of work in to helping me along and was always willing to take the time to explain things over and over again. I would also like to thank the faculty at UM and especially my committee members for always being available to answer the many questions I had and to attempt to help me in any way possible. Thanks to Dr. Rosenberg and his group whose work a large portion of my thesis is based on. I had the opportunity to discuss many various problems and possible solutions to my work with them and without their support I doubt my project would have gone far. I would also like to thank Dr. Rosenberg for the generous donation of the polymers used in my study. Thanks to Dr. DeGrandpre and his group for the assistance with many technical issues and fore being readily available help in my project.
I would also like to thank my fellow group members for the support, knowledge and especially the ability to make my work enjoyable.
I would like to thank all the other students at UM who made my stay there a most enjoyable experience.
Finally I would like to thank my family for their love and support throughout the years.

Table of Contents:

List of Figures

List of Equations

List of Tables

List of Abbreviations and Mathematical Symbols

2-PAM	Prolidoximine
AChE	acetylcholinesterase
APTS	aminopropyl trimethoxy silane
ATChI	acetylthiocholine iodide
β	double layer
CDI	N,N'-carbonyl diimidazole
CE	capillary electrophoresis
CZE	capillary zone electrophoresis
D	diffusion coefficient
DFP	diisopropylfluorophosphate
ε_0	permittivity in vacuum
E	Electric field strength
E_A	activity energy
EOF	Electroosmotic flow
f	frictional coefficient
F_d	frictional retarding force
F_E	moving force experienced by a particle
FITC	fluorescein isothiocyanate
FOCap	fiber optic capillary
GMBS	N-γ-maleimidobutyloxy succinimide ester
HPLC	high-pressure liquid chromatography
I	electric current
i.d.	internal diameter
κ	conductivity
LCW	liquid core waveguide
L_d	capillary length from the window to the detector
L_t	total capillary length
MEKC	Micellar electrokinetic chromatography
MPTS	3-(mercaptopropyl)trimethoxy silane
N	theoretical plates
η	viscosity
P	dissipated electric power
PAA	Polyallylamine
PAMAM	polyamidoamine
PEI	Polyethyleneimine
PEG	poly(ethylene glycol)
q	charge on a particle
r	radius
R	molecular gas constant
σ	surface charge
S	capillary cross section

SFX	6-(fluorescein-5-carboxamido)hexanoic acid,succinimidyl ester
T	Temperature
t	time
TCCPS	trichlorochloropropyl silane
t_{eo}	time of electroosmotic marker
UV	ultraviolet
V	voltage
v	velocity
v_{eo}	Velocity of the electroosmotic flow
v_{ep}	Electrophoretic velocity of a charged species in an electric field
ν	Viscosity
$w_{1/2}$	full width at half maximum
μ_0	intrinsic mobility
μ_{eff}	effective mobility
μ_{eo}	Electroomotic mobility
μ_{ep}	Electrophoretic mobility
ζ	Zeta potential

Chapter 1: Introduction and Overview

This thesis will discuss the modification of silica capillaries for analytical applications. Chapter 1 is a brief overview and introduction to the thesis. Chapter 2 will introduce silica capillaries; their production, properties and structure. Chapter 3 will introduce capillary electrophoresis (CE) theory and basics. Chapter 4 describes the modification of silica capillaries for use in capillary electrophoresis applications. Chapter 5 describes the modification of fiber optic capillaries (FOCaps) for use as a sensor for the detection of chemical warfare agents. Chapter 6 is a summary and a discussion of possible future work.

Chapter 2 describes fused silica capillaries, their production and properties. Both types of silica capillary described in this thesis are produced in similar fashion. An additional step is added in the manufacturing of FOCaps by the addition of a fluorine-doped layer that will be described in Chapter 5. Chapter 2 also describes the chemistry of fused silica surfaces and a review of the chemistries used for modification of the surfaces. Because of the adaptability of the silica surface a vast amount of research has been developed to modify the surface and attach almost any functionality desirable. The internal surface chemistry where the chemical modification takes place is identical for both systems studied.

Chapter 3 is an overview of CE principles and properties. The chapter also provides a rationale and justification for the experimental research described in Chapter 4.

Chapter 4 describes the adaptation of existing silica modification technology for use in capillaries and demonstrates the benefits of these modified capillaries over

existing modifications and bare fused silica capillaries. The results show that covalent modification with polyamines, followed by quaternization of secondary and tertiary amines, generates surfaces with unprecedented chemical stability as well as reproducible and stable electroosmotic flow in the direction of the anode. Applications of these capillaries for separation of representative cationic and anionic species are presented. The results also show that, while individual modified capillaries provide reproducible flow, the reproducibility between different modified capillaries is not as good.

Chapter 5 presents the development and evaluation of a chemical sensor for warfare agents based on FOCap technology. The principles behind the chemical warfare agent sensor, which is based on the immobilization of fluorescein modified acetylcholinesterase (AChE-FITC), are presented. Previous work demonstrating the principle and viability of this approach on fiber optics are described, as is the rationale for the adaptation of this approach to capillary fiber optics. Various schemes for the immobilization of acetylcholinesterase (AChE) are evaluated and compared, and are found to give similar enzyme activity. Immobilized recombinant acetylcholinesterase (rAChE) is shown to provide better catalytic activity, as predicted, but the overall conversion rate and applicability were limited by the small quantity of rAChE available. Results are presented that demonstrate the utility of the capillary fiber optic sensor approach using immobilized commercial AChE and evanescent absorbance spectroscopy by detecting nerve agent mimics. Ultimately, however, the sensitivity and applicability the fused silica capillary fiber optic approach is shown to be hampered by the existence of a high background fluorescence relative to the fluorescence signal.

Chapter 6 summarizes the results of the two studies, and suggests possible future directions for the development and application of fused silica capillaries in analytical chemistry.

Chapter 2: Background and introduction to silica capillaries

Due to unique and advantageous properties, fused silica capillaries have found use in a wide range of applications. Silica capillaries have found use in analytical chemistry, gas and fluid delivery, drug delivery systems, flow cells, micro pipettes, liquid core light guides, hollow wave guides and micro optical elements. Since its first use in the late 70's the range of capillary tubing internal diameters has grown and specification tolerances have continually improved to meet the demands of the column manufacturing industry.

Probably the most common applications of fused silica capillaries for analytical chemistry are in separation science. The advent of fused-silica capillaries for gas chromatography (GC) was a major technological development; for the story of their discovery see Dandeneau and Zerenner. [1, 2] Not only have fused-silica capillaries revolutionized GC, but they have led to major advances in new separation technologies such as capillary electrophoresis (CE), capillary LC and capillary electrochromatography (CEC). Silica based columns provided many advantages over the preceding borosilicate technology and became the accepted standard in many analytical instruments. [3]

2.1 Silica Properties

Silica materials are preferred over other materials, such as quartz, Teflon and polymers such as polytetrafluoroethylene (PTFE), due to their low catalytic surface activity and the ability to physically and chemically modify the silica surface. [4] Also,

fused silica is inexpensive, optically transparent across the UV and visible spectra and can be drawn into capillaries.

The commercially available glasses which are used for fabrication of capillary columns contain silica, SiO_2, as the major component. Warren [5] has shown that the silica in glass has the usual tetrahedral arrangement of four oxygen atoms bonded to each silicon atom. The silica tetrahedra are linked together at slightly distorted angles to give a three-dimensional polymer. [6] Various metal oxides can be added to silica during the glass manufacturing process in order to modify some of its chemical and physical properties; for a review of these properties see [7].

Glass is generally considered to be an inert substance in regard to adsorptive effects and catalytic activity. In capillary chromatography column applications, however, glass manifests undesirable activity that can result in severe peak tailing or complete adsorption when polar compounds are chromatographed. [8-13] This surface activity can be attributed to the silica surface structure and to impurities found in the near surface region of the glass matrix. The metallic oxides added during the manufacturing process can act as Lewis acid sites when at or near the surface of the glass. [14-17] Lewis acids function as adsorption sites for lone-pair donor molecules such as ketones and amines. The strength of the adsorption depends on the properties of the adsorbed molecule and of the electron-accepting Lewis acid sites.

Fused silica is produced by the thermal oxidation of high purity silicon tetrachloride, usually within an oxygen-hydrogen flame [18]:

$$SiCl_4 + O_2 + 2H_2 \rightarrow SiO_2 + 4HCl \quad (2.1)$$

The resulting deposition product is low metal ion content silicon dioxide. This product is the raw material used to draw a wide range of capillary tubing products. The bulk composition of fused silica materials contains very few metallic impurities and is therefore unlikely that the surface would contain a large number of Lewis acid sites. It is the absence of these adsorptive sites that gives fused silica its higher degree of intrinsic inertness.

2.2 Surface Hydroxyls

The most important chemical and structural detail of the silica surface is the hydroxyl groups that are attached to the surface silicon atoms. These silicon atoms are presumably tetrahedrally coordinated to three other oxygen atoms and thus to the bulk silica. Several types of hydroxyl groups are found. Hydroxyl groups attached to adjacent individual silicon atoms are termed vicinal. [19] When two hydroxyl groups are attached to the same silicon atom, they are termed geminal. Also, there are hydroxyl groups within the silica structure which are usually termed intraglobular hydroxyls. [20-23]

Surface hydroxyls that are hydrogen bonded to one another are described as being “bound.” Those which are not involved in any interaction are described as “free.” Whether two adjacent hydroxyl groups are bound or free is determined by the distance of one hydroxyl group from the oxygen atom of the adjacent hydroxyl group. Hydroxyls separated from adjacent oxygen atoms by more than 3.1 Å appear to be incapable of hydrogen bonding. [24-26] For optimum hydrogen bonding, the hydroxyl-oxygen distance should be between 2.4 to 2.8 Å. [27, 28]

Since vicinal hydroxyl groups on regular flat surfaces are separated by at least 3.1 Å, it is unlikely that they are hydrogen bonded to one another. Geminal hydroxyl groups also are probably not bonded to their partners because a five- or six-membered ring is normally needed for intramolecular hydrogen bonding. Triplet OH groups ($-Si(OH)_3$) should also be free from internal bonding. [29, 30]

If it is assumed that a silicon atom on the surface must complete its tetrahedral coordination with a hydroxyl group, the number of surface hydroxyls can be calculated from geometric considerations. [31, 32] By assuming one hydroxyl group per surface silicon atom, there are approximately eight groups per nm^2. However, experimental determinations indicate that at ambient temperatures the surface hydroxyl concentration corresponds to less than five groups per nm^2. [33-35]

The hydrogens on the surface hydroxyl groups, also called silanol groups, are partially acidic due to d-electron cloud vacancies in the silicon atoms. [36] As a result, the silanol groups are available as proton donors for hydrogen bonding sites. Although the mechanism of adsorption is more complicated than an electrostatic hydrogen bond interaction, the adsorption closely resembles hydrogen bonding. [37] In addition to the specific interactions of the silica surface with polar molecules, a weak non-specific dispersion type of interaction is observed that is independent of the degree of surface hydroxylation and independent of the electron density distribution of the adsorbate. [37-39]

In general, the free hydroxyl groups are the strongest surface adsorption sites. Water interacts strongly with these groups and can form several molecular layers. The

adsorbed water can then act as specific adsorption sites for molecules containing high electron densities in the same way as free surface hydroxyls. [40]

2.3 Surface Modification

In order to improve efficiency and reproducibility of chemical coating procedures, the silica surface should have the maximum number of hydroxyl groups per unit surface area. As discussed above it is generally accepted that there are 4-5 silanol groups per nm^2 on the surface of fused silica capillaries. [41] This is smaller than the theoretically calculated value of 7.8 silanols per nm^2 due to the presence of the previously mentioned germinal and vicinal silanol groups. The chemical status and quality of silica can be quite different from one batch to another; therefore to improve reproducibility of modification, surface pretreatment methods are often employed. Most groups employ an alkaline solution, usually potassium or sodium hydroxide ranging in concentration from 0.1 to 1M. A washing step with diluted hydrochloric acid is often used to remove adsorbed metal ions and excess sodium or potassium ions.

The remaining silanol groups provide an excellent surface for chemical modification. In chromatographic applications, the development of coatings covalently bonded to the capillary wall has led to significant improvements in separation efficiencies of a wide variety of solutes. There are two common approaches to creating anchors to the silica surface; using the silanols to create siloxane bonds (Si-O-Si) or creating Si-C bonds directly with the surface silicon atoms. The most common organosilanes used in wall modification are trifunctional modifiers such as $RSiX_3$, trimethoxy or triethoxy silanes. The organic functionality, R, is strongly bonded to the

surface through the siloxane bonds. The limited stability of the Si-O-Si-C linkage has received much attention, because such siloxane bonds are only stable in the pH range from 3 to 7.5. [41] At lower or higher pH, hydrolysis can occur, resulting in loss of surface modifier.

In an effort to overcome these problems, bonded silicas bearing direct Si-C linkages have been developed. They involve the sequential reaction of the silica substrate with a chlorinating agent, such as thionyl chloride, and an alkylating reagent, such as a Grignard or organolithium compound:

$$\text{Si-OH} \xrightarrow{SOCl_2} \text{Si-Cl} \xrightarrow{R-M} \text{Si-R} \quad (2.2)$$

where –M = -Li or MgBr. The resulting Si-C bond is quite stable and resistant to hydrolysis.

2.4 Glass Capillary Drawing

The first glass capillary column drawing machine was designed and built by Desty *et al.* [42] Two pairs of rollers, one before an electrically heated furnace and one after, control the draw ratio, and thus, the length and diameter of the column. As the capillary is drawn from the molten glass in the furnace, it is forced through a heated coiling tube to form a helix. Typical operating temperatures vary between 600° and 750°C depending on the type of glass. For a more detailed description of the drawing process see Novotny and Zlatkis. [4]

2.5 Fused Silica Capillary Drawing

In 1975 Desty modified his original glass drawing machine to attain the necessary drawing temperature for quartz. [43] The electrical heating oven was replaced with a special propane/oxygen burner. The inability to build suitable coiling tubes was the limiting factor in the use of this prototype machine and only preliminary work was successfully accomplished. The discovery by Dandeneau that thin wall capillary columns of high flexibility could be drawn straight and then coiled to normal column dimensions by bending them into the desired shape has proved to be a most significant advance in the capillary column technology. [1, 2] Generally the wall-thickness of a flexible fused silica capillary column is less than 25 μm.

Fused silica is drawn at high temperatures (1800°-2200°C, depending on the bore) and is generally produced using advanced fiber optics technology and a clean-room atmosphere. The capillary can be used as a fiber optic so that infrared laser radiation can be beamed continuously through the capillary. When coupled to a microprocessor-controlled feedback, this provides a method of obtaining extremely uniform and precisely drawn capillary tubing. Induction furnaces, graphite furnaces, and hydrogen/oxygen burners have been used in fused silica drawing machines to reach the high temperatures necessary. The more elaborate systems use a graphite furnace or induction furnaces.

Although thin-walled fused silica columns have a high tensile strength, this strength is greatly reduced by slight surface imperfections, microcracks, or minute scratches caused by dust particles or fingerprints. [1, 2] The newly drawn surface may also be susceptible to atmospheric corrosion. As a result, a polymeric sheath is applied

directly to the capillary tubing as it emerges from the drawing furnace. This material needs to be mechanically durable and thermally stable to high temperatures to be suitable for a range of applications. Initially silicone rubber and graphite impregnated polymethacrylate were used, but these proved to have insufficient stability. Since then, polyamide and polyimide polymers have been used. These are stable to temperatures of 350°C and to over 400°C for short periods of time. The exact structure of the polyimide used by various manufacturers is proprietary, but some possible structures are given in Figure 2.1.

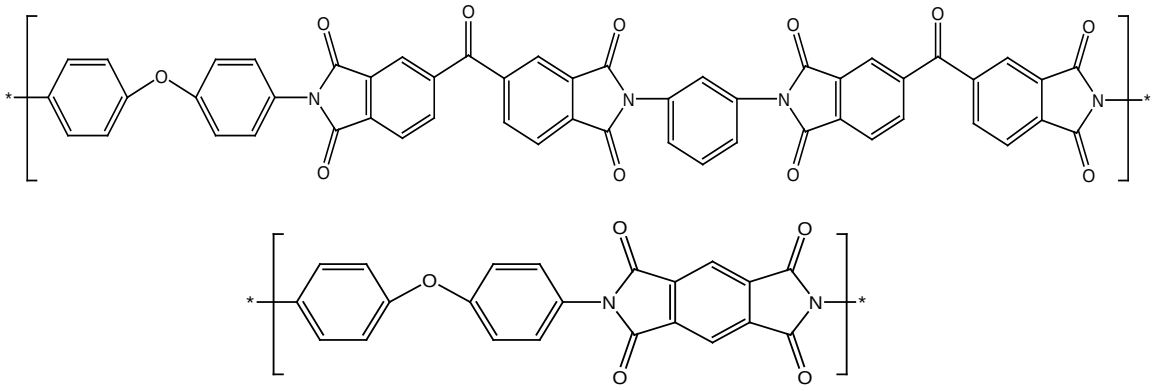

Figure 2.1: Possible chemical structures of polyimide coatings used to impart improved mechanical stability to fused silica capillaries.

The polyimides are thought to stack and form strong intermolecular interactions through a series of charge transfer complexes. This contributes to the excellent mechanical and thermal stability of the coating.

2.6 Summary

The preceding overview of the chemistry and manufacture of fused silica capillaries establishes several important details regarding their properties. First, it

should be clear that after the drawing process the surface is considered to be inert and devoid of water. Also the capillaries and surface are composed of high quality silica with few impurities. After hydration, a surface is generated which is rich in silanol groups that can be used for chemical modification. Finally, the physical strength and durability of the capillaries depend on the application of a chemically, physically and thermally robust polymer coating. Commercially-available capillaries are most often coated with a polyimide.

In the following chapters I will show how the unique properties of silica capillaries can be used to our benefit for analytical purposes. In particular I will show how the optical properties of silica capillaries can be used to create a sensor and how the surface chemistry can be modified to benefit separations in capillary electrophoresis. Some limitations of the state of the art capillary technology described above also become apparent in the course of these studies.

Chapter 3: Introduction to Capillary Electrophoresis

Capillary electrophoresis has become a powerful analytical technique in separation science in recent years due to its advantages over other separation methods. CE requires small sample volumes and little or no sample preparation, provides extremely high separation efficiencies, offers rapid separation times, and is easily automated. One major challenge in CE is optimization of the many physiochemical factors that affect the electrophoretic mobility and separation of analytes.

The first separations using high electric field strength in free solution with 3mm internal diameter capillaries were performed by Hjerten in the 1960's. [44] However, to reduce detrimental effects of convection it was necessary for Hjerten to rotate the capillary. In the1970's techniques using smaller internal diameter capillaries were successfully developed. Superior heat dissipation permitted the use of higher field strength without the need for capillary rotation. Jorgenson and his group solved two major problems, namely low sensitivity of the detection systems for narrow-bore tubes and electroosmosis. Instead of suppressing electroosmosis by using electrically inert capillaries, he took advantage of the unique plug flow profile of the electroosmotic flow and demonstrated the extremely high resolution of CE in 1981. [45] The first CE instruments were laboratory-constructed models but commercial automated instruments have been available since 1987.

3.1 Basics of Capillary Electrophoresis

The basic components of a capillary electrophoresis instrument, shown in Figure 3.1, are a capillary, high voltage supply, inlet and outlet containers for the buffer solutions, detector and data acquisition and control systems (personal computer).

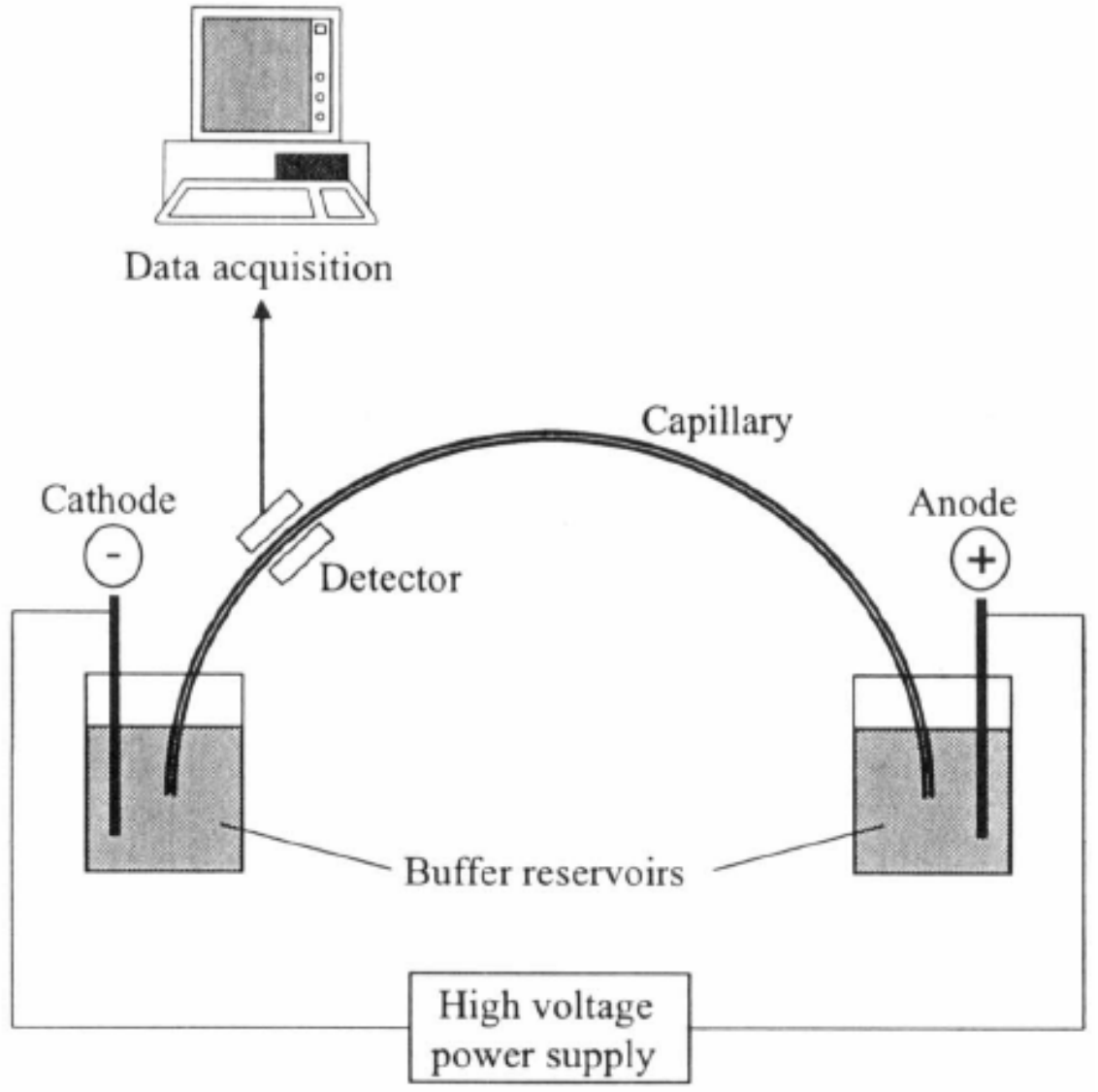

Figure 3.1: Basic configuration of a CE instrument

The capillary is typically made of fused silica with an external polyimide coating for flexibility and strength (as described in Chapter 2). Capillaries made from glass,

quartz, Teflon, and polymers such as PTFE have also been used. [46-48] Fused silica has several advantages: it is inexpensive, optically transparent across the UV and visible spectra and easy to draw into capillaries. The capillary inner diameters are usually 10-100μm while the outer diameter ranges from 150-385μm. The ends of the capillary are immersed into separate inlet and outlet vials containing the background electrolyte. The voltage required to drive the CE separations is provided by a high voltage power supply connected to two electrodes, usually made of platinum or other chemically inert metal, which are positioned along with the capillary ends into the buffer vials.

To perform a CE separation, a capillary filled with buffer has the inlet buffer vial replaced with a vial containing the sample solution. A small plug of sample is then injected into the capillary either electrokinetically or hydrodynamically. With hydrodynamic injection, a pressure difference is generated between the inlet and outlet ends of the capillary causing the sample solution to flow into the capillary. In electrokinetic injection, the sample is driven into the capillary under an applied electric field by the combined effects of electrophoretic migration and electroosmotic flow. After the sample has been injected the buffer vial is re-introduced to the capillary inlet and separation is initiated by applying a voltage to the capillary.

Under the applied electric field, the analyte molecules migrate according to their electrophoretic mobilities. Analytes can be detected either on-column or post-column. For on-column detection a small section of the polyimide coating on the fused silica capillary is removed, typically by burning, to create the detection window. The output from the detector is then sent to a personal computer for processing where the height or area of the peak is used as a measure of the concentration of the analyte in the sample

solution. Since many parameters in CE are temperature dependent, active temperature control systems are essential to obtain good reproducibility. Most instruments rely on built-in air flow cooling systems but others employ liquid coolants.

CE separations usually have greater speed and efficiency than those attained in HPLC or conventional electrophoresis. The running costs of CE are also lower due to the fact that capillaries and buffers are much less expensive than HPLC columns and high grade HPLC solvents. Efficiencies and analysis times are improved relative to HPLC and conventional electrophoresis because the capillary format allows the separations to be carried out at high electric field strength without the deleterious effects of Joule heating, and because all band broadening mechanisms except for longitudinal diffusion are minimized or eliminated.

3.2 Fundamentals of Capillary Electrophoresis

3.2.1 Electrophoretic Mobility

In the presence of a uniform electric field, E, an ion or charged particle experiences a moving force, F_E, which is equal to the product of its net charge, q and the electrical field strength, E,

$$F_E = qE \qquad (3.1)$$

When the ion begins to move through the solvent, it also experiences a frictional retarding force, F_d which is proportional to its velocity, v:

$$F_d = -vf \qquad (3.2)$$

where f is the frictional coefficient. For a spherical ion, this frictional coefficient is given by Stokes' law[49] as:

$$f = 6\pi\eta r \qquad (3.3)$$

Where η is the viscosity of the medium, and r is the hydrodynamic radius of the ion. With no other significant force acting on the ion (such as electrostatic interaction), the accelerating and retarding forces counter balance quickly resulting in a steady state ion velocity. The steady state velocity from a combination of equations 3.1, 3.2, 3.3 is:

$$v = \frac{qE}{6\pi\eta r} \qquad (3.4)$$

The velocity of the ion is proportional to the electric field strength. This proportionality constant of ion velocity per unit field strength is called electrophoretic mobility, μ_{ep} and is given by:

$$\mu_{ep} = \frac{v}{E} = \frac{q}{6\pi\eta r} \qquad (3.5)$$

Equation 3.5 shows that the electrophoretic mobility of an ion depends on its charge and size and or shape, and the viscosity of the medium. Equation 3.5 predicts that the electrophoretic separation of charged analytes is governed by the differences in their charge to size ratio. It is the simplest equation used in CE and works well for spherical and large ions.

However, there are a number of important limitations to this equation. Firstly, the equation refers to infinite dilution where the ionic strength and ion-pairing are negligible or absent. As a result, the electrophoretic mobility computed using equation 3.5 is referred to as the absolute or intrinsic mobility (μ_0) at infinite dilution. Secondly, the equation fails to predict selectivity changes among analyte ions in various solvents. Finally, the equation is also unable to describe the electrophoretic mobility of small inorganic anions. The electrophoretic mobility of an ion is also a function of temperature, because temperature will affect the viscosity according to:

$$\eta = j\, e^{(EA/RT)} \qquad (3.6)$$

Where j is a constant, E_A is the activity energy for the viscous flow, R is the molecular gas constant, and T is the temperature. The factors influencing electrophoretic mobility must be controlled in order to make consistent separations possible.

3.2.2 Joule Heating

The conduction of electric current through an electrolytic solution results in the generation of heat because of frictional collisions between mobile ions and buffer molecules. This is referred to as Joule heating, and at the high voltages applied in CE it can be substantial. Joule heating increases the temperature at the center of the capillary relative to that of the wall. The temperature difference leads to a viscosity difference, as seen in equation 3.6, that affects the migration rate of the solutes. Efficient heat dissipation is the primary reason for performing electrophoretic separations in a capillary format. During the passage of an electric current, I, through a capillary of cross-section S (m^2) filled with an electrolyte having a conductivity κ ($\Omega^{-1}m^{-1}$), the Joule heat produced per unit volume per second is:

$$P = I^2/\kappa S^2 \qquad (3.7)$$

where P is the dissipated electric power (Wm^{-1}). From equation 3.7 we see that using a smaller radius capillary leads to lower Joule heat produced at constant applied potential and buffer composition. The excellent heat dissipation is the reason small capillaries can be used to generate fast, very efficient separations. This fact was demonstrated very effectively by Jorgenson and Lukacs [45] and many others after their work.

3.2.3 Electroosmosis

A fundamental process in CZE is electroosmosis, which is the flow of bulk mobile phase under an applied potential field. In an unmodified fused silica capillary the surface is negatively charged because of ionized silanol groups. When the surface comes in contact with an electrolyte solution, there is a buildup of positive ions in solution near the surface to balance the fixed negative charges on the surface. Some of the excess ions are free to move within the liquid while others are immobilized on the surface. An electric double layer which consists of the stagnant layer and a diffuse layer is formed on the capillary surface. The potential at the interface between the charged surface and the start of the diffuse layer is called the zeta potential, denoted by ζ. The zeta potential depends on the nature and number of surface charges per unit area on the capillary wall (σ), the dielectric constant of the buffer (ϵ) and the thickness of the double layer (d) and is given by:

$$\zeta = \frac{\sigma d}{\epsilon_0 \epsilon} \qquad (3.8)$$

where ε_0 is the permittivity in vacuum.

Under the influence of a tangential electric field, a slipping plane is formed because of the electrical force acting on the excess ionic charge in the diffuse layer. This causes movement of the solution in the near surface region. A uniform flow of the bulk liquid in the capillary is reached because of the frictional forces arising from the viscosity of the liquid. This flow is called electroosmotic flow (EOF) and is given by: [50]

$$v_{eo} = \mu_{eo} E = \frac{\epsilon \epsilon_0 \zeta}{\eta} * E \qquad (3.9)$$

Experimentally, the electroosmotic mobility can be measured using the following equation:

$$\mu_{eo} = \frac{v_{eo}}{E} = \frac{L_d L_t}{t_{eo} V} \qquad (3.10)$$

where L_d is the capillary length to the detector (cm), L_t is the total capillary length (cm), V is the applied voltage and t_{eo} is the migration time of a nonionic electroosmotic flow marker.

A flat flow profile results because the flow originates at the diffuse region of the double layer and the tube diameter is much larger than the thickness of the electrical double layer. As opposed to parabolic flow generated by pressure driven systems, the plug flow has a flat velocity distribution across the capillary cross-section with a deviation of only a few nanometers. The unique flat flow profile contributes to low band broadening and aids in the remarkable separation efficiencies associated with CE.

As can be seen from equation 3.9 the rate of electroosmotic flow depends on several variables. Flow is most rapid under conditions that increase the zeta potential and the double layer thickness, or decrease the solution viscosity. From equation 3.8 we see the zeta potential is dependent on the charge per unit area at the capillary surface. For fused silica the EOF is a strong function of the solution pH because the ionization equilibrium of the silanol groups on the capillary surface is pH dependent. [51, 52]

3.2.4 Migration, Efficiency and Resolution

In CZE the individual ions move at an electrophoretic velocity, v_{ep}, given by equation 3.4 in a plug of liquid which is itself moving at a velocity v_{eo} given by equation

3.9. The observed or apparent electroosmotic mobility (μ_{app}) is a combination of the electroosmotic mobility (μ_{eo}) and electrophoretic mobility (μ_{ep}) given by:

$$\mu_{app} = (\mu_{eo} + \mu_{ep}) \qquad (3.11)$$

The magnitude and direction of μ_{eo} is influenced by parameters such as the pH, buffer concentration, and chemical modification to the capillary surface. The electrophoretic mobility of the ion may be affected by the pH and buffer chemistry. The apparent mobility can be altered by changing the electroosmotic mobility, electrophoretic mobility or both.

As formalized by the van Deemter equation, there are multiple ways that peaks broaden in chromatography including multiple flow path, longitudinal diffusion and mass transfer. Since the EOF profile is essentially flat and CE uses open tubular capillaries without packing material, only longitudinal diffusion should contribute to zone broadening. [45, 53]

In the absence of other types of broadening, the variance, σ_l^2, of the zone after time, t, is given by the Einstein equation:

$$\sigma_l^2 = 2D * t = 2D \frac{Ld}{(\mu app)E} \qquad (3.12)$$

And according to Giddings the efficiency of a chromatographic system can be expressed in terms of a number of theoretical plates, N, defined as[54]:

$$N = L_d^2 / \sigma_l^2 \qquad (3.13)$$

Combining equations 3.12 and 3.13 the efficiency in CZE is given by:

$$N = \frac{(\mu_{app})EL_d}{2D} = \frac{\mu_{app} V_d}{2D} \qquad (3.14)$$

where V_d is the voltage drop between the injection end of the capillary and the detector. This implies that high efficiency is directly proportional to the μ_{app} of the analyte or in other words the faster the molecules migrate, the better the separation efficiency. Also equation 3.13 indicates that high applied potential must be maintained to obtain maximum efficiencies. According to equation 3.14 separation efficiency is independent of column length and proportional to voltage while migration time is inversely proportional to the voltage. As a result, shorter capillaries can be used without increasing the applied voltage, allowing for fast separations while maintaining the same efficiency. Jorgenson *et al.* have shown that high efficiency separations can be achieved with CE using high voltage and very high efficiencies are possible using shorter capillaries with very high field strengths. [45, 55, 56]

If peaks have a Gaussian profile the number of theoretical plates can be calculated using the peak migration time (t_m) and the full width at half maximum ($w_{1/2}$) as given by:

$$N = 5.545\left(\frac{t_m}{w_{1/2}}\right)^2 \qquad (3.15)$$

This equation is only valid for Gaussian peaks, otherwise asymmetry should be taken into the calculation. The resolution that can be achieved in CE is given by

$$R_s = \frac{\sqrt{N}}{4}\frac{\mu_2 - \mu_1}{\mu_{avg}} \qquad (3.16)$$

In which N is the plate number, μ_1 and μ_2 are the apparent mobilities of two analytes to be resolved, and μ_{avg} is the average of μ_1 and μ_2. Resolution can be enhanced at the expense of analysis time when μ_{avg} approaches zero, which can be achieved by adjusting the electroosmotic mobility to be nearly equal in magnitude and opposite in sign to the

average electrophoretic mobility of the analytes. Conversely, resolution suffers and analysis time is reduced when the electroosmotic mobility is large and has the same sign as the electrophoretic mobility of the analytes. Capillaries with reversed (anodic) EOF flow can thus be used to decrease the analysis time for anions at the expense of resolution, or enhance the resolution for cations at the expense of analysis time.

Although the basic CE theory predicts that the only source of band broadening is from longitudinal diffusion, there are other dispersive processes associated with CE. In order to achieve diffusion limited separation efficiency, all the other processes have to be minimized. Efficiency can be expressed in terms of all the other band broadening processes by:

$$N = t^2_{mig} / \sigma^2_{tot} \qquad (3.17)$$

where σ^2_{tot} is the total zone variance associated with all the sources of band broadening and t^2_{mig} is the migration time. The total zone variance can be defined as:

$$\sigma^2_{tot} = \sigma^2_{Diff} + \sigma^2_{Inj} + \sigma^2_{Det} + \sigma^2_{Heat} + \sigma^2_{Ads} \qquad (3.18)$$

Where σ^2_{Diff} is the variance due to longitudinal diffusion, σ^2_{Inj} is the variance due to the injection, σ^2_{Det} is the variance due to detection σ^2_{Heat} is the variance due to Joule heating and σ^2_{Ads} is the variance due to adsorption of solutes to the capillary wall. Although the variance due to diffusion decreases with fast migration times, contributions from other sources of band broadening can increase with high voltage. One of the significant sources of band broadening in fast separations is Joule heating. Individual sources of band broadening and current practices to minimize their effects will be discussed in the following sections in detail.

As discussed above, Joule heating is a necessary consequence of applying an electrical potential across a conductive medium. This heating could affect the separation efficiency in various ways, including convective mixing, zone broadening, viscosity changes and variation in migration time. The temperature difference between the center of the capillary and the surrounding medium depends on the inner diameter, wall thickness of the capillary, and the efficiency of the heat transfer. The magnitude of the thermal gradient is directly proportional to the square of the capillary radius.

By using small inner diameter capillaries with thick walls for separation, joule heating can be minimized due to improved heat dissipation from the capillary walls. The use of small capillaries limits the amount of current through the capillary due to high resistivity minimizing the heat generation. Disadvantages of using small diameter capillaries are stringent requirements of highly efficient injection schemes and detection systems. The use of low conductivity buffers can reduce the amount of current generated and is particularly useful with larger diameter capillaries.

Wall adsorption of analytes also degrades the separation efficiency and leads to irreproducible migration times. The negative surface of the bare fused silica capillary interacts with positively charged analytes leading to non-equilibrium effects during electrophoresis. Analyte adsorption leads to retention during the separation, which is considered to be a major source of band broadening during the separation of large analytes such as proteins and peptides. Many methods such as capillary modification are designed to minimize the interaction between analytes and the capillary wall.

3.3 CE Injections

The quantity Q of a solute injected into the capillary by direct on-column injection is given by:

$$Q = l\pi r^2 C \qquad (3.19)$$

Where l is the length of the sample zone, r is the radius of the capillary and C is the solute concentration. The injection of a sample zone can be accomplished by electromigration or by hydrodynamic flow. For either method, the capillary must be moved from the buffer reservoir in which electrophoretic separations are performed to the sampling vial to initiate sample injection.

3.3.1 Electromigration injection

In this method, an injection voltage is applied for a brief period of time, causing electromigration of the sample into the capillary. [45, 55, 57] The length of the sample zone can be determined by the velocity of electroosmotic flow v_{eo} and electrophoretic migration v_e by:

$$l = t_i (v_e + v_{eo}) \qquad (3.20)$$

where t_i is the time over which the injection voltage is applied. By combining equations 3.19 and 3.20 we obtain:

$$Q = t_i(\mu_e + \mu_{eo})\pi r^2 C \qquad (3.21)$$

Because of the electrophoretic migration component of electromigration injection, sample bias can occur for ionic solutes with different ion mobilities.

Electromigration injection can be used to concentrate the sample at the column head by using the stacking effect. Sample stacking is the process that occurs when a

voltage is applied along a capillary tube containing a sample plug with a lower specific conductivity than that of the surrounding run buffer. Since the electric field strength is inversely proportional to the specific conductivity of the liquid, the field strength is higher along the sample plug compared with the running buffer. In this way, the electrophoretic velocity, which is proportional to the field strength, increases and the ionic analyte zone is narrowed.

3.3.2 Hydrodynamic injection

Hydrodynamic sample injection can be achieved by three different methods: gravity, pressure and vacuum. [57, 58] In pressure injection, the capillary is kept in a pressurized sample vial and sample injection is controlled by manipulating the applied pressure. For vacuum injection, a vacuum is applied to the detection end of the capillary while the other end of the capillary is kept in the sample vial. For gravity injection, the sample is held above the detection end of the capillary to be injected and by varying the height and time the amount of sample injected can be controlled. The volume of sample (V_t, nL/s) injected per unit time is defined by the Poisseuille Equation: [59]

$$V_t = \Delta P d^4 \pi / 128 \eta L \qquad (3.22)$$

Where ΔP is the pressure drop, d is the capillary internal diameter, η is the solution viscosity and L is the capillary length. For gravity injection, the pressure drop can be calculated by:

$$\Delta P = \rho g \Delta h \qquad (3.23)$$

Where ρ is the density of the analyte solution, g is the gravity constant and Δh is the height difference between the sample vial and the buffer container. [57]

3.4 CE Detection

CE utilizes similar detection methods to those used in liquid column chromatography. The commonly used methods are absorbance detection, fluorescence detection, refractive index, conductivity detection, and amperomeric detection. Mass spectrometry is also becoming a more routine detection method. Both on and off column detection methods are used in CE with on column detection being the most commonly used.

Absorption detection is a nearly universal detection method and both UV and visible light can be used due to the favorable spectral properties of fused silica capillaries, which have a transmission cut-off at 170nm. Early work in CE featured the use of modified HPLC UV detectors. [60-65] Jorgenson *et al.* designed UV detectors to overcome some of the problems associated with modified detectors. This technique is predominately used in commercial CE instrumentation. Light for the detection is obtained by a lamp, a light emitting diode (LED) or by a laser. The selected light is focused into the separation capillary and the difference in the absorbance coefficient between the analyte and the running buffer is utilized for detection. The sensitivity of absorbance measurements depend on the path length, which is defined by the capillary internal diameter and is usually less than 100μm in CE. Because of this several methods have been designed to increase the path length without affecting the resolution. [65] These methods include utilization of a bubble capillary, utilization of a "Z" bend in the capillary, and multiple reflections in capillary and absorbance measurements along the capillary axis. The concentration detection limits using UV-Vis-CE for protein and small

organic molecules is approximately 10^{-6} M, which is mainly limited by the size of the capillary. However, UV-Vis-CE is not a universal detection method because ions that do not possess high absorption coefficients such as inorganic salts and ions cannot be directly detected.

To overcome the limitations of UV-Vis detection, such as detecting molecules with little or no absorbance, indirect detection is frequently employed thus making UV-Vis a universal detection method. In indirect detection, additives with a high absorption coefficient are added to the buffer creating a strong signal throughout the analysis. When the sample is introduced, analyte zone displace the buffer additive in the background, which changes the background signal enabling the detection of the solute. LODs for indirect detection in CE are reported to be in the range of 10^{-6} to 10^{-5} M.

3.5 Chemical Modification of Capillary Surfaces

Fused silica capillaries have many advantages for CE, but the interior surface chemistry also presents significant limitations. The surface chemistry makes it difficult to control or generate reproducible electroosmotic flow, and also presents challenges for elimination of analyte-wall interactions.

3.5.1 Electroosmotic Flow Control

It has been shown that EOF plays an important role in capillary electrophoretic separations. As seen in equations 3.14 and 3.16, the electroosmotic flow affects both the separation efficiency and the resolution. If the rate of the EOF is high enough, all solutes (cations, anions and neutrals) will migrate in the same direction. In fact, the separation

of neutral molecules in electrokinetic capillary chromatography is based partly on electroomosis.

EOF arises from the surface charge properties of the capillary tubing. Different tubing materials or different surface properties of the same kind of tubing will produce different EOFs. The chemistry of the surface of silica is dominated by the heterogenous chemistry of the silanol. Silanols are polar, mildly acidic (pk_a=6.5), and reactive. Due either to the physical heterogeneity of the amorphous silica surface or due to metal impurities in the silica matrix there are a variety of silanol sites, as described in Chapter 2. These silanol sites are known to vary in activity, acidity, and reactivity. This gives rise to irreproducible electromigration in bare fused silica.

An additional motivation for alteration and control of electroosmotic flow is to effect more rapid separations. In general the μ_{eo} in bare fused silica capillaries is greater than the μ_{ep} of most analytes. At neutral pH this allows for simultaneous determination of both positively and negatively charged species when the detector is placed at the cathodic end of the capillary. However, in the case of high mobility analytes such as small ions, the μ_{ep} values are close to or greater than that of μ_{eo}. Because of this some of these anions migrate faster than the EOF but in the opposite direction. This results in the inability to detect these ions. However, when coatings are used to reverse the EOF these ions migrate in the same direction as the EOF and are thus rapidly detected.

The control of EOF can be accomplished by modifying the capillary surface, which can be done by covalently covering the ionic groups on the surface, and/or by permanently modifying the surface with a polymer or other chemistry. Different coatings give rise to different EOFs and by selecting appropriate chemical modification

the EOF can be manipulated. Tunable EOF can be the basis of optimizing separations in capillary electrophoresis.

3.5.2 Adsorption Elimination

As discussed above, adsorption of analytes to the capillary walls can lead to significant band broadening, poor migration time reproducibility, and poor sample recovery. [66, 67] Reduction or elimination of interactions of analytes with the capillary wall is critical for high performance separations. Because bare fused silica has a negatively charged surface at most pH values, the wall interactions can be severe for positively charged species. Adsorption of the analytes onto the bare capillary wall occurs through electrostatic attraction although nonspecific interactions may be present. [66]

3.5.3 Surface Modification

Fortunately the silica surface lends itself to modification with a wide variety of reagents yielding an assortment of surfaces that provide a wide range of surface chemistries. Silica support materials were originally modified with a physisorbed liquid. Later, the surface was modified by covalently bonding a reagent to the surface to form a bonded phase material. The original covalent modifiers were alcohols, which reacted with the silanol sites to yield an ether linkage. A variety of reagents have been employed since that time, with the most popular being the reactive silanes, which bond to the surface by reaction with silanol sites to form a silyl ether linkage. More recently,

physisorbed and covalently bonded polymeric films have been used to modify silica support materials.

Permanent modification of the capillary wall appears to be the most attractive approach to controlling protein-wall interactions as well as the extent of EOF. The reactive surface silanol groups provide excellent opportunities for chemical alteration of the capillary surface; there are many commercially available silation reagents that can be used to immobilize various hydrophilic, biocompatible polymers onto the capillary surface. Coated capillary surfaces with suitable polymers have been shown to be able to provide much improved electrophoretic separations of proteins, and this approach has been widely accepted, as will be discussed in the next section.

A number of surface modifications have been reported in the literature. These coating techniques are classified as permanent or dynamic based on the nature of the attachment of the coating to the capillary wall.

3.6 CE coatings:

Chemical modification of the fused silica capillary surface has become a common approach to introduce and maintain a reproducible and uniform electroosmotic flow, eliminate or reverse the direction of the electroosmotic flow, and/or to reduce surface adsorption of analytes. This approach utilizes the advantages of fused silica capillaries, while attempting to eliminate the problems associated with the silica surface.

Chapter 4: Chemical Modifications of fused silica Capillaries for Capillary Electrophoresis Applications

4.1 Introduction

Since capillary electrophoresis (CE) in fused silica capillaries was developed in the early 1980's [45], the technique has developed into a powerful analytical tool capable of separating many species ranging from large biomolecules to small organic and inorganic ions. [41, 68-75] Fused silica capillaries provide a number of advantages for the technique, including good thermal conductivity, UV transparency and uniform diameter. [76] However, insufficient migration time reproducibility caused by variations in the chemistry of the fused silica surface often limits its applicability, particularly in regulatory environments. Applicability of CE with fused silica capillaries can also be limited for certain applications by robust cathodic electroosmotic flow, or by adsorption of analytes, buffer impurities, or sample matrix components to the silica surface.

Insufficient reproducibility in migration times is typically due to run-to-run variations in the electroosmotic flow (EOF) caused by poor control over the zeta potential at silica surfaces. Analytes migrate along the length of the capillary at a rate proportional to the sum of their intrinsic electrophoretic mobility and the electroosmotic mobility as described in Chapter 3. Under a constant set of buffer conditions, the electrophoretic mobility of an analyte is reproducible and constant. Given careful control of the separation conditions, variations in the overall migration velocity are thus most often linked to variations in the EOF. The ζ for silica surfaces results from ionization of the surface silanols, and is thus negative and pH dependent. Observed

variability in the electroosmotic flow in silica capillaries is directly related to variations in ζ caused by changes in hydration and ionization of the silica or adsorption of buffer or sample components to the surface.

Another significant limitation of fused silica capillaries for CE is that the hydrated silica surface provides a highly active surface for adsorption of solutes, especially proteins. Interactions between bare fused silica capillaries and the analytes of interest can cause reduced efficiency, loss of reproducibility, decrease in electroosmotic flow (EOF), and peak broadening.

Chemical modification of the fused silica capillary surface has become a common approach to introduce and maintain a reproducible and uniform electroosmotic flow, eliminate or reverse the direction of the electroosmotic flow, and/or to reduce surface adsorption of analytes. This approach utilizes the advantages of fused silica capillaries, while attempting to eliminate the problems associated with the silica surface. An ideal surface modification should satisfy the following [41]:

a. The bonded phases should completely cover the original silica and the functions introduced should not interact with biopolymer solutes over a wide range of conditions;
b. The coating should exhibit a defined or reproducible composition;
c. The bonded phases should have high chemical stability, and in particular should be resistant to alkaline and acidic hydrolysis produced by aqueous solvents routinely used in CE.

Capillary modifications are described as being either static or dynamic, based on the attachment to the silica surface. [73, 77, 78] Static coatings involve covalent bonding between the wall and the coating material, while dynamic coatings involve non-

covalent adsorptive interactions. Characterization of the properties of coated capillaries is generally done by measuring the EOF and its dependence on the pH of the buffer, [73] characterization of their performance for the separation of selected analytes, and determination of their chemical stability.

Dynamic coatings are an attractive option because of the ease of use and generally homogeneous coating. Dynamic coatings are typically prepared by rinsing the capillary with a solution containing a surface modifier. Neutral polymers are often used, because they eliminate the electrostatic interactions between the analyte and the wall. Charged surface coatings were developed for specific separation problems such as fast separation, reversed EOF, and separation of complex analyte mixtures. However, dynamic coatings require occasional regeneration, and the addition of the coating agent into the separation buffer is often necessary. Significant concentrations of modifier present in the buffer or bleeding of modifier from the surface can interfere with analyte detection. [79] Also, additional buffer additives can reduce the stability or effectiveness of the surface coating, and surface modifier in the run buffer may alter separation selectivity or bring about undesirable changes in buffer properties.

Covalent modification of the surface has also been used to mask or reverse the EOF and reduce surface-analyte interactions. [71, 73, 79-86] This method eliminates the need to regenerate the surface coating or to incorporate the surface modifier into the run buffer. Coated capillaries prepared using covalent bonding generally exhibit longer working lifetimes than those prepared using physical adsorption method. [87] Several effective surface modification schemes have been implemented and developed over the last several years, see reviews. [71, 73] However these coatings are often only usable in

a narrow pH range or suffer from reproducibility issues. Since covalently-modified surfaces can not be as easily regenerated as dynamically modified surfaces, it is critical that they be highly resistant to chemical attack by buffer media and capillary rinse solutions. This last issue has been a significant limitation of the approach, since the standard silanization chemistry that is often used to covalently modify silica surfaces is only stable in a relatively narrow pH range. [45, 53, 71, 73, 88]

Previous attempts to create stable positively charged surfaces have not been able to generate anodic flow at all pH's and have shown that the EOF in covalently bonded PEI capillaries decreases quickly above pH 8. [68, 78, 84, 89-96] To our knowledge, no studies have demonstrated stable surfaces resistant to degradation by acidic or basic washes. [79, 90, 91, 96] Guo *et al.* demonstrated an extremely stable amino-silica glass capillary, but above pH 6.3 the flow was in the cathodic direction due to the negative charges on the silanols. [97]

Recent developments in silica gel polyamine composite technologies for the extraction of toxic metals from waste streams by the Rosenberg group have shown superior stability and resistivity to acidic and basic solutions. [98, 99] The group has developed several composites which have significant advantages over commercially available polystyrene resins. The composites consist of linear or branched water-soluble chelating polyamines covalently bound to a silica gel support, as illustrated in Figures 4.1-3. The novel design of these composites leads to remarkable durability. [100-102]

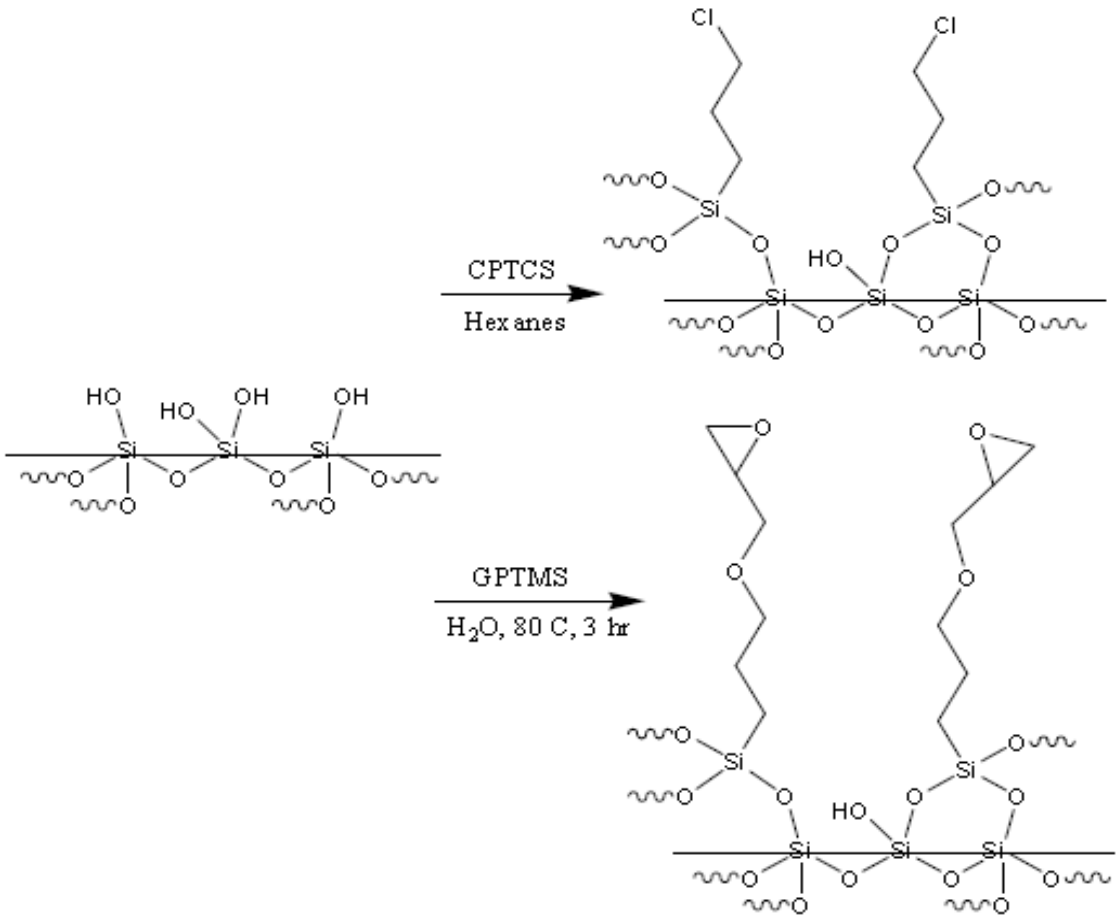

Figure 4.1: Synthetic route of silane anchor attachment for CPTCS and GPTMS modifications

The illustrations in Figures 4.1-4.3 are intended to be representative of possible surface structures. Given the very small surface areas, it was not possible to confirm the surface chemistry using spectroscopy. Spectroscopic studies have been conducted on silica-polyamine composites of similar chemistry [98-100] and provide some insight into the chemical structures that may exist on the modified capillaries. These studies show that silica modification with CPTCS results in a distribution of structures with three (28%), two (59%) or one (13%) siloxane bonds to the surface. [98] The CPTCS gave a

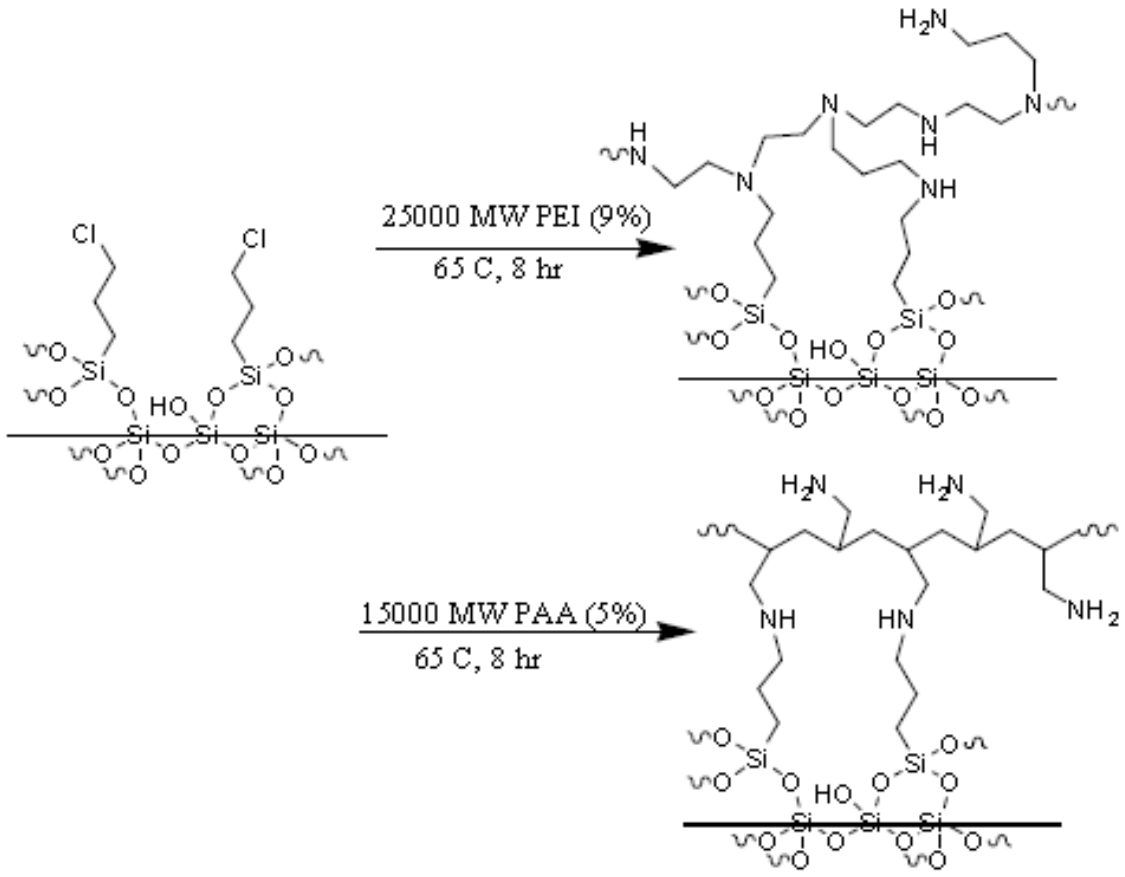

Figure 4.2: Schematic representation of PEI and PAA attachments to CPTCS silane anchors.

surface concentration of 4.5 to 5.7 (±0.7) μmol/m^2, as compared to a typical silanol concentration of up to 8 μmol/m^2. [98] Spectroscopic studies also indicate that when PAA is reacted with CPTCS modified silicas, approximately 40% of all amines are bound to the surface silane layer. For PEI 83% of the primary and secondary amines are bound to the surface, assuming that tertiary amines are not quaternized under the

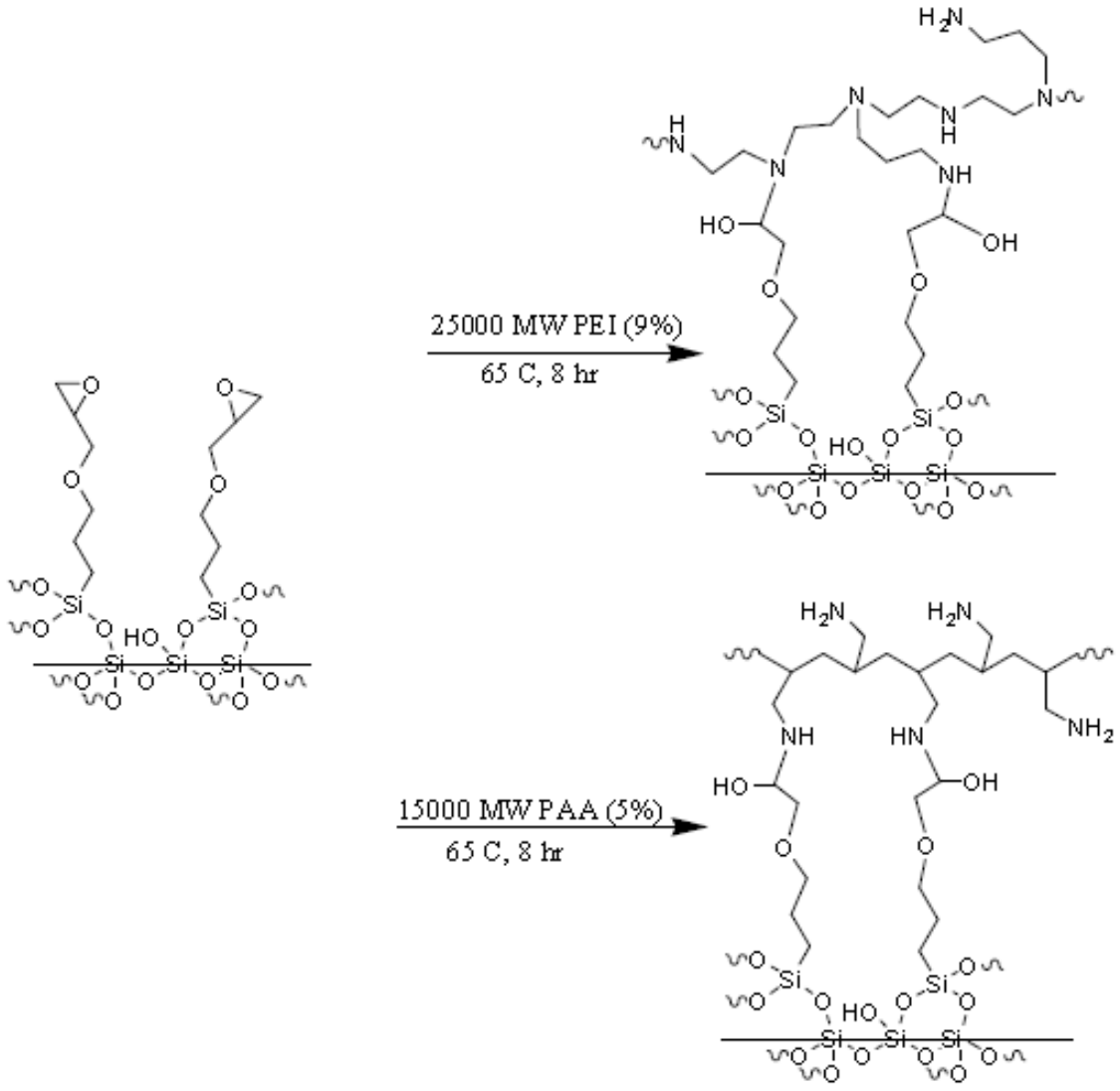

Figure 4.3: Schematic representation of PEI and PAA attachment to GPTMS silane anchors.

reaction conditions. [98, 99] It has been postulated that the remarkable chemical stability of the modification chemistry results from the multiple sites of attachment of the silane anchors and polymers, as well as restricted access of hydrolysis agents to the underlying silica surface.

The purpose of this study is to adapt and develop the silica polyamine composite chemistry described above for application to the covalent modification of fused silica capillaries to generate a positively charged covalently-bound coating that is highly resistant to chemical attack. To achieve this, the capillaries were modified with a silane anchor, followed by covalent modification with amino containing polymers. The covalently bound polymers were then modified to generate cationic quaternary ammonium groups. The resulting modified capillaries were then shown to provide a robust and reproducible EOF and to be remarkably resistant to attack by acidic and basic solutions. The modified capillaries also showed consistent flow over a wide pH range and similar separation performance compared to similar dynamically coated approaches.

4.2 Experimental

4.2.1 Instrumentation

All measurements were performed on an Agilent 3D CE system equipped with a UV detector. Separations were performed with the capillaries thermostated at 25°C and all analytes except acetone were detected at 200nm. Acetone was detected at 254nm. Fused silica capillary with dimensions of 50μm ID × 360μm OD was purchased from Polymicro Technologies (Phoenix, AZ). A detection window was burned into the capillary approximately 8.5cm from the end of the capillary using a homemade device.

4.2.2 Reagents

Nicotinamide, quinine, phenyltoloxamine citrate salt, potassium thiocyanate, potassium bromide, ammonium formate, polyethyleneimine (PEI, 25,000 MW), (3-

chloropropyl)trichlorosilane (CPTCS) were purchased from Sigma (St. Louis, MO). Polyallylamine (PAA, 15,000 MW) was obtained from Changzhou-Synegetica, Ltd. (Changzhou City, China). Potassium iodide was purchased from Merck (Rahway, N.J.). Sodium nitrite was purchased from J.T. Baker (Phillipsburg, N.J.). Tris(hydroxymethyl)aminomethane (TRIS), 3-glycidoxypropyl-trimethoxysilane (GPTMS), sodium phosphate monobasic monohydrate and sodium phosphate dibasic heptahydrate were purchased from Acros Organics (New Jersey, USA). Ammonium acetate was purchased from EMD (Darmstadt, Germany). Hexanes (J.T. Baker) were dried and stored over molecular sieve. Deionized distilled water purified using a Barnstead (Dubuque, Iowa) NANOpure Infinity system was used for all synthetic solutions and for the preparation of all CE buffers. The pH of all running buffers was adjusted to the desired value using concentrated HCl (Merck) or NaOH (EMD). All running buffers were filtered through Whatman (Maidstone, England) 0.8μm nylon membrane syringe filters before use.

4.2.3 Procedure:

New capillaries of 50-100cm in length were cleaned and prepared for modification by rinsing with 500μL 1M NaOH, 250μL DI, and then filling with 1M H_2SO_4. The ends of the capillaries were sealed by an oxygen-house gas torch and the capillaries were then placed in an 80°C bath for 3h, then flushed with DI and air then placed in a 120°C oven for 1h. Following this cleaning and preparation, the capillary surfaces were modified with either CPTCS or GPTMS following with the general procedure described by Hughes *et al.* [98] and illustrated in Figure 1. Cleaned

capillaries were removed from the oven and flushed with humidified house air for one minute in an effort to create a uniformly hydrated capillary surface. The capillary was then flushed with 50μL of 5% solution of CPTCS in hexanes, followed by 500μL of hexanes, MeOH and air. For modification with GPTMS, cleaned capillaries were removed from the oven, and filled with a 1% GPTMS in DI, pH~ 6.5, sealed and placed in 80°C bath for 3h. Capillaries were then flushed with 500μL DI, MeOH, and finally air.

Silanized capillaries were then further modified by polymer attachment as illustrated in Figures 4.2 and 4.3. The capillaries were filled with either 9% PEI (25000MW) or 5% PAA (15000MW), sealed as described above, and placed into a 65°C bath for 8h. The capillaries were removed from the bath and flushed with 500μL each of DI, 4M NH_4OH, water, MeOH, and air.

Polymer modified capillaries were then methylated to form the quaternary ammonium groups by filling the capillaries with 5% MeI in DMSO, sealed, and heated in a 65°C bath for 6h. Capillaries were removed from the bath and flushed with 500μL each of water, dilute HCl, water, and MeOH. The capillaries were then flushed with air.

All capillaries then underwent initial conditioning before being used in CE. Initial conditioning of unmodified capillaries consisted of flushing for 10min with 0.1M NaOH, 10min with water, and 5min with the run buffer. Initial conditioning for polymer-coated capillaries consisted of flushing for 10min with DI, then 10min with run buffer.

4.3 Results and Discussion

4.3.1 EOF in Modified Capillaries

The coatings implemented here were intended to mimic amorphous silica gel polyamine composites, such as those created by Hughes *et al.* [98, 99] and illustrated in Figures 4.1 and 4.2. These composites have demonstrated minimal shrink-swell, can be used at high temperatures, and have improved stability and improved usable lifetimes over commercially available technologies. In their studies, Hughes *et al.* utilized CPTCS for the initial silanization. However, our initial experiments showed that capillaries were frequently clogged during silanization with CPTCS. This was most likely caused by rapid polymerization of the trichlorosilane in the presence of small and variable amounts of water in the capillary. Substitution of GPTMS for CPTCS and following the schemes illustrated in Figures 4.1 and 4.3 eliminated the capillary clogging problems, presumably due to the lower reactivity to the trimethoxy silane. A comparison of EOF magnitude, reproducibility and stability using the two anchors is presented below.

Given the very small surface areas, it was not possible to confirm the surface chemistry using spectroscopy. It is assumed that the surface chemistry on the modified capillaries is similar to that illustrated in Figures 4.1-4.3 and to that determined in previous spectroscopic studies with silica-polyamine composites of similar chemistry. [98, 99]

As illustrated in Figures 4.2 and 4.3, the polymer modified surfaces likely contain a mixture of primary, secondary and tertiary amine sites, depending on the polymer chemistry used. These amine sites are ionizable, and modification with either polymer would result in a pH-dependent positive zeta potential. In an effort to produce

a more permanent and pH independent surface charge, and also to have a more consistent surface chemistry, the polymer-coated surfaces were methylated to produce quaternary ammonium sites.

Modified capillaries were initially characterized for the magnitude, direction, and reproducibility of the electroosmotic flow. The electroosmotic mobility (μ_{eo}) was calculated from the observed migration time of a nonionic flow marker using equation 3.10.

The flow is reversed (in the anodic direction) in all of the modified capillaries relative to the unmodified silica capillary. Figure 4.4a compares the average absolute values of the μ_{EOF} for the first 100 runs in a blank fused silica capillary to that in a capillary modified with GPTMS and PEI and then methylated with MeI. Figure 4.4b shows the EOF vs. run. Both sets of measurements were made using pH 7 10mM TRIS buffer using nicotinamide as the nonionic flow marker. Analysis of the results shows that the difference between the EOF magnitudes is significant at greater than 95% confidence, and that the variance of the flow is significantly lower in the modified capillary at greater than 95% confidence. From Figure 4.4b we can see that both capillaries show a gradual decrease in EOF vs. run, but it is much less for the modified capillary indicating a very stable surface.

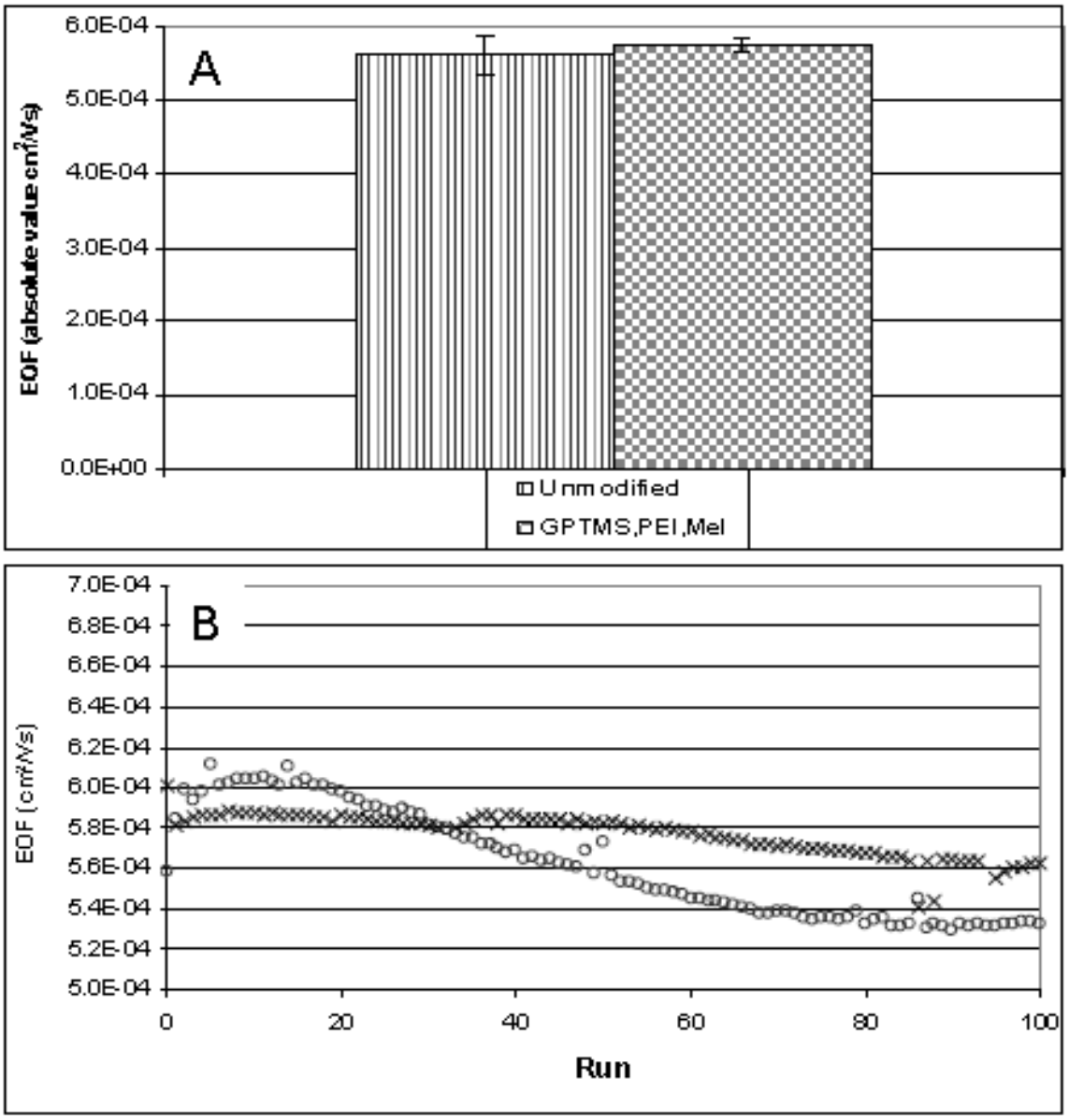

Figure 4.4: Comparison of the absolute values of the μ_{EOF} for the first 100 runs in a blank fused silica capillary to that in a GPTMS, PEI,MeI modified capillary, measured in pH 7 10mM TRIS buffer. A. Average values and standard deviations. B. Absolute value of EOF vs. run number, comparing unmodified (o) and GPTMS,PEI,MeI modified (x) capillaries. Separation conditions -25kV, 25°C, 100mbar/s hydrodynamic injection. Acetone was used as the neutral marker and detected at 254nm. Unmodified capillaries were rinsed for 2min with 0.1M NaOH and 1 min with buffer between injections. GPTMS,PEI,MeI modified capillaries were rinsed for 1min with pH 2 HCl followed by 1min with run buffer between injections.

The EOF was then investigated as a function of buffer chemistry and pH, and as a function of polymer chemistry used to modify the surface. These results are presented in Figure 4.5. The methylated capillaries demonstrated an electroosmotic flow in the anodic direction at all pH's examined, due to the presence of quaternary amine groups on methylated PEI and PAA. The EOF in PAA modified capillaries is lower than that of the PEI modified capillaries at all pHs and buffer chemistries studied, for an average decrease of 20% in the EOF over all conditions. This result indicates that the PAA modified surfaces have fewer amine sites and thus are less positively charged.

The modified capillaries show constant EOF even above pH 8 due to the presence of the quaternary amine groups, which provide positive charge and permanent anodic flow at all pHs. The magnitude of the flow is buffer dependent, however, showing a loss in flow in higher pH phosphate buffers. This decrease in the flow indicates that phosphate anions are adsorbing to the surface and decreasing the overall positive charge. The other buffers, which included ammonium formate, ammonium acetate and TRIS, do not show the same trend in this pH range indicating no ion adsorption.

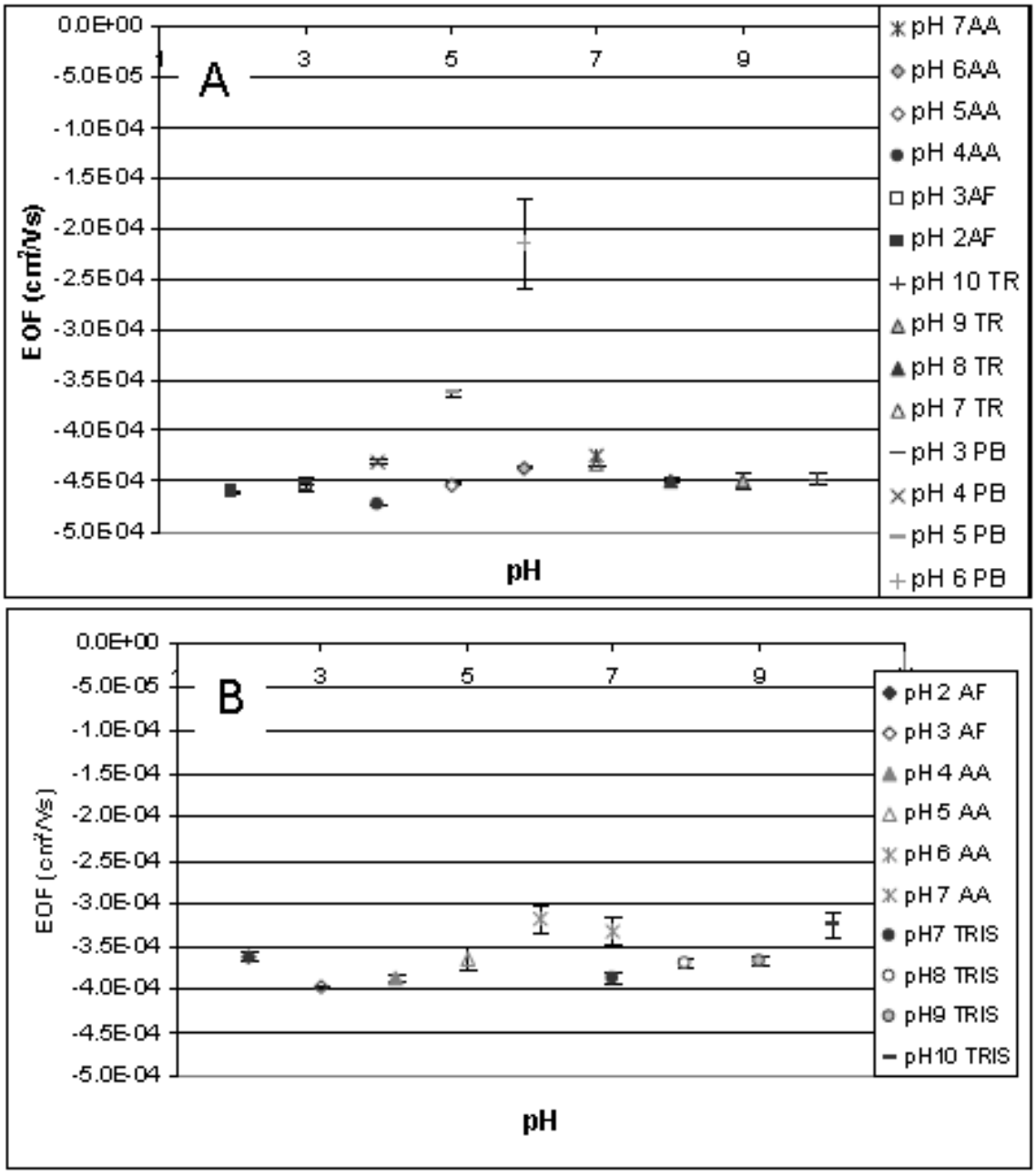

Figure 4.5: μ_{EOF} in modified capillaries as a function of pH and with various buffer chemistries. A. GPTMS,PEI,MeI modified capillary. B. GPMS,PAA,MeI modified capillary. Buffers are 20mM ammonium formate (AF, pH 2-3), 20mM ammonium acetate (AA, pH 4-7), 20mM phosphate (PB, pH 3-7) and 20mM TRIS (TR, pH 7-10). Separation conditions same as Figure 4.4. Acetone was used as the neutral marked and detected at 254nm.

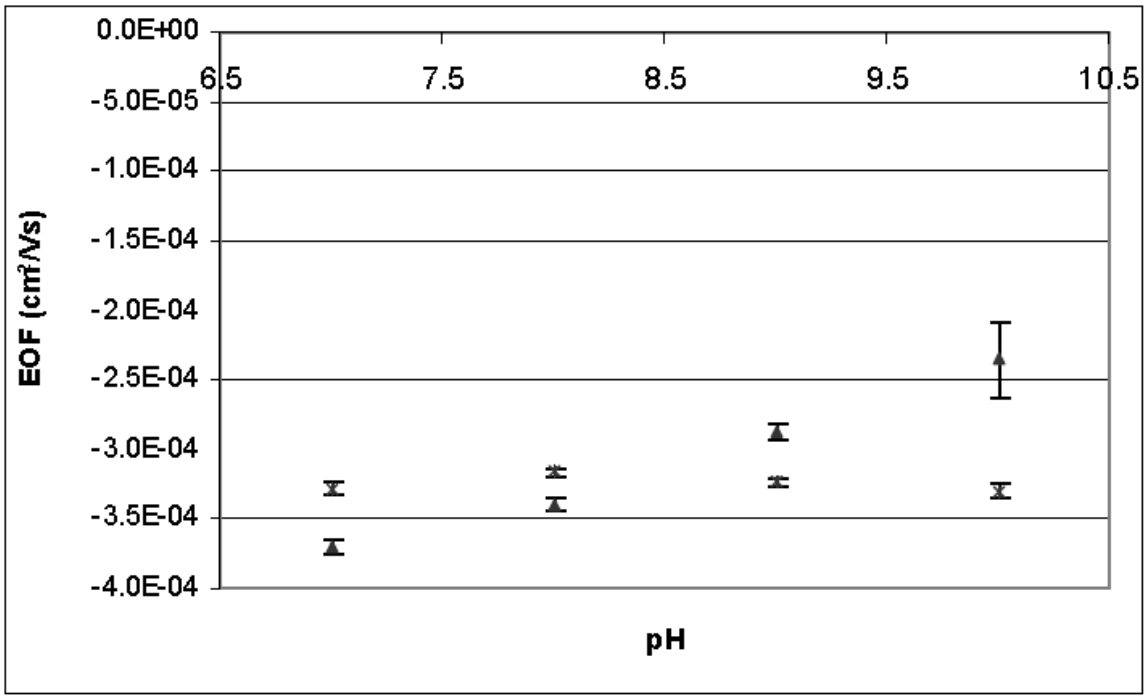

Figure 4.6: Comparison of EOF in GPTMS,PEI (▲) and GPTMS,MeI (Ж) in 20mM TRIS. Separation conditions same as Figure 4.4. EOF average of 6 runs.

GPTMS,PEI modified capillaries were then compared before and after the methylation reaction to confirm that the pH-independent flow is a result of the methylation procedure. Figure 4.6 shows the difference between methylated and non-methylated capillaries as a function of the buffer pH. The results illustrate that methylation to the quaternary amines gives a surface with a fixed or permanent charge, and thus constant μ_{eof}, in the pH range studied. The decrease in the protonation of imine groups of PEI in the non-methylated capillary with increasing pH causes the wall to be less positively charged and thus results in a decrease in EOF. [1, 5, 8] The large deviation at pH 10 in the non-methylated capillary is not a true standard deviation as it represents a trend to lower EOF over time beginning at $-2.64*10^{-4}$ cm^2/Vs and decreasing with repeated measurements to $-1.86*10^{-4}$ cm^2/Vs. This is likely a result of

the slow equilibration of the imine sites with the buffer. The methylated capillaries do not show this effect because of the permanent charge on the surface.

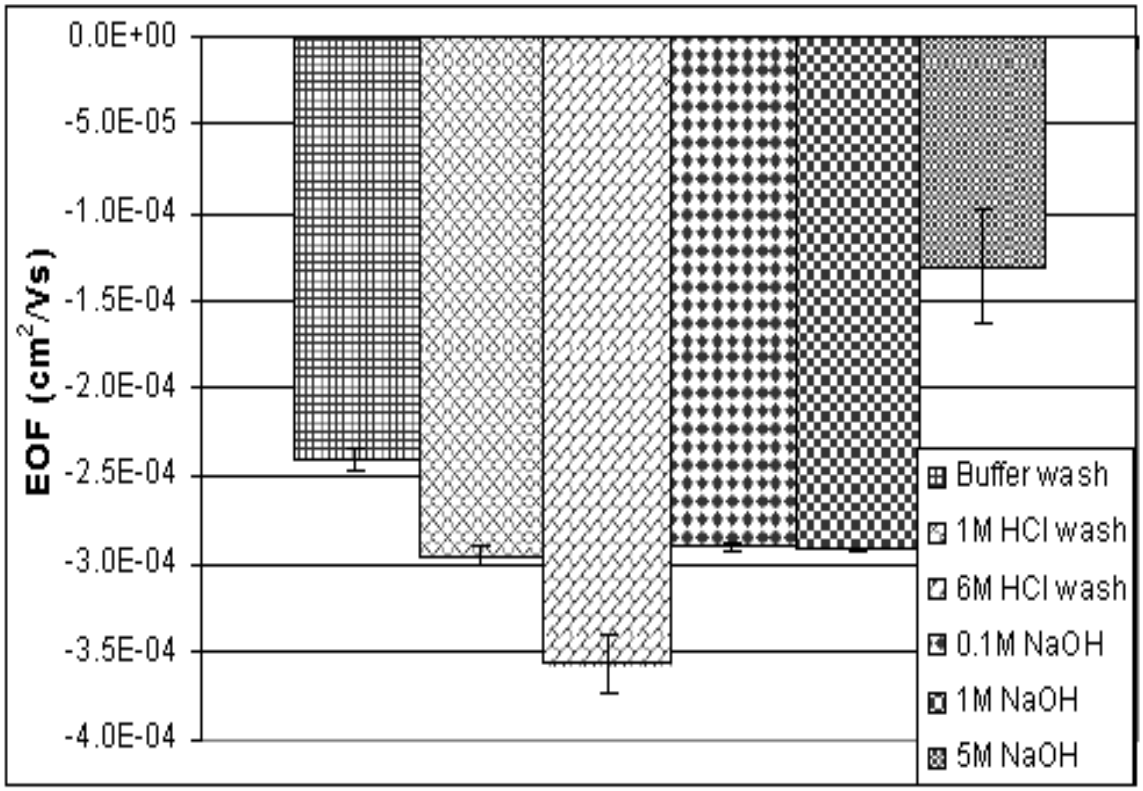

Figure 4.7: EOF in a CPTCS,PAA,MeI capillary after various capillary rinse conditions. Separation conditions same as Figure 4.4, pH 4 phosphate buffer, acetone detected at 254nm used as neutral marker.

The durability of the surface modifications was tested using various capillary wash conditions before measuring acetone as the EOF marker in pH 4 phosphate buffer. The CPTCS,PAA,MeI capillary showed very good hardiness to extreme pH's. The results in Figure 4.7 are the average EOF of three runs, washing the capillary for 1min with an acidic or basic solution and then 1min with buffer. It can be seen that washing with a mild acidic or basic solution gives a more negative EOF and greater reproducibility than just washing with buffer. There is no statistical difference in the

EOF between measurements taken after washes of 1M HCl, 0.1M or 1M NaOH. Remarkably, the capillaries can be washed with concentrated acid and base and still retain reproducible anodic EOF. Washing with 6M HCl actually temporarily generates a more robust anodic EOF, implying that the capillary modification remains intact and possibly that the immobilized polymer becomes highly ionized in the presence of strong acid. When the EOF is analyzed again using a 1M HCl wash the EOF returns to its original value. Washing with 5 M NaOH, however, causes a significant permanent decrease in the magnitude of the EOF, most likely because of loss of polymer modifier from the surface through hydrolysis of the siloxane anchor chemistry. The durability of GPTMS,PEI,MeI capillaries is demonstrated in Figure 4.4, where the capillary showed minimal loss in EOF after 100 runs each employing a wash with 0.01M HCl (pH 2).

As mentioned above, early experiments using CPTCS as the silane anchor often resulted in clogged capillaries, but GPTMS did not cause this problem. GPTMS is less reactive than CPTCS but has been used in previous studies to anchor PEI. [9] Studies were conducted to determine if substitution of the silane anchor had any detrimental effect on EOF magnitude, reproducibility, or stability. No statistically significant difference was observed in the magnitude or reproducibility of the EOF in pH 7 TRIS buffer, while the GPTMS anchor gave significantly greater EOF in pH 4, 5 and 6 phosphate buffers. No observable difference was noted in the chemical stability of the surfaces modified with the two silane anchors.

The reproducibility of the coating procedure was examined by comparing the EOF of eleven GPTMS/PEI/MeI modified capillaries synthesized on different days over a 13 month period. Each capillary was made according to the conditions described in

section 4.2.3, and each gave robust and reproducible EOF. However, statistically significant and substantial differences were observed between different modified capillaries. The combined EOF average was $-4.57*10^{-4} \pm 7.83*10^{-5}$ cm^2/Vs and the average with the high and low capillaries removed was $-4.54*10^{-4} \pm 4.64*10^{-5}$ cm^2/Vs.

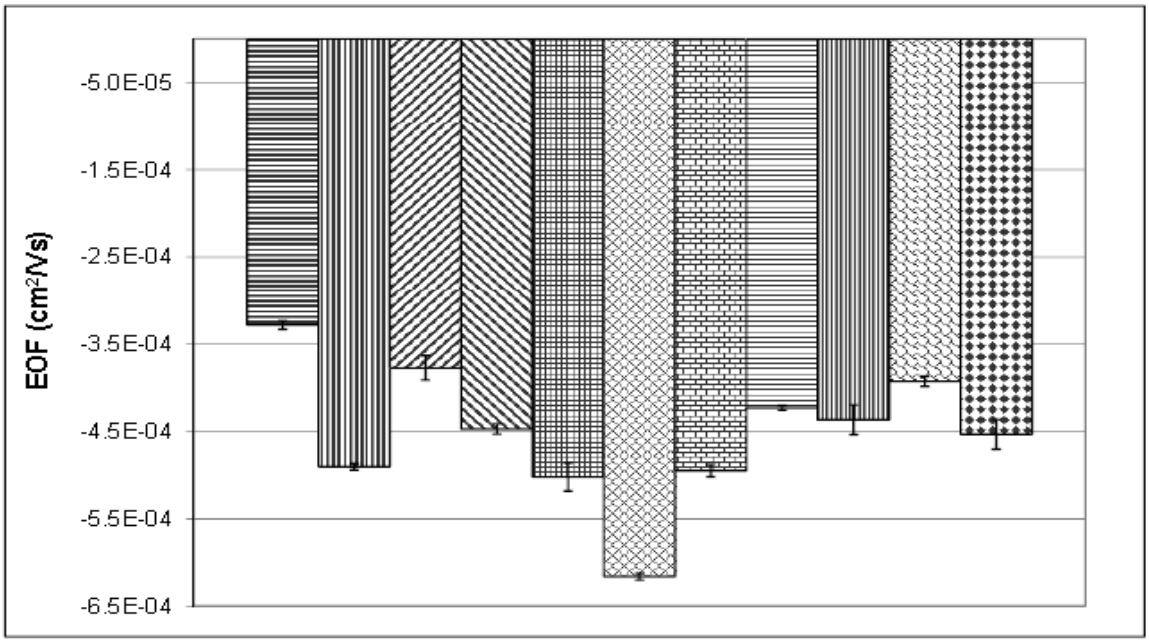

Figure 4.8: EOF of GPTMS,PEI,MeI modified capillary produced on different days over a period of 13 months. Separation conditions same as Figure 4.4, pH 7 20mM TRIS.

4.3.2 Representative Applications

Small inorganic anions have electrophoretic mobilities that are of nearly the same magnitude but opposite in sign to the EOF in fused silica capillaries, resulting in very long migration times. For most CE methods, therefore, an EOF modifier is added to the running buffer to reverse the electroosmotic flow and reduce analysis times significantly. PEI has been used previously as a covalent or dynamic coating agent for the separation of small inorganic ions. [68, 91, 94, 96] Given the positive charge and anodic EOF over a wide pH range, the modified capillaries introduced here are also

suitable for the fast separation of inorganic anions. Separations of four UV active inorganic anions in the modified capillaries are presented in Figure 4.9. Comparative separations in unmodified capillaries were not obtained due to the extremely long analysis time required, as discussed in sections 3.2.4 and 3.5.1. The separation with both modification chemistries is very fast, with all four anions migrating within 2.5min. The ions migrate with the same electrophoretic mobility in both modified capillaries. The apparent difference in migration time is due to the fact that a longer capillary was used for the PEI,MeI capillary. The analysis time with these capillaries is approximately the same as that obtained in static coated PEI capillaries. [68, 93] A curious result, however, is that the migration order is not the same as in previous studies, with a reversal in the migration order of iodide and nitrite. This may be due to ion exchange interactions with the modified surfaces. The peak tailing for thiocyanate and to a minor extent iodide is likely due to electrophoretic effects.

As discussed in the introduction, the anodic EOF in modified capillaries allows for improved resolution of cationic species that may be difficult to resolve using unmodified capillaries with cathodic EOF. This improved resolution results from the opposing effects of electrophoresis and EOF, and is achieved at the cost of analysis time. This was demonstrated for the current capillaries using the cations nicotinamide, quinine and phenyltoloxamine. The average resolution between quinine and phenyltoloxamine in modified and unmodified fused silica capillaries are presented in Table 4.1, and

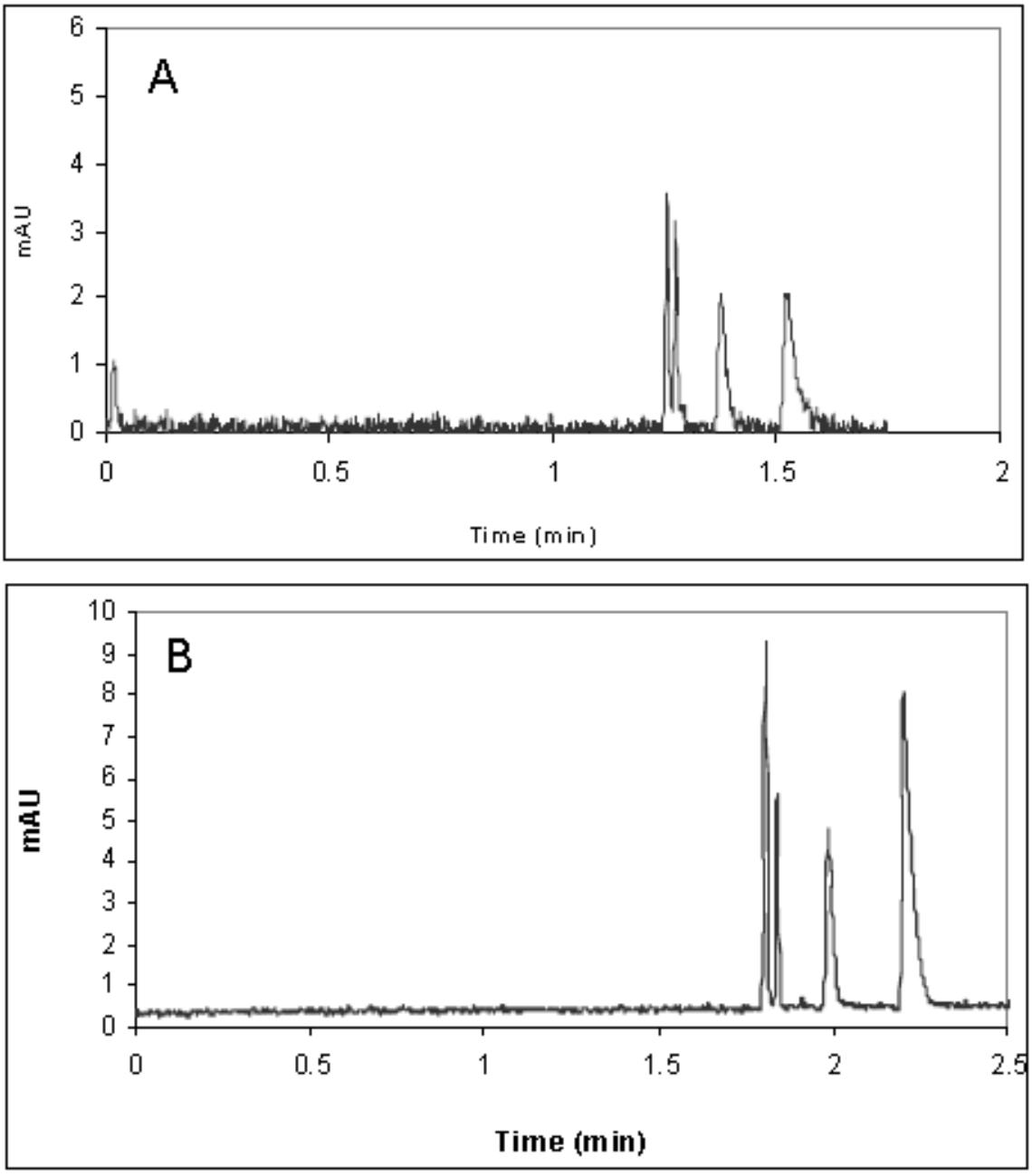

Figure 4.9: Electropherograms of four anions at pH 7 in modified capillaries. Peaks: 1=bromide, 2=nitrite, 3=iodide, 4=thiocyanate. A. GPTMS,PAA,MeI capillary, total length 48.3cm, effective length 39.8cm. Injection: 250mbar/s hydrodynamic. B. GPTMS,PEI,MeI capillary, total length 60.3cm, effective length 51.7cm. Injection: 300mbar/s hydrodynamic. Run conditions: 20mM TRIS, -25kV, detection at 200nm.

representative separations in a blank and modified capillary are presented in Figure 4.10 and 4.11. When the flow is reversed in the modified capillary phenyltoloxamine and

quinine migrate after the neutral marker. As expected, the modified capillaries provide improved resolution over blank capillaries at all pH's studied. The resolution is not as great at pH 10 because phenyltoloxamine has a pKa of 9.1, the species becomes ionized and the migration changes.

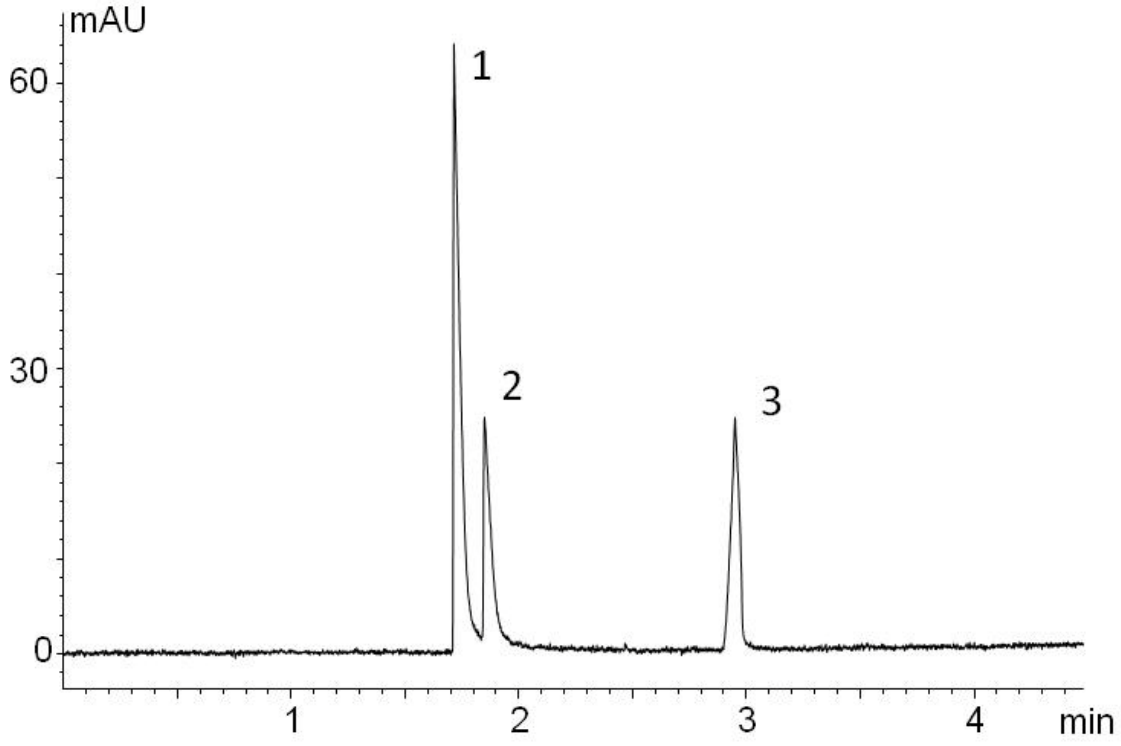

Figure 4.10: Electropherogram of three positively charged species at pH 4.99 in unmodified capillary. Peaks: 1=nicotinamide, 2=phenyltoloxamine, 3=quinine. Buffer 10mM PB. Injection: 20mbar/s hydrodynamic. Run voltage +15kV. Total length 34.0cm, effective length 25.5cm, detection at 200nm.

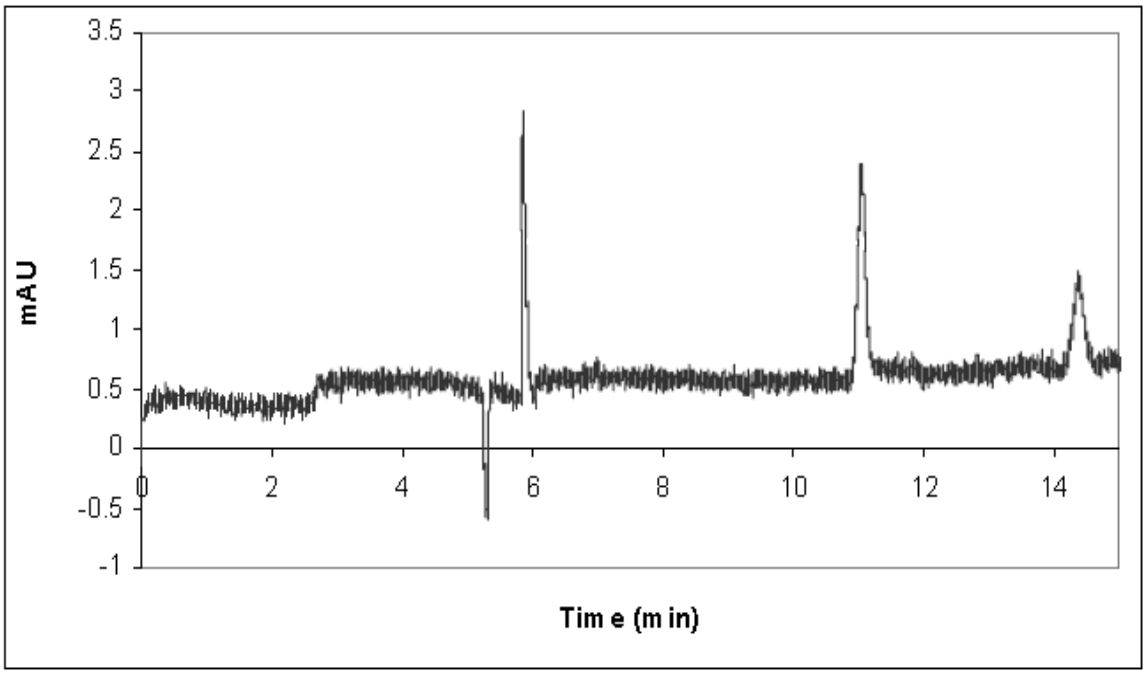

Figure 4.11: Electropherogram of three positively charged species at pH 4 in GPTMS,PEI,MeI capillary. Peaks: 1= acetone, 2=nicotinamide, 3=phenyltoloxamine, 4=quinine. Buffer 20mM PB. Injection: 250mbar/s hydrodynamic. Run voltage -25kV. Total length 60.3cm, effective length 51.7cm, detection at 200nm.

Table 4.1: Average Resolution between quinine and phenyltoloxamine in different buffers.

	pH 7 TRIS	pH 8 TRIS	pH 9 TRIS	pH 10 TRIS	pH 3 PB	pH4 PB	pH 5 PB
GPTMS,PEI,MeI	6.63 ± .28	6.45 ± .25	3.26 ± .10	2.48 ± .24	18.5 ± 2.51	8.41 ± .91	6.66 ± 2.2
Unmodified	1.90 ± .24	4.20 ± .38	2.05 ± .56	2.34 ± .29	9.28 ± 1.88	3.22 ± .22	3.88 ± .40

4.4 Concluding Remarks

The use of PEI and PAA coated capillaries reverses EOF and offers a suitable alternative to the use of cationic surfactants and buffer modifiers for the separation of negatively and positively charged species. The modification chemistry utilized generates capillaries with excellent chemical stability and strong anodic flow even after exposure to extremely acidic and basic wash solutions. The EOF in the capillaries is very

reproducible for 100 injections or more. Methylation of the immobilized polymers provides nearly constant flow over the entire pH range studied. Utilizing the modified capillaries, the separation of simple anions is very fast and offers good resolution, while cationic analytes migrate against the EOF and thus have longer migration times and much improved resolution.

To the author's knowledge, no other covalently modified capillaries have demonstrated the same level of stability for as many injections or with such strongly acidic or basic rinse solutions. The stability of this covalent surface modification chemistry means that this approach offers a competitive alternative to dynamically coated capillaries, with the advantage that these surfaces do not need to be regenerated, no buffer modifiers are required, and modifier bleed is likely to be very low or nonexistent.

The reported modification procedure did not lead to suitable reproducibility in the electroosmotic flow for different capillaries. This is most likely caused by small differences in the hydration of the surface before modification with the reactive silane. Efforts to reproducibly hydrate the surface before modification were apparently not successful. Improved capillary to capillary reproducibility might be achieved by development and application of improved methods to achieve reproducible surface hydration and modification.

Chapter 5: Development and Characterization of a Capillary Biosensor for Chemical Warfare Agents

In this chapter I describe efforts to develop a biosensor for organophosphorous nerve agents utilizing a fused silica capillary waveguide as a platform. The goal and rationale of the studies were to exploit the benefits of a new and promising technology called fiber optic capillaries (FOCaps) to develop a field usable sensor. The need for such a sensor will be discussed in the following sections along with similar research and the benefits of FOCaps. A modification of existing chemistry was employed to immobilize acetlycholinesterase (AChE) onto the surface of FOCaps. Several immobilization chemistries were tested and K_m and V_{max} of AChE were measured for each chemistry. From these results it was determined that all immobilization chemistries were similar in that no statistically significant differences in enzyme performance were observed. Based on these results a fiber optic capillary (FOCap) sensor was developed and employed to detect warfare agent stimulants paraoxone and DFP. Paraoxone was detected at a concentration level of 1.15μM and DFP was detected at 0.05μM.

5.1 Definition of the Problem:

Chemical warfare agent detection is an important defense concern for both civilian and military agencies. Terrorism is regarded as one of the key challenges facing our society today, with the events of 2001 in the United States and subsequently in the United Kingdom graphically demonstrating the threat to our way of life. There is a growing concern that terrorists will resort to non-conventional means of attack such as

the use of chemical and biological agents. The 1st UK–US Conference on Chemical and Biological Sensors and detectors held in April 2007 highlighted the considerable research investment being made to develop detection systems that can provide rapid warning of these agents. This part of the dissertation describes efforts to develop a simple, robust and portable chemical warfare agent sensor through adaptation of existing approaches to a new technology.

5.2 Organophosphate Warfare Agents

Some common representatives of the major classes of chemical warfare agents are shown in Figure 5.1. The nerve agents represent one of the most important and lethal classes of chemical warfare agents. Their rapid and severe effects on human and animal health stem from their ability to block the action of acetlycholinesterase, a critical nervous system enzyme that is responsible for the breakdown of the neurotransmitter acetylcholine. Among the nerve agents, the organophosphates are of particular concern because they are generally stable, easy to disperse and highly toxic. They can be absorbed through the skin, by ingestion, or by respiration.

The acyl pocket of the active center, the choline subsite of the active center and the peripheral anionic site of AChE constitute three distinct binding domains for inhibitory ligands. [103] The catalytic triad consisting of Ser203, His447, and Glu334, reside at the base of a narrow gorge approximately 20 Aº deep. [104] . The catalytic mechanism is similar to other hydrolases, where the serine hydroxyl group is rendered highly nucleophilic through a charge-relay system involving the glutamate carboxyl group, the imidazole on the histidine, and the hydroxyl of the serine. [105, 106]

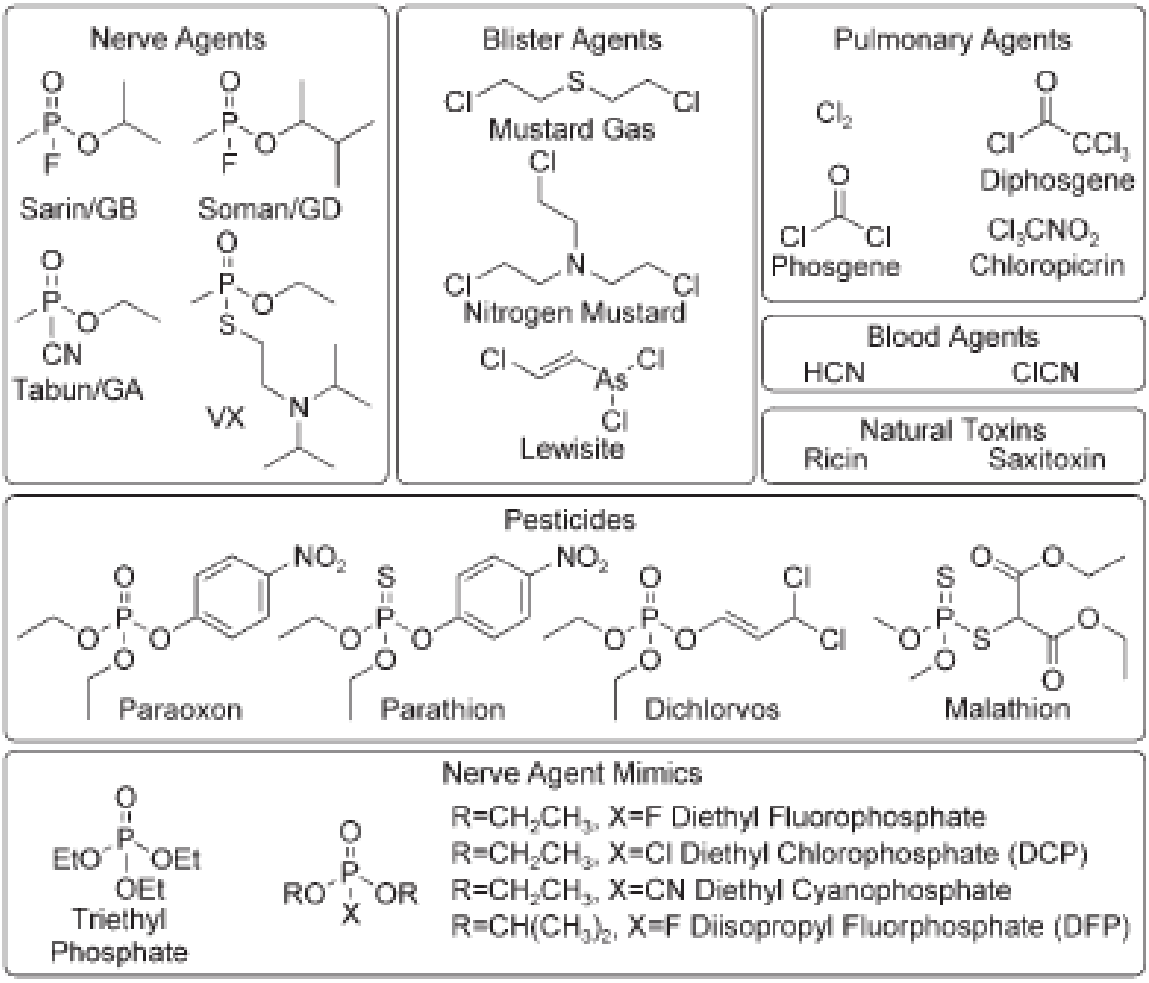

Figure 5.1. Major classes of chemical warfare agents, pesticides and nerve agent mimics and chemical structures of common representatives. [110]

Radic *et al.* found site specific mutants of mouse AChE that can alter the activity of the enzyme. [107] They identified three specific regions where mutations caused alterations to the enzyme activity. The first domain is in the acyl pocket, the second is a region near the lip of the gorge, and the third region is found in the region where the choline moiety associates during catalysis.

Reversible inhibitors such as propidium and the peptide toxin fasciculin, bind to the peripheral anionic site on AChE. [108, 109] Virtually all organophosphates (OPs) and carbamates inhibit AChE by reaction with serine residue within the active site.

Specifically, inhibition is caused by a chemical reaction between the phosphorus containing moiety of the OP compound and the hydroxyl functionality of the serine residue, resulting in a phosphorylated enzyme. (Scheme 5.1). [110]

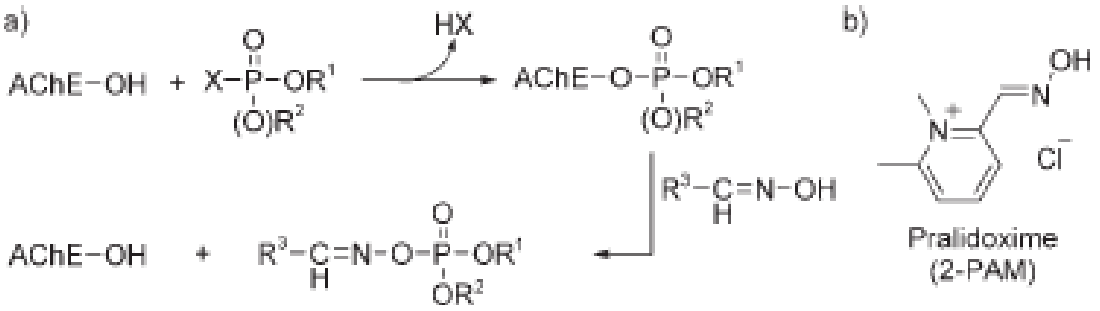

Scheme 5-1. a) Inhibition scheme of AChE by organophosphates and reactivation by an oxime and b) structure of the enzyme reactivating agent pralidoxime chloride, 2-PAM. [110]

Compared to the normal acylated intermediate complex, the phosphorylated enzyme is very stable, resistant to hydrolysis and breaks down very slowly, leading to a loss of enzyme function. [111] This results in a buildup of acetylcholine in the body, which can lead to organ failure and eventual death.

The enzyme function can be restored with compounds that can dephosphorylate the enzyme, such as pralidoxime chloride (2-PAM), and as a consequence such compounds can be used as antidotes (Scheme 5-1). The reactivation occurs by hydroxyl ion attacking the phosphorylated serine residue, removing the phosphate moiety and releasing active enzyme. Stronger nucleophiles such as oximes are better at reactivation and 2-PAM can reactive AChE faster than other oximes because it has a very small ligand.

5.3 Sensors for Organophosphate Nerve Agent Detection

Traditionally, detection and quantitation of these hazardous chemicals relied on physicochemical means such as thin layer chromatography, mass spectrometry and gas liquid chromatography. Several additional approaches have been used to detect organophosphorus compounds, including but not limited to: potentiometric methods [112], colorimetric methods [113], surface acoustic wave spectroscopy [114], gas chromatography/ mass spectrometry [115], and interferometry. [116] Although these methods are sensitive and specific, in most cases they are time consuming, difficult to interpret, and require specialized laboratories and qualified technicians. Further, most of these technologies do not address the need for sensitive and reliable portable sensors to monitor the presence of these agents in the field.

Alternatives to these traditional approaches include field deployable bio-sensors. Biosensors incorporate a biological sensing element (eg enzymes, antibodies or receptor proteins) and physical transducers (electrode, silicon chip or fiber-optic). The signal in such sensors is the result of specific interaction between the analyte of interest and the bioreagent.

Many biosensing schemes for organophosphate nerve agents utilize enzymes. For example, the presence of any AChE inhibitors such as organophosphates can be determined if changes in AChE enzyme activity can be reliably converted to an analytical signal. Organophosphate hydrolase (OPH), which catalyzes the hydrolysis of organophosphates to produce phosphoric acid, has also been used in biosensors. Several groups have used immobilized AChE [117-132] and OPH [133-137] to detect pesticides

and other organophosphates. [127, 129, 138-141] The AChE-based sensors rely on the fact that hydrolysis of acetylcholine by AChE produces a proton per substrate molecule, resulting in an increase of the acidity. This acidity increase can be measured in solution with the help of a pH-sensitive molecule.

A very convenient and simple method of chemical detection is through generation of an optical event, such as a change in absorption or fluorescence intensity or spectrum. [127, 142-146] Rogers *et al.* [147] utilized this approach by labeling AChE with the pH sensitive fluorescein isothiocyanate (FITC) and immobilizing the enzyme-dye adduct on a quartz fiber attached to a fluorescent spectrometer. In the absence of organophosphorous inhibitors, the labeled AChE was able to hydrolyze acetylthiocholine, resulting in a pH reduction. The pH decrease leads to a reduction of the FITC fluorescence intensity, due to the interruption of the fluorophore's conjugation upon protonation. [148] If this bio-sensor was first exposed to the CWA mimic diisopropylfluorophosphate (DFP) and subsequently to acetylcholine, 90% of the enzyme activity was lost, as quantified by a less pronounced reduction of the fluorescence intensity. The enzyme activity could be restored by treating the biosensor with 2-PAM, which removed the bound phosphorus from the enzyme and thus "reset" the sensor. This biosensor was capable of detecting the organophosphorus pesticide paraoxone in the nM range when it was exposed to a solution that contained the analyte for ten minutes. It was unable to detect the pesticides malathion or parathion, even at mM concentrations, indicating selectivity of the sensor for different OP compounds.

Fluorescein is used in numerous applications because of its very high molar absorptivity at the wavelength of an argon laser, large fluorescence quantum yield and high photostability. The dye has strong fluorescence in alkaline solutions and as the pH decreases so does the luminous intensity. Previous reports have related this fluorescence variation to the existence of different protolytic forms of the dye, shown in Figure 5.2, and the occurrence of protolytic reactions in the excited state. [149-151] The neutral fluorescein molecule has a much lower molar absorptivity than other forms due to the formation of the lactonic modification, which does not adsorb in the visible spectrum. An explanation for the low fluorescence yield of the neutral molecule proposed by Martin *et al.* is that the molecule undergoes internal conversion or intersystem crossing processes. [152] Martin *et al.* also observed that the monoanion has a much lower molar absorptivity at 490 nm and a shift in the absorbance maximum to lower wavelengths relative to the dianion. Fluorescence quantum yield of the monoanion was estimated by Martin *et al.* to be 0.25-0.35, compared to 0.93 for the dianion. Although a shift in the pKa of the xanthene hydroxyl group is expected on excitation, spectral studies indicate that proteolytic equilibrium is not achieved during the lifetime of the excited state: excitation of the monoanion results in fluorescence of the monoanion with very little or no fluorescence from the dianion. [152] The combination of reduced absorptivity at 490 nm and reduced fluorescence quantum yield results in diminished fluorescence intensity for the monoanion relative to the dianion.

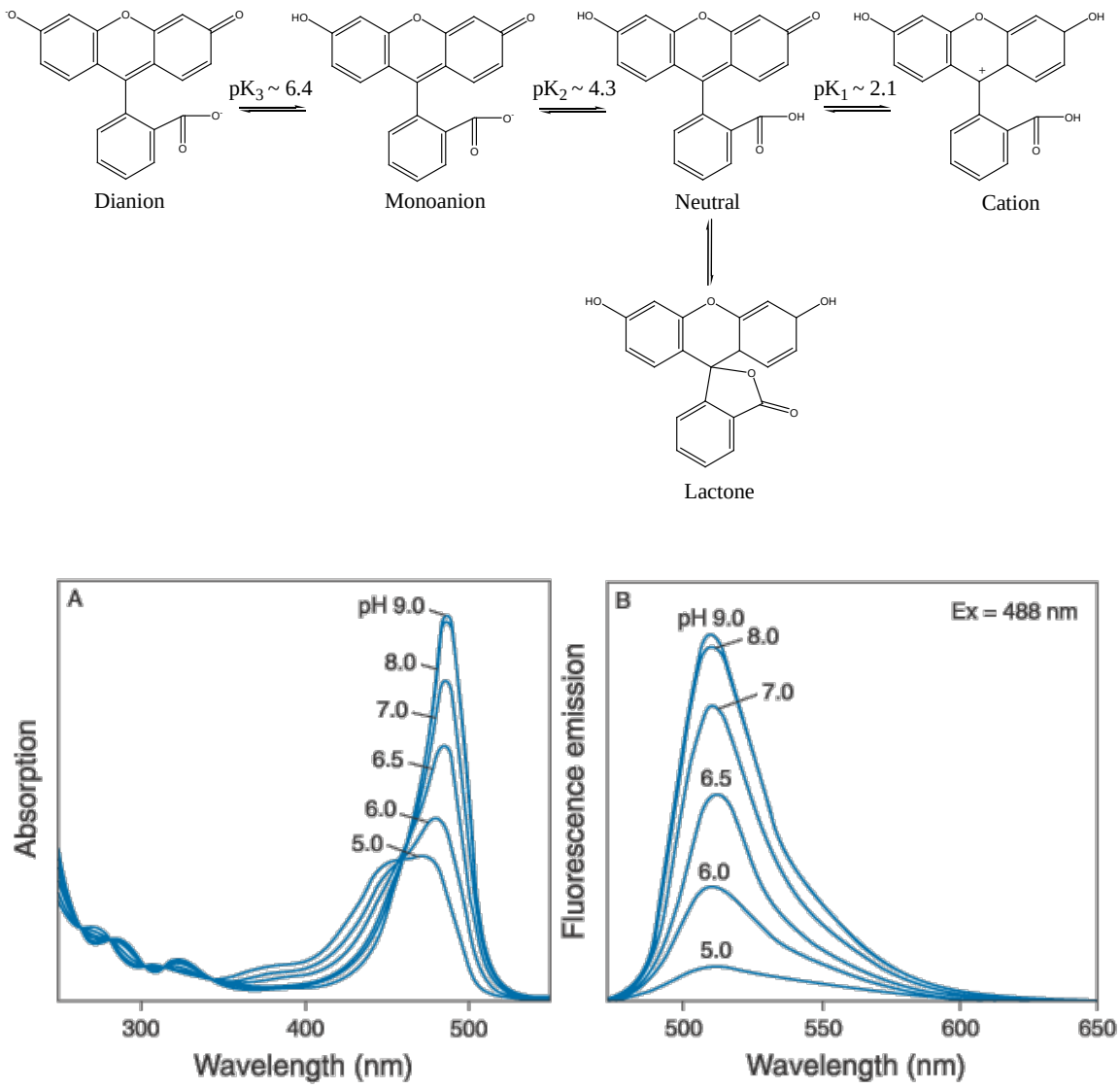

Figure 5.2: Ionization equilibria of fluorescein, and the corresponding A) absorption and B) emission spectra of Fluorescein. (Taken from Invitrogen.com)

Jin *et al.* [127] relied on the inhibition of AChE in the presence of a pH-dependent fluorescent dye. In this system the proton resulting from the hydrolysis of the acetylcholine resulted in an increase of the fluorescence intensity of 2-butyl-6-(4-methylpiperazin-1-yl)benzo-[de]isoquinolin-1,3-dione). The change of the fluorescence peak intensity was correlated with the OP concentration. A flow injection analysis setup

allowed for detection of the OP derivative paraoxone in the 10^{-8}M range after an incubation time of ten minutes.

A second family of enzymatic sensors utilizes OPH in conjunction with a pH-responsive fluorescent dye. This enzyme works differently from AChE, in that it catalytically hydrolyzed the organophosphate. As a result, sensors involving OPH allow for a more direct measurement of organophosphate molecules, instead of measuring enzyme inhibition. OPH is widely used in CWA biosensors because its catalytic site is able to hydrolyze a wide range of OP compounds that contain P-O, P-F, P-S, or P-CN bonds. [153] The stoichiometric hydrolysis produces two protons which can be directly correlated to the amount of OP substrate present.

To create an OPH-based CWA sensor, Rogers *et al.* [143] labeled the enzyme with FITC and coated this complex onto poly(methyl methacrylate) beads to create a biosensor. The fluorescence signal from this biosensor was monitored in a buffer solution. Upon addition of OP analytes, such as paraoxone, a decrease in pH in the local environment occurs and a decrease of FITC's fluorescence intensity was observed. The decrease of FITC's fluorescence intensity could be directly related to the concentration of analyte. The detection limit for paraoxone, defined in the study as three times the standard deviation of experiments with the neat buffer solution, was in the μM range.

Cao *et al.* [144] labeled OPH with FITC and deposited this complex onto silanized quartz slides in the form of Langmuir-Blodgett films to create organized monolayers of the enzyme-based sensors. These thin films reduce the problems associated with thicker films, which include the longer times required for the substrate to diffuse into the thicker film and the tendency of enzymes on the surface of the thick film

to act as barriers for the analyte, thus reducing access to the enzymes within the film. Cao *et al.* demonstrated that the enzyme-based sensor LB films show enhanced sensitivity, detecting the analyte at nM concentrations. Orbulescu *et al.* [145] further demonstrated that covalently immobilized fluorescently labeled OPH on a silanized quartz substrate results in an increase of the enzyme stability, while a detection limit in the nM concentration range can be maintained.

Another biosensor that incorporates OPH in combination with a fluorescent dye was developed by Russell *et al.* [146] In this sensor OPH was covalently functionalized with the pH dependent fluorescent label carboxy seminaphthofluorescein (SNAFL-1) and with a poly(ethylene glycol) (PEG) acrylate derivative. The acrylated fluorescent enzyme was photopolymerized in the presence of PEG diacrylate, trimethylopropane triacrylate, and tetraacrylated PEG to yield microspheres of a sensor-containing, lightly cross-linked polymer that formed hydrogels upon immersion in water. This system has several specific advantages over the above mentioned FITC-labeled OPH biosensors, namely that SNAFL-1 is a “self-referencing” fluorescent dye. It features a broad fluorescence band that stretches from 500 to 700nm. The fluorescence intensity of SNAFL at 620nm is unchanged upon exposure to OP analytes, while the intensity around 550nm experiences a reduction. Thus, monitoring the ratio of the emission intensities at 620 and 550nm allows one to generate a “referenced” signal that limits problems with effects such as photobleaching, concentration changes, and sensor noise. It is also claimed that the PEG hydrogel further provides a protective environment for the enzyme; thus potentially inhibiting degradation and fouling. The OPH/SNAFL/PEG

sensors investigated allowed the detection of paraoxone in the aqueous solution, in concentrations as low as 10^{-7}M.

Sensor systems that rely on enzyme/fluorescent dye systems have the potential to be used in portable electronic devices. Viveros *et al.* [154] reported an OPH biosensor in which the fluorescent dye carboxynaphthofluorescein (CFN) was covalently bound to the enzyme. The complex was reported to operate well in combination with a fiber-optic biosensor assay. The fluorescence intensity of CNF decreased with decreasing pH, and through correlation of the fluorescence intensity with the concentration of the OP, a detection limit of 10^{-8}M was claimed.

5.4 Fiber Optic Sensors

Fiber optic sensors have received considerable attention as an alternative method for rapid chemical analysis because of their adaptability to a wide variety of assay conditions. Optical sensors have certain advantages over potentiometric sensors such as no direct electric connections, reduced drift problems and suitability for continuous monitoring. [147] Traditional optical sensors measure intrinsic absorbance, scattering or fluorescence of the analyte of interest. In many cases, analytical selectivity and sensitivity can be considerably improved by use of fiber optic based sensing schemes.

Optical and fiber optic chemical sensors have been reported extensively in literature since the 1970's. Fiber optic sensors have since found applications in chemical [155-157], biochemical [158-161], biomedical and environmental sensing. [162-165] In general, fiber optic sensors are classified as intrinsic and extrinsic type sensors. In the extrinsic type of sensors the optical fiber is only used as a means of light transport to an

external sensing system i.e. the fiber structure is not modified in any way for the sensing function. Examples of extrinsic fiber optic sensors include fibers terminated in active layers e.g. optode [166], fibers having end face mirrors or fibers confronting other transducer elements or fibers. [167] The intrinsic fiber optic sensors differ from extrinsic sensors, where light does not have to leave the optical fiber to perform the sensing function. In the intrinsic fiber optic sensors, the optical fiber structure is modified and the fiber itself plays and active role in the sensing function. Examples of intrinsic fiber sensors include fibers with Bragg gratings, modified claddings or micro or macrobends. [168]

Fiber optic intrinsic sensors provide numerous advantages over conventional sensors, which include immunity to electromagnetic interference, small and compact size, sensitivity, remote sensing, ability to be multiplexed and the ability to be embedded into various textile structures. [168, 169] Well-designed intrinsic sensors have the characteristics of high sensitivity, selectivity, and reliability and can perform measurements in specific-sites and in real-times. Research and development work for fiber optic sensors is generally composed of four major steps: 1) selection and characterization of the selective chemical sensitive material, such as polyaniline and polypyrrole, 2) design of the optical fiber sensing element, 3) development of optical fiber modification process and 4) fiber optic sensor characterization and optimization. [168]

Evanescent wave absorption spectroscopy is an effective sensing technique more often employed with fiber-optic chemical sensors. [170] A sensor utilizing evanescence is configured so that light propagates within the fiber core and an evanescent field

penetrates into the sensing region. The evanescent absorbance sensitivity depends upon the exposed length of fiber and the penetration depth of the evanescent field. [171-173] Fiber optic evanescent sensors are not widely commercialized yet primarily due to the difficulties in handling bare fibers and the need for custom sample cell fabrication. [174]

In most of the recently reported optical fiber chemical sensors the interaction of a chemical species diffused or trapped into the cladding layer of an optical fiber with the evanescent wave of light guided inside the optical fiber has been detected as a sensing signal. [173, 175-177] In these sensors, in order to bring the analyte molecules from the sample into the evanescent wave field of an optical fiber, the sample has to be directly in contact with the cladding of the optical fiber during the sensing process. When a conventional optical fiber is used to fabricate an evanescent wave based optical sensor, the jacket of the fiber has to be removed for the sample to contact with the cladding layer. However, the length of the exposed sensing region is limited by the fragility of conventional optical fibers. This is a significant limitation because the sensitivity of an evanescent wave sensor usually increases linearly with the transducer length.

5.5 Capillary Sensors

Capillary tubing with waveguiding capabilities can also be used in optical sensing applications. A capillary waveguide serves as a long path length cell with a small but well defined volume and is capable of sampling liquids or gases. The self contained and protected inner sample volume can be probed along the entire capillary length. Capillary waveguides can also be coupled to existing detectors, commercial instruments and inexpensive light sources. Generally capillaries functioning as optical

waveguides are in two categories, based upon their light guiding and sensing properties. The first type is referred to as a liquid core waveguide (LCW), which provides increased sensitivity in the detection because the light can travel directly through the solution filled capillary over long pathlengths. [178] The second type of capillary waveguide has light propagation restricted to the wall and employs evanescent absorbance as a method to probe the inner surface of the capillary. [179, 180] Glass capillaries can serve as a substrate for physical adsorption of chemically sensitive coatings or covalent immobilization of reagents in the designing of evanescent sensors. [181] The function of the capillary depends upon the waveguide structure and the refractive index of the medium filling the capillary core. [182]

Recently a new type of fiber optic capillary has become commercially available. The construction and chemistry of these capillaries are very similar to the fused silica capillaries described in Chapter 3. FOCaps are specifically designed for evanescent sensing but can also operate as a liquid core waveguide when filled with high refractive index solvents.

There are still few examples of capillary waveguides used as evanescent sensors. A short glass capillary was used as an evanescent wave sensor for ammonia after coating the inner surface with a vapor sensitive dye. [183] FOCap sensors or optrodes with inner coating for absorbance and fluorescence sensing of gases have also been developed. [184] However, these waveguides do not use evanescent sensing and instead operate by allowing light to propagate from the capillary wall into the gas sensitive inner coating.

The FOCap has a fused silica wall with a doped fused silica cladding and a polyimide outer coating. (see Figure 5.3) This type of waveguide is ideal for evanescent

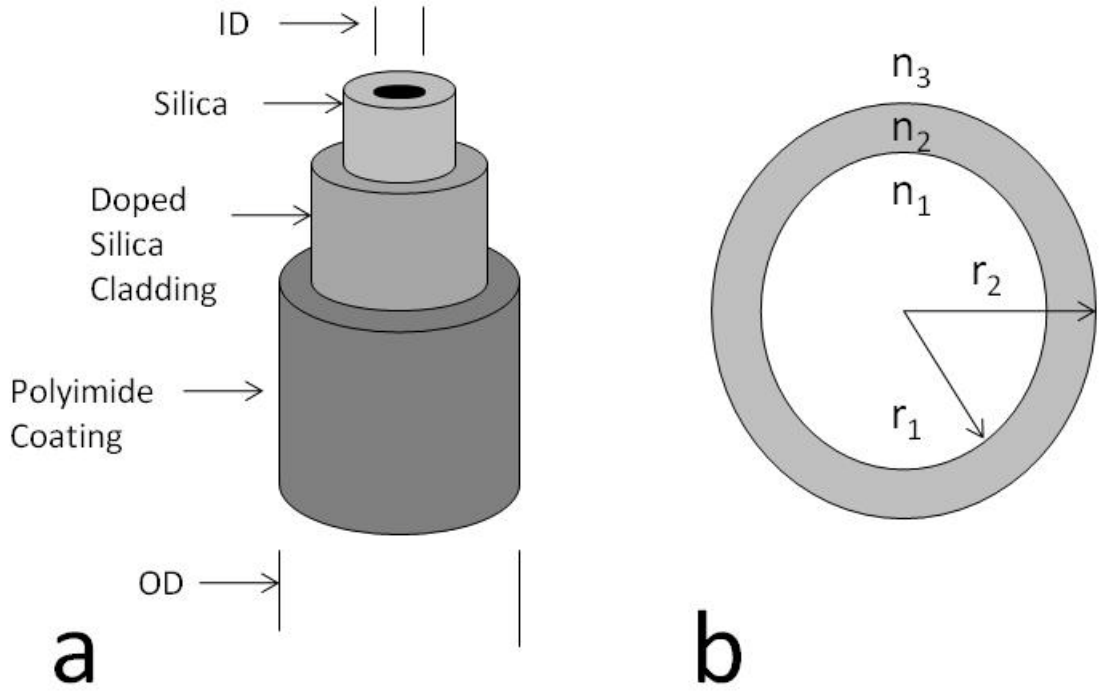

Figure 5.3 a) Schematic of Fiber optic capillary b) Front face geometry of FOCap composed of three regions having refractive indices n_1, n_2, and n_3. The core has a radius r_1 and the outer wall radius r_2. The clad layer n_3 is considered to be infinitely thick in regards to light guiding properties.

sensing because light propagation is confined to the capillary wall when the core is filled with solution with refractive index below that of the cladding. For a detailed description of the light guiding properties in FOCaps see Keller *et al.* [174] Because of the FOCap properties these capillaries are best adapted to evanescent monitoring of immobilized chemistries along the inner capillary wall. The evanescent penetration of the electric field of light into the FOCap core has an amplitude E that decreases exponentially from a maximum of E_0 with decreasing radial distance (r_1) from the center of the capillary (Figure 5.2). The depth of penetration d_p in Equation 5.1, is the radial distance from the

wall and into the core where the E-field amplitude reaches e^{-1} of the maximum. Equation 5.1 shows that d_p increases with wavelength λ and decreases with lower launch angles θ:

$$d_p = \frac{\lambda}{2\pi(n_1^2 \sin^2\theta - n_2^2)^{1/2}} \qquad (5.1)$$

where n_2 and n_1 correspond to the refractive indices of the capillary wall and core, respectively.

The sensor described here utilizes a similar sensing chemistry and protocol to the previously reported systems described above, but was designed with specific differences that were anticipated to improve the performance. The sensor is a fiber optic based enzyme biosensor in which flourescein isothiocyanate (FITC)-labeled AChE is immobilized on the inner walls of a FOCap. The optical signal resulting from the pH decrease caused by the hydrolysis of acetylthiocholine was monitored, as was the effect of treatment with AChE inhibitors.

The current project is an effort to improve detection of organophosphate nerve agents over similar sensing schemes reported previously by using a recombinant AChE (rAChE) and evanescent spectroscopic detection in a fiber optic capillary. The rAChE offers benefits over commercially available AChE in that it more closely resembles human AChE and has fewer impurities. [185] The capillary waveguide serves as a long path-length cell with a small but defined volume that can be easily coupled to inexpensive light sources, detectors and existing commercial instruments. [174, 186, 187] The hypotheses are that the improved enzyme activity of the rAChE, along with the improved sensing capabilities of the capillary fiber optic sensors, will improve detection limits and sensor robustness. This technology also has the possibility to be adapted to provide small hand held sensors for field applications.

5.6 Experimental

5.6.1 Enzyme Attachment Chemistry

In order for the fiber optic capillary sensor to function effectively, the enzyme must be permanently attached to the inner surface of the capillary while maintaining enzyme activity. Different attachment chemistries were investigated to determine if higher enzyme activity or loading could be achieved by alternate attachment methods. The chemistries studied to activate the surface for enzyme immobilization were: 1) aminopropyltrimethoxy silane (APTS), glutaraldehyde; 2) 3-Mercaptopropyl trimethoxy silane (MPTS), N-γ-maleimidobutyloxy succinimide ester (GMBS); 3) APTS, glutaraldehyde, PAMAM generation 4 dendrimer, glutaraldehyde; 4) Glycidoxypropyl trimethoxy silane; 5) trichlorochloropropyl silane (TCCPS), polyallylamine (PAA), glutaraldehyde; 6) N,N'-carbonyl diimidazole (CDI), polyamidoamine (PAMAM) dendrimers, glutaraldehyde. Figure 5.4 shows the main attachment chemistries used to immobilize AChE.

Initial experiments were conducted using Nucleosil 1000-10 silica particles (Macherey-Nagel, Germany) as a high surface area model of the capillary surface. A common wash procedure was used to clean and rinse the silica particles before chemical modifications. Particles were placed in a 10 mL test tube, a known quantity of wash solvent or solution was added, and the tube was vortexed for 30 seconds. The tube was then sonicated for the reported period of time in a small bench-top sonicator (Branson, Danbury, CT) and centrifuged for 5 minutes. The supernatant wash solution was then decanted and discarded.

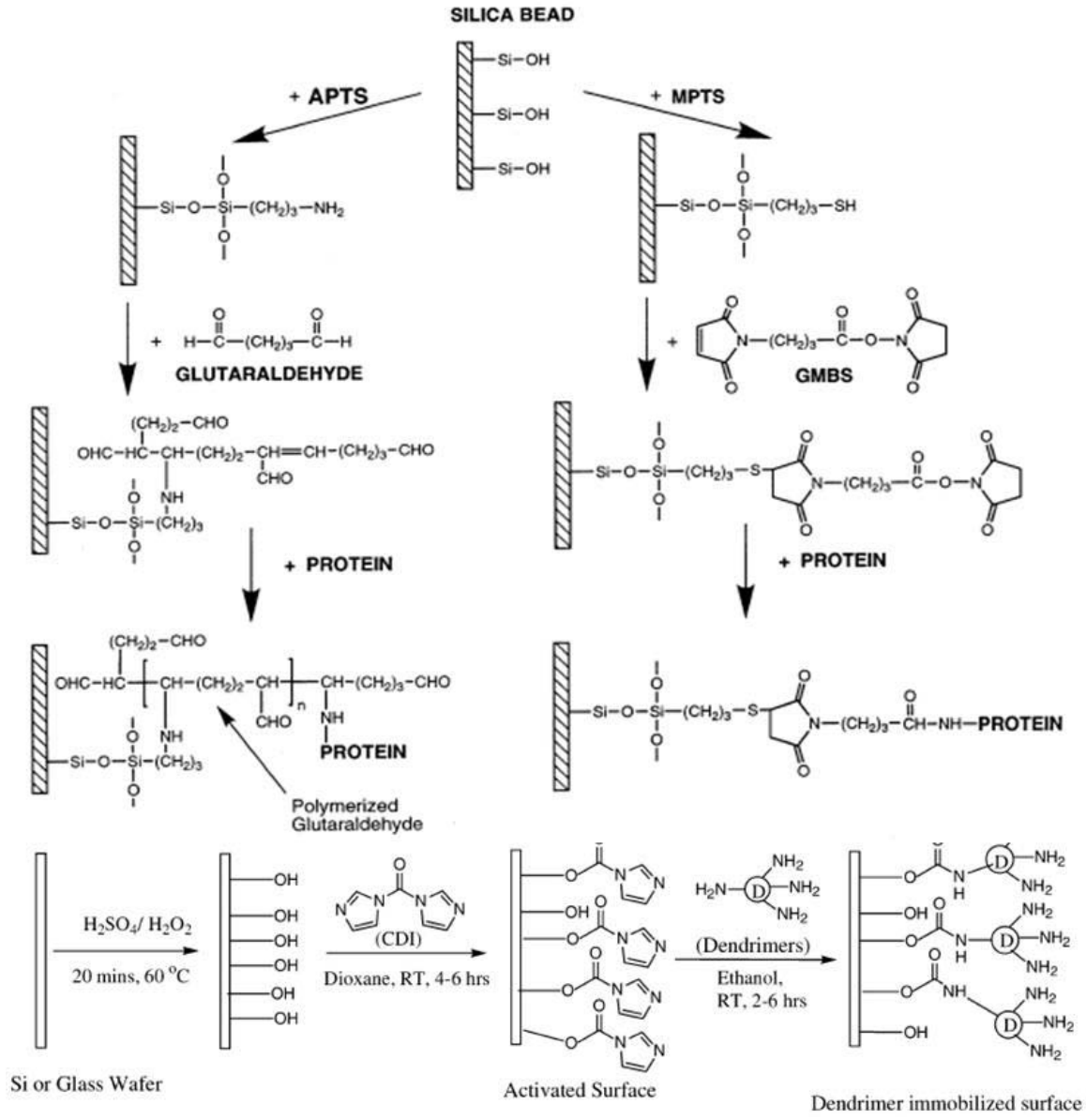

Figure 5.4: Main attachment chemistries used to immobilize AChE on silica surface

Silica particles were cleaned prior to modification. Silica (300mg) was washed with 5mL of MeOH (Acros) with 15 minutes of sonication. The particles were then washed with 5mL distilled deionized water without sonication. This wash process was repeated for a total of three times. Five mL of DI was added and the system was

vortexed for 30s and heated in boiling water for 15min. The particles were then centrifuged for 5min, and the supernatant decanted. Five mL of 10% hydrogen peroxide was added and the suspension was heated in boiling water for 1h. The particles were then centrifuged for 5min and the supernatant decanted. The particles were washed three times with 5mL DI as described above. Methanol was added (5mL), the suspension was vortexed for 30s, and heated in boiling water to evaporate the MeOH. Then the particles were placed in a 140ºC oven until they were ready to be used.

Treatment with APTS: A 10% APTS solution was prepared by diluting 95% 3-aminopropyltrimethoxy silane (Acros) in DI and adjusting the pH to 7.0 using glacial acetic acid. 200mg of Nucleosil 1000-10 silica particles were placed in a 10mL test tube and 5mL of 10% APTS solution were added. The tube was sonicated for 10min and stirred using a hotplate in an 80ºC water bath for 3h. The modified particles were washed three times with 5mL DI, without sonication.

Treatment with glutaraldehyde: A 10% glutaraldehyde solution was prepared by adding 100mL 50% glutaraldehyde (Sigma) to 400mL DI. Five mL of this 10% glutaraldehyde solution was added to the particles and stirred for 1h at room temperature. The modified particles were then washed three times with 5mL DI without sonication.

Treatment with MPTS: All the materials were placed inside a glove bag and the glove bag was flushed three times with nitrogen. A 10mL test tube was loaded with 200mg of silica particles and 5mL of low water toluene (J.T. Baker) and the tube was sonicated for 10min. (3-mercaptopropyl)trimethoxy silane (MPTS, 100μL) was added and the solution stirred for 2h at room temperature. The mixture was then removed from

the glove bag, centrifuged for 5min and the supernatant decanted. The particles were washed with 5mL toluene with 30 s of sonication, and then washed with 5 mL of ethanol with 30s of sonication.

Treatment with GMBS: A GMBS solution was prepared by adding 3mg N-γ-maleimidobutyryloxy succinimide ester (GMBS) to 5mL MeOH. The GMBS solution (5mL) was then added to the MPTS modified particles and the suspension was stirred for 1h at room temperature. The modified particles were washed twice with 5mL EtOH without sonication.

Treatment with PAMAM: A 1% PAMAM solution was prepared by adding 0.5mL 10% PAMAM generation 4 solution (Sigma) to 4.5mL EtOH. Five mL of this 1% PAMAM solution was added to and the suspension was stirred at room temperature for 24h. The modified particles were washed three times with 5mL EtOH without sonication. Five mL of the 10% glutaraldehyde solution was added to the particles and stirred for 1h at room temperature. The modified particles were washed three times with 5mL DI without sonication.

Treatment with CDI: A 110mM solution of 1,1'-carbonyldiimidazole (CDI) was prepared by adding 88.8mg of CDI to 5mL dioxane (Mallinckrodt). A 10mL test tube was charged with 200mg of silica particles and 5mL of CDI solution and the suspension was stirred for 24h at room temperature. The modified particles were washed twice with 5mL EtOH without sonication.

Treatment with GPTMS: A 10% GPTMS solution was prepared by diluting 95% γ-glycidoxypropyltrimethoxy silane (Acros) in DI. A 10mL test tube was charged with 200mg of silica particles and 5mL 10% APTS solution was added. The suspension was

sonicated for 10min and stirred in 80ºC water bath for 3h. The modified silica was washed three times with 5mL DI without sonication.

Treatment with TCCPS: A 1% TCCPS was prepared by adding 50μL trichlorochloropropyl silane (TCCPS, 95% Sigma) to 5mL of hexane. A 10mL test tube was charged with 200mg of silica particles and 5mL 1% TCCPS solution, flushed with N_2, covered with parafilm and stirred for 24h. The modified particles were washed twice with 5mL hexanes without sonication.

Treatment with PAA: 4.5mL of 15% polyallylamine (PAA, Summit Chemicals, NJ) and 0.5mL MeOH were added and the tube was placed in 70ºC water bath for 48h. The modified particles were washed two times with DI, once with 4N NH_4OH, two more times with DI and once with MeOH once, without sonication.

Attachment of AChE: In each case the final modification of particles with AChE was carried out by addition of 3mL of 100mM phosphate buffered saline (PBS) (Sigma) and 100μL of 0.25mg/mL AChE (Sigma) or 0.05mg/mL rAChE (provided by Katie George, University of Montana) to the pretreated particles and the suspension was placed on vertical shaker for 17h in a cold room (4°C). After AChE attachment, the particles were separated from the modification solution by vacuum filtration and 3 mL of PBS was added to each sample for testing using Ellman's method. All AChE modified particles were and stored in PBS at 4°C

In order to evaluate each attachment chemistry the enzyme kinetics for AChE immobilized on silica beads was measured using Ellman's method. [188] Using an Agilent 8453 UV-Vis instrument with biochemical analysis software the initial rate was determined for various acetylthiocholine iodide (ATChI) substrate concentrations (0-

1mmol). These data were then entered into Sigma Plot and were fit to the Michaelis-Menton equation. The kinetics of enzyme catalyzed reactions are generally governed by the Michaelis-Menton equation as follows:

$$v_0 = \frac{V_{max}[S]}{K_m + [S]} \qquad (5.2)$$

where v_0, [S], V_{max}, and K_m represent the initial rate of product generation, the substrate concentration, the maximum rate and the Michaelis-Menton constant, respectively. Lower values of K_m indicate higher enzyme activity and high V_{max} indicate more enzyme present on the silica beads.

5.6.2 FOCap Measurements

Based on the results of the bead study, APTS was chosen as the preferred AChE attachment chemistry because it was the simplest chemistry and achieved comparable AChE activity and load. The attachment chemistry was adapted from that detailed in section 5.4.1. A 2m section of ID_{50} FOCap was filled with a 10% APTS solution and the ends of the capillary were sealed with an acetylene/house gas torch and the capillary was placed in an 80°C water bath for 3h. The FOCap was then flushed with air, 500μL DI, air and then filled with a 10% glutaraldehyde solution and allowed to react for 1h at room temperature. The FOCap was then flushed with air, 500μL DI, and air and then filled with a 0.25mg/mL AChE (type V-S from Sigma) solution and placed in a refrigerator @ 4°C for 18h. A fluorescein isothiocyanate (FITC) or 6-(fluorescein-5-carboxamido)hexanoic acid,succinimidyl ester (SFX) solution was prepared by adding a small amount of FITC or SFX (Invitrogen) to 3mL of 100mM bicarbonate buffer. The FITC concentration was determined by measuring the absorbance at 484nm of 10mL of

FITC solution in 3mL PBS, and calculating the concentration using Beer's Law with the absorption coefficient 72,200 $M^{-1}cm^{-1}$. The AChE modified FOCap was flushed with air, 500μL PBS, air and then filled with the FITC solution and placed in the refrigerator @ 4°C for 6h. Finally the FOCap was flushed with air, 500μL PBS, and air and then filled with PBS and stored at 4°C.

Each FOCap containing immobilized FITC-modified enzyme was connected to an Agilent 8453 UV-Vis instrument using a fiber optic coupling device described in detail by Keller *et al.* [174, 187] The coupling device consisted of a commercial support (Custom Sensors and Technology, Inc.) mounted on the UV-Vis instrument that transmitted the light through fiber optics which were connected at the opposite ends to Upchurch Scientific "T" connectors. Each "T" connector had an optical fiber from the instrument in one end and the FOCap mounted directly across from the fiber. The third, perpendicular, "T" connection was connected to a syringe pump at the inlet of the FOCap and to a waste container via tubing at the opposite end, allowing solution to be pumped through the FOCap. All measurements on modified capillaries were blanked against unmodified FOCaps before measurements were taken.

To determine if there was a difference between the absorbance spectrum from FITC or SFX two capillaries were modified as described in the preceding paragraphs where one was modified with FITC and the other was with SFX. Each capillary was connected to the UV/Vis instrument using the connecter described above, flushed with 500mL buffer, and then filled with 50mM PB pH 7.2. The absorbance spectra were then measured and compared. The process was repeated by filling capillaries with 50mm PB at pH 8, 7, 6.5, and 6 and the absorbance spectrum was measured.

Modified capillaries were flushed with 50mM pH 7.5 PBS for 10min. The capillary was then flushed with 500μL 50mM pH 7.5 PBS, the flow was stopped and the absorbance of FITC was measured at 494nm for 3min. The change in absorbance resulting from any pH change over the first 30s was calculated and this was considered the initial rate. This process was repeated using 500μL of ATChI solution with known concentrations from 0.1-25mM. Each measurement was repeated three times.

The response of the sensor was determined using fresh AChE/FITC modified FOCaps. A 5mM solution of ATChI was flushed through the capillary, the flow was stopped and the absorbance was monitored at 494nm for 30s and repeated three times. Next the capillary was flushed with a 0.5mM 2-PAM, the flow was stopped and the change in absorbance was monitored again. After conducting the measurements in the absence of inhibitor, nerve agent mimics DFP (10μM and 50nM) and paraoxon (5.65μM and 1.15μM) were flushed through the capillary and the flow was stopped for 5min. Then 500μL of 5mM ATChI were flushed through the FOCap, the flow was stopped, and the absorbance was measured for 3min. The measurement was repeated three times. Capillaries were then exposed for 5 minutes to 0.5 mM 2-pyrimidine aldoxime methiodide (2-PAM, which reactivates AChE), and the ATChI measurements were repeated.

5.7 Results

5.7.1 Immobilized Enzyme Activity

To study the various attachment chemistries silica beads were employed as a model surface. Silica beads have the same surface chemistry as silica capillaries but

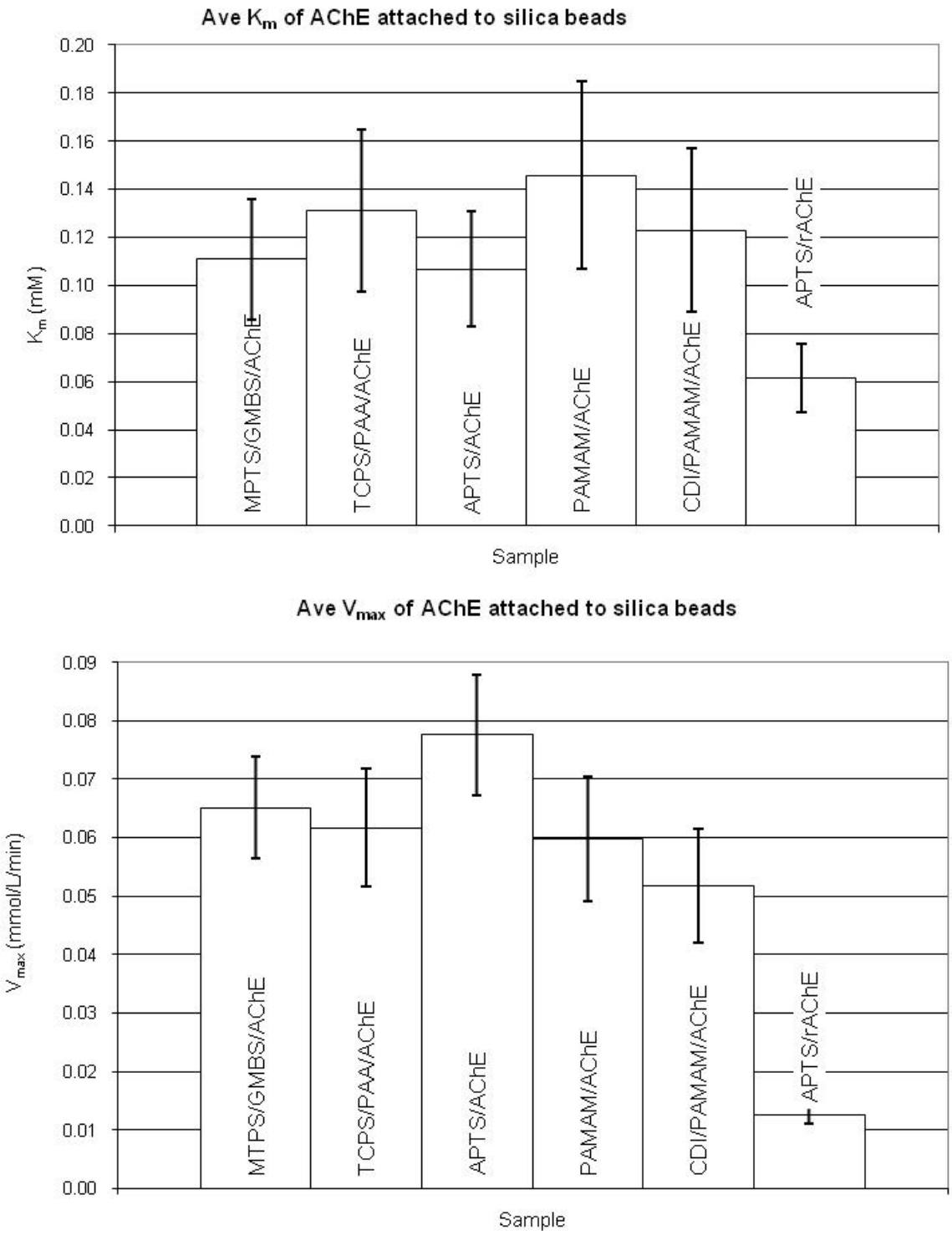

Figure 5.5: Measured K_m and V_{max} values for AChE bound to silica gel. Abbreviations same as in section 5.4.1

have a much higher surface area and therefore more enzyme can be loaded onto the surface. Several methods were attempted to determine the amount of AChE immobilized on the silica surface. However, each method encountered interferences from either the silica beads themselves or with the attachment chemistry and thus no direct measurement of AChE loading on the silica beads was possible. Therefore, to study the immobilized enzyme we employed Ellman's method for measuring AChE activity. Figure 5.5 presents the results comparing various immobilization chemistries for AChE, and for a single immobilization chemistry for the rAChE, on silica particles.

The attachments via GPTMS, and CDI did not give measurable enzyme activities and the results are not presented. Possible explanations for these results will be discussed in the following section. The K_m values of all of the chemistries tested were within one standard deviation of each other, as were all of the V_{max} values except that for the recombinant AChE. The reproducibility of kinetic results for each sample of modified silica was good as indicated by R^2 values greater than 0.95 of the Michaelis-Menten plots, but the reproducibility between samples was not as good. This is likely due to poor reproducibility in the immobilization of the enzyme and may have resulted from varied fractions of the enzyme attaching to the silica in orientations that limit access to the active site. No statistically significant differences ($p \leq 0\ .05$) in K_m or V_{max} were observed as a function of immobilization chemistry. V_{max} is significantly lower for the rAChE than for the AChE ($p \leq 0.05$). The ratio of V_{max}/K_m can be used as a measure of enzyme efficiency. [189, 190] A larger ratio of V_{max}/K_m indicates a faster reaction at low substrate conditions. The efficiency of the enzyme is ultimately limited by the rate

of diffusion of the substrate to the enzyme, thus the diffusion of substrates sets an upper limit.

Table 5.1: Results from enzyme attachment experiments

Table 5.1	K_m (mM)	V_{max} (mM/min)	V_{max}/ K_m
APTS/AChE	0.12 ± .03	.081 ± .011	.69 ± .19
PAMAM/AChE	0.14 ± .03	.059 ± .008	.42 ± .09
MPTS/GMBS/AChE	0.11 ± .03	.065 ± .010	.59 ± .18
TCPS/PAA/AChE	0.10 ± .03	.053 ± .008	.51 ± .16
APTS/rAChE	0.07 ± .02	.018 ± .002	.28 ± .08
CDI/PAMAM/AChE	0.12 ± .04	.052 ± .011	.43 ± .17

Although the recombinant AChE had a K_m value equal to or less than the commercial AChE, it had the lowest V_{max} and efficiency values. The limited supply of this recombinant enzyme meant that only a very small amount was available to be immobilized on the silica particles. More tests with greater quantities of rAChE would be needed to determine if this was the cause of the low V_{max} value, which is five times lower than the other V_{max} values. The lower efficiency for this enzyme is somewhat surprising, and the cause of this result is not immediately clear. However, due to the high cost and long production time of the recombinant AChE further tests are not possible at this time. All further experiments were performed with AChE purchased from Sigma.

It was anticipated that immobilizing PAMAM dendrimers or polyallyl amine (PAA) on the surface would allow a higher loading of enzyme on the silica beads and would result in higher V_{max} values. However, the results indicate that there is no significant increase in the amount of active enzyme immobilized using these

chemistries. Both PAMAM immobilization approaches yielded lower efficiency values, although these results are not significant at 95% confidence.

Overall, since there are no statistically significant differences in the enzyme activities, it seemed appropriate to use the simplest immobilization chemistry for further studies. The efficiency for the APTS immobilization chemistry is equal to or greater than the other immobilization chemistries and therefore this was selected as the preferred immobilization chemistry for use in future experiments.

5.7.2 AChE-FITC on FOCaps

Silica FOCaps were modified first with APTS, glutaraldehyde, and AChE as described in section 5.3.2. AChE modified surfaces were then modified with FITC or SFX (Figure 5.6). No differences were observed between the spectra of FITC or SFX bound to AChE, as shown in Figure 5.7. The capillaries were filled with phosphate buffer at different pHs and the UV/VIS spectrum was measured via a UV/VIS-fiber optic coupler using evanescent wave absorption spectroscopy. The results can be seen in Figure 5.8, and show that as the pH decreases so does the absorbance signal at 494nm. Therefore, by monitoring the absorbance at 494nm, it is possible to detect changes in pH inside the capillary. [8]

Figure 5.9 shows the dependence of the change in absorbance vs. the ATChI concentration for three capillaries modified as described in section 5.3.2. The results were measured in change in absorbance and thus the signal is negative because the signal at 494nm decreases as the pH decreased from acetic acid produced. Based on

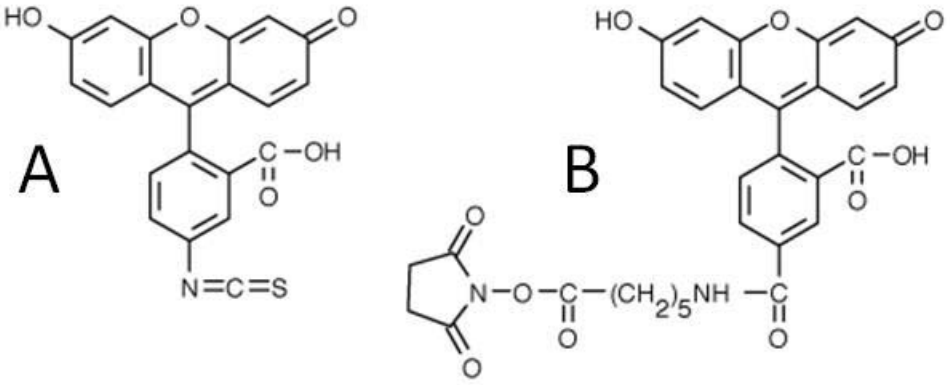

Figure 5.6: Structures of A) fluorescein-5-isothiocyanate 'Isomer I' (FITC) and B) 6-(fluorescein-5-carboxamido)hexanoic acid (SFX)

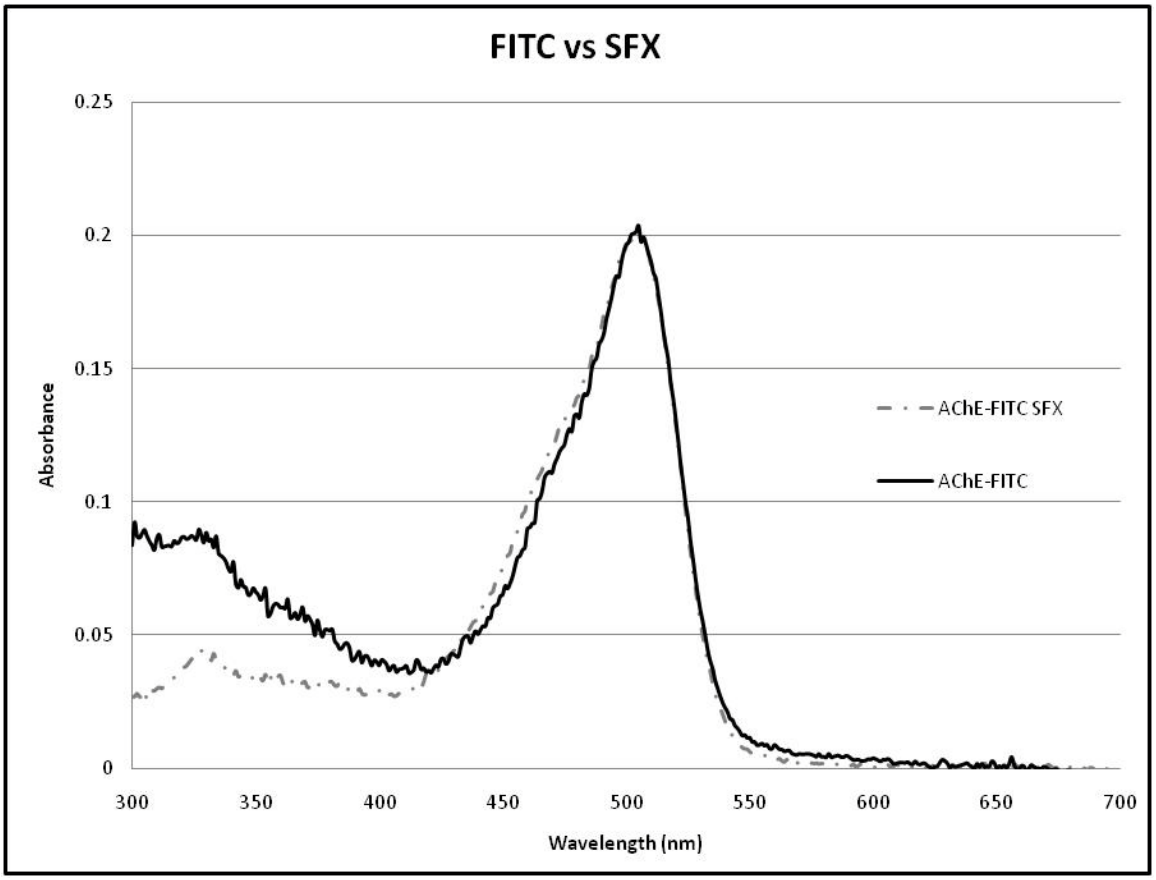

Figure 5.7: Comparison of evanescent absorbance spectrum from two capillaries modified with different fluorescein probes as described in section 5.5.2. Both were modified with APTS, then enzyme was bound using glutaraldehyde. The immobilized enzyme was then modified with fluorescein probe. The solid black line represents FITC and the dashed gray line represents SFX.

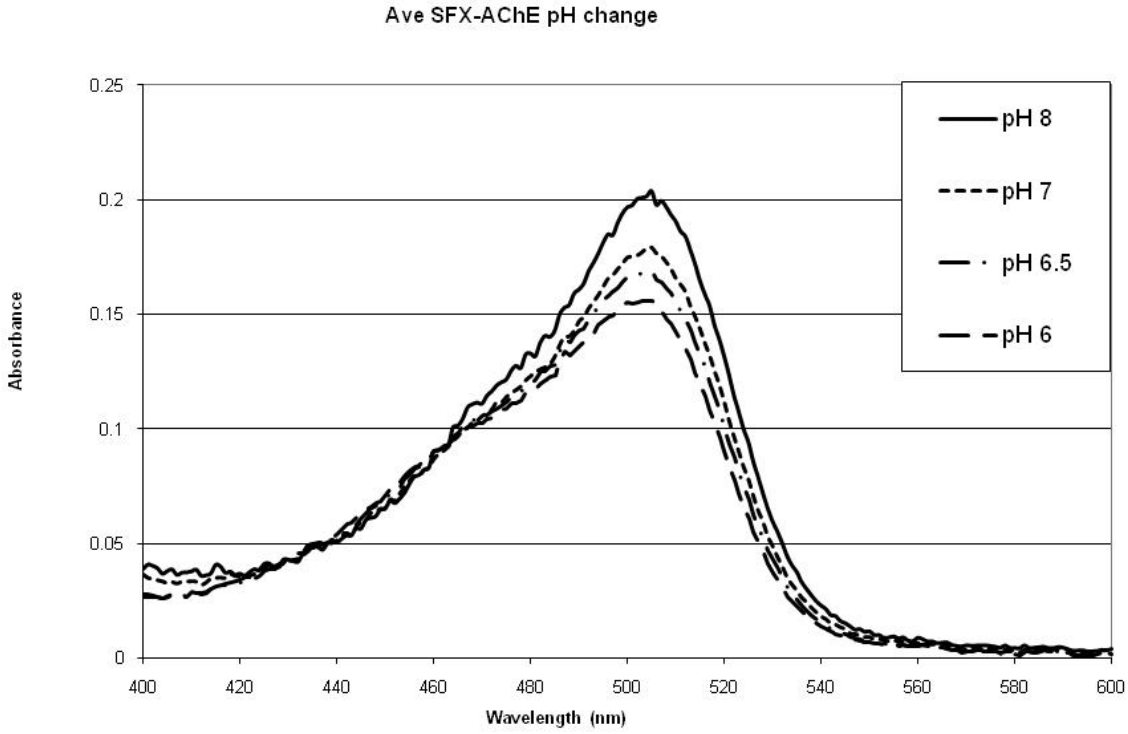

Figure 5.8: Change in absorbance spectrum of AChE-6-(fluorescein-5-carboxamido)hexanoic acid,succinimidyl ester(SFX) cap in PB at different pH's as described in section 5.5.2

these results 5mM ATChI was chosen as the ATChI concentration for future experiments because it gave a large and reliable change in signal.

5.7.3 Exposure of AChE-FITC Capillaries to Paraoxon and DFP

These experiments were conducted to determine whether paraoxon or DFP (Figure 5.10), which are known inhibitors of AChE and are used as warfare agent surrogates, could be detected with this system. Experiments showed that exposure of the AChE/FITC modified capillary to paraoxon or DFP inhibits the activity of the enzyme and generates a detectable difference in optical response.[143, 147] This response was characterized in an AChE-FITC modified capillary.

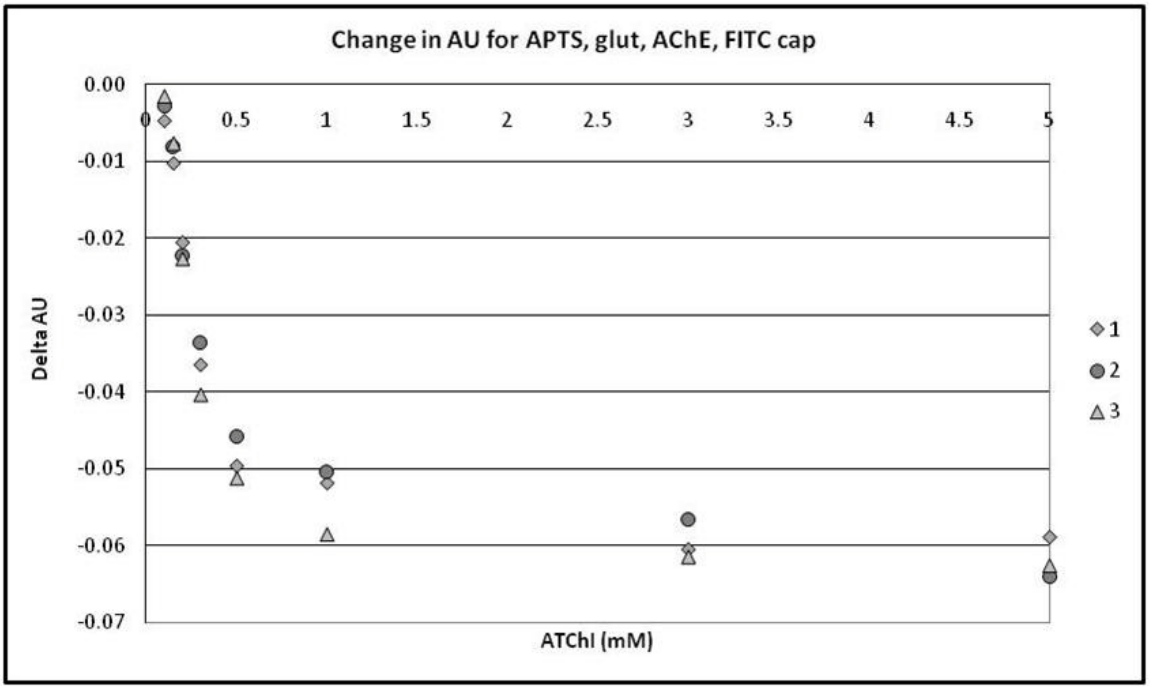

Figure 5.9: Change in absorbance over 30 s vs ATChI concentration for 3 capillaries modified using the same synthesis of APTS, glut, AChE, FITC. Capillaries in pH 7.5 PBS, measured at 494nm, as described in section 5.5.2

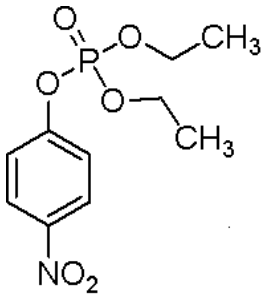

Left:
Paraoxon

Right: DFP

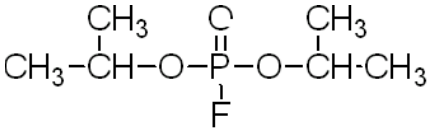

Figure 5.10 Structures of the nerve agent mimics paraoxon and DFP.

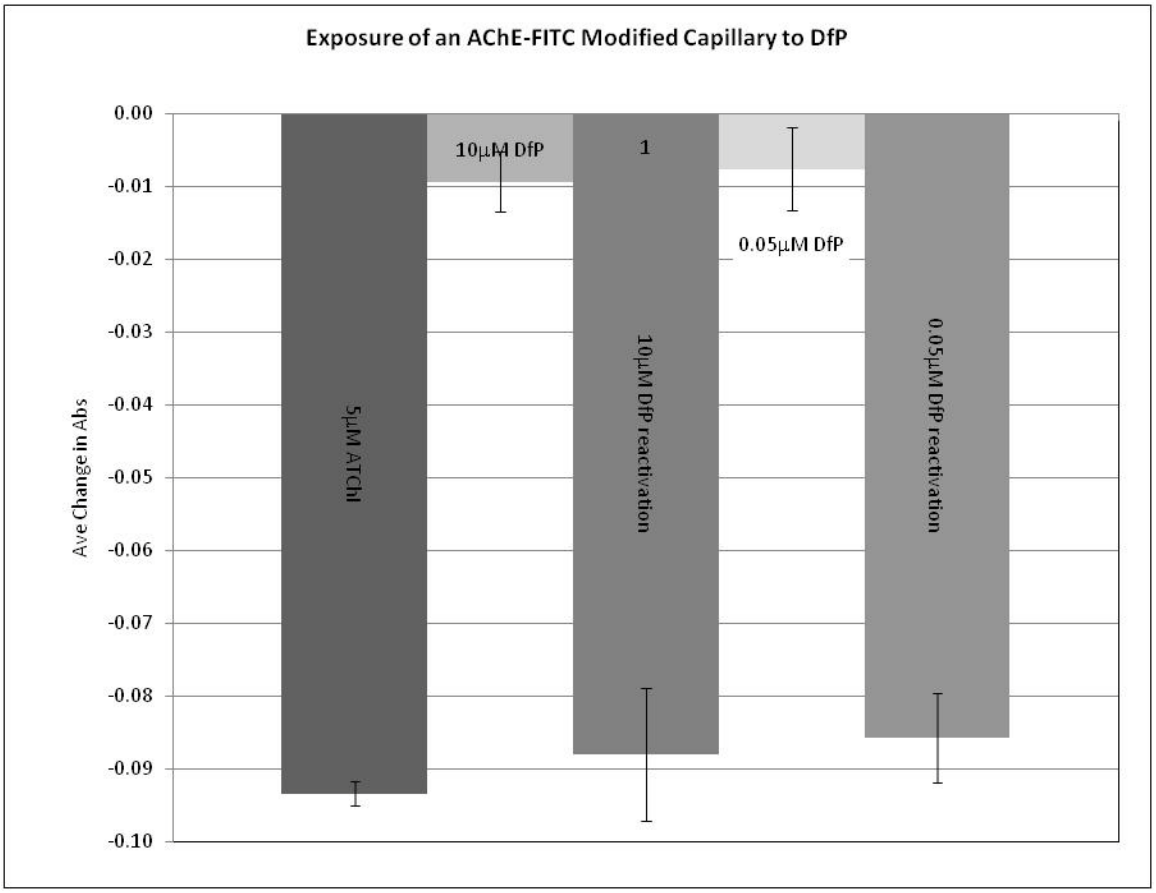

Figure 5.11: Average of three runs on the exposure of an AChE-FITC modified capillary to DFP and reactivation using 2-PAM, as described in section 5.5.2

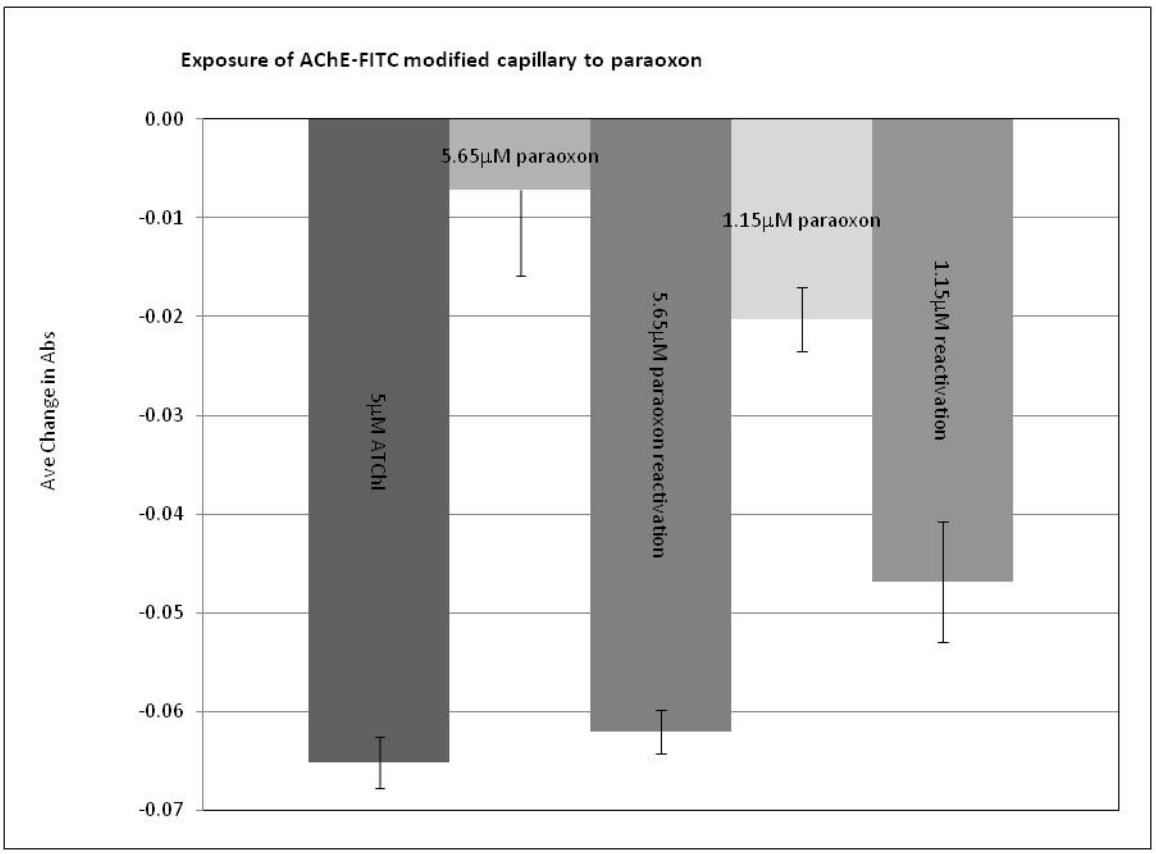

Figure 5.12: Average of three runs on the change in absorbance after exposure of an AChE-FITC modified capillary to paraoxon and reactivation using 2-PAM, as described in section 5.5.2

The exposure of the capillary to 2-PAM showed no change in the FITC spectrum. The results in Figure 5.11 show that exposure of the capillary to 10μM concentrations of DFP produced reduction in the signal of 99.1%, which indicates essentially no AChE activity. After exposure to 2-PAM the signal was restored to 94.2% of its original value. 0.05μM DFP also decreases the change in absorbance by 99.1%, and exposure to 2-PAM again restored signal to 91.8% of its original value, indicating good reactivation. This demonstrates the ability of the FOCap system to detect the

presence of low concentrations of warfare agents and for the system to be regenerated by 2-PAM.

Using the same procedure as above, fresh AChE/FITC FOCaps were generated and exposed to paraoxon. Examining the data from Figure 5.12 we see that the measured change in absorbance after exposure to 5μM paraoxon is between 76-89% less than that before any exposure. The FOCap is then exposed to 2-PAM and the signal was regenerated to 85-95% of its original activity. After exposure to 1.15μM paraoxon the change in absorbance was 67.3% lower and the signal was restored to 75.6% after 2-PAM.

Several important conclusions can be made from the data. The sensor does respond to the AChE inhibitors and the signal can be restored using 2-PAM. Each time the signal is regenerated it is somewhat reduced relative to the original or the previous active signal. Perhaps longer exposure to 2-PAM could improve signal regeneration. Both species can be detected at $\leq$ 1μM concentrations using this method. The system is more sensitive to DFP, which was easily detected at 0.05 μM.

5.6.4 Fluorescent Measurements of AChE-FITC Capillaries

Although the sensitivity of this sensor toward more active AChE inhibitors such as VX or tabun would likely be greater, it remains important to explore avenues to improve the sensitivity and reduce the detection limits. One approach to accomplish lower detection limits would be to utilize FITC fluorescence rather than absorbance. The initial sensor concept was to conduct the experiments in the same manner as the UV/Vis experiments above, but monitor the fluorescence signal of FITC inside the FOCaps

using evanescent detection. As it has been demonstrated the conversion of ATChI provides a detectable change in the absorbance spectrum of FITC, it seemed likely that the system could be easily adapted to fluorescence measurements. [117] To do this a Jobin Yvon Fluorolog 3 was equipped with a fiber optic interface which allowed fibers to be coupled to the system in a similar manner to the UV/Vis system. FITC has an absorbance max at 495nm, but 485nm excitation was used because using 495nm excitation caused large amounts of excitation light to appear in the emission spectra. A fluorescence emission spectrum of a blank FOCap was compared to the spectrum obtained from an AChE-FITC modified capillary measured at 485nm excitation, see Figure 5.13. From Figure 5.13 it appears that background emission from the FOCap dominates the emission spectrum in both cases.

The FOCaps have a polyimide coating on the outside of the capillary to make them more physically robust, as described in Chapter 2. The current hypothesis, based in part on work by Eric Paprocki, [191] is that the high background emission we observed is caused by this polyimide coating. The structure of the polyimide used by Polymicro Technologies is proprietary, and therefore we can only speculate at the reason for the emission. Although the exact structure is not known, it can be assumed that it is similar to those presented in Figure 2.1. The material may contain aromatic groups and the functional groups can stack to create very stable charge transfer complexes. The presence of aromatic groups and charge transfer complexes could cause the emission observed in our studies. It is also possible that the emission is from impurities in the polyimide, in the doped fused silica cladding, or in the fused silica itself.

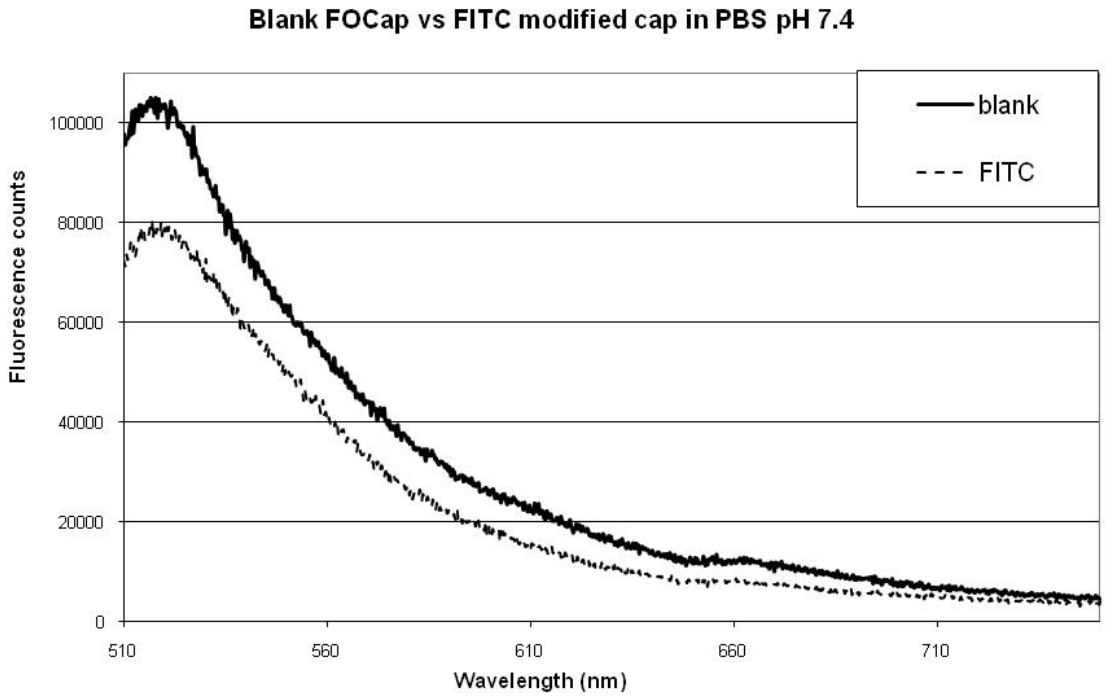

Figure 5.13: Fluorescence of blank (solid line) and AChE-FITC modified (dashed line) FOCaps filled with PBS pH 7.4 using 485nm excitation

This background emission was so high that we were unable to detect or distinguish the FITC spectrum. Various methods were attempted to reduce or remove the background fluorescence, but all proved unsuccessful.

In subsequent work, fluorescein immobilized directly on the surface of FOCaps was detected using evanescent fluorescence techniques. [191] In those studies, FITC was immobilized directly on the capillary wall. The direct attachment may have enhanced the signal relative to the background due to increased loading of fluorescein on the surface and greater proximity of the immobilized fluorescein to the surface, as opposed to the binding of FITC to an enzyme employed in my experiments. Still, background fluorescence from the FOCap was a significant problem in those studies, and reliable measurement of fluorescein fluorescence could only be achieved by

removing the polyimide from the first and last 0.5 cm of the capillary.[196] This resulted in a reduced background emission that could be subtracted from the FITC spectrum to give interpretable results, but rendered the FOCaps fragile and difficult to handle. Additional subsequent experiments have demonstrated successful detection of a fluorescent dye in solution and surface-bound pyrene, without removal of the polyimide coating from the ends of the capillary. [190] In these cases, a significant background emission of 7-10% of the total signal was observed, but this background was reproducible enough that it could be subtracted from the total signal to obtain good results. Although direct quantitative comparisons can not be made, it is thought that the improved signal to background emission in those experiments is likely due to higher signal resulting from higher fluorophore concentrations at the capillary wall, and not due to a lower background signal.

In the configuration described here, the very high level of background emission relative to analytical signal made fluorescent detection of FITC with this system impossible. This problem could be solved by developing and using FOCaps with low background emission, or perhaps by modification of the current capillaries by removal of polyimide from both ends. Alternatively, a pH sensitive fluorescent probe whose emission and excitation are much different from those of polyimide could be employed. However, these options are not currently available or are unpractical, so the future of this sensor will depend on improving the UV/Vis detection method until these technologies become available.

5.7 Discussion

Several chemistries were examined to immobilize AChE on silica surfaces and it was determined that there was no difference in the activity or loading of the main chemistries tested apart from the inactive GPTS and CDI chemistries. The attachments via GPTS, and CDI did not give measurable enzyme activities. One possible explanation could be due to the fact that the linkers between the enzyme and the surface are relatively short and may require the enzyme to deform to bind to the surface. This deformation could result inadequate access to or alteration of the active site and thus result in loss of activity. It might be necessary for the linker to be a certain length to allow immobilization of the enzyme without loss in activity. Another explanation for decreased enzyme activity is that during the enzyme immobilization the attachment occurred in the region near the lip of the gorge as described in section 2.2. If the attachment occurs in this region access to the active site would be severely limited and as described by Radic *et al.* would adversely affect the activity. [107] However, it's not likely that the attachment chemistry would affect the other two sites determined by Radic *et al.* because of the inaccessibility of the active site within the gorge.

It was hoped that a higher activity could be achieved using rAChE, but due to the limited supply available to us full analysis was not possible. For this reason commercially available AChE was used for further experiments. Because there was no significant difference in the attachment chemistry used, APTS/glutaraldehyde was chosen to apply to further experiments because it was the simplest method.

The ATPS/glutaraldehyde chemistry was adapted to FOCaps and then the pH sensitive fluorophore FITC was bound to AChE. In the pH range of this study, the

dianion and monoanion are the main species present and the resulting spectrum is a combination of the two. As demonstrated by Martin *et al.* the monoanion has a much lower absorption intensity than the dianion, therefore when the pH is decreased a decrease in the absorbance intensity occurs. [152]

Solutions of the substrate ATChI could be pumped into the capillary and when the flow was stopped the pH began to decrease due to the buildup of acetic acid. When the activity of the enzyme was interrupted using nerve agent mimics the rate of decrease in the pH was diminished. As demonstrated in Figure 5.9 and 5.10, inhibition of AChE was detected with concentrations as low as 0.05μM DFP and 1μM paraoxon. When these results are compared to the results of others discussed in section 5.1 our results are comparable to the results of Rogers *et al.*, but not as sensitive as Russsell *et al.* and Jin *et al.* The other researchers used fluorescence detection and our results are only preliminary results from absorbance measurements.

It was anticipated that further improvements in detection could be achieved using fluorescence detection. However, it was determined that the polyimide coating on the FOCap caused large background emission in the region that overlapped with the emission of FITC. Future sensors could overcome this problem by using pH sensitive fluorophores that have an absorbance and emission different that of the FOCap. Another anticipated advantage of the FOCap sensor is that increasing the length of the capillary would increase the available signal as demonstrated by Paprocki and Keller. [192]

In conclusion we proved the concept of the FOCap AChE sensor worked well using absorbance, but further improvements in detection could not be accomplished

using fluorescence at this time. However, the technology could provide superior detection limits compared to previously reported sensors discussed above.

Chapter 6: Summary, Conclusion and Future Work

6.1 Summary and Conclusions:

This thesis demonstrated the versatility of silica capillaries and the advantages of using silica capillaries in instruments. The versatility of fused silica capillaries is demonstrated to be a function, in large part, of the ability to chemically modify the silica surface using a variety of chemistries.

In Chapter 5 a sensor was described based on a new technology called FOCaps. These capillaries are manufactured in a similar methods to mass produced capillaries and they can function as long path waveguides. By the chemical immobilization of an enzyme-fluorophore complex on the inner surface of the capillary and flowing a solution of ATChI through the capillary the activity of the enzyme could be monitored. In the presence of an AChE inhibitor, such as a chemical warfare agent, the activity of the enzyme is reduced and the change in activity can be detected. The sensitivity is not as great as some of the published sensors, but we did not achieve fluorescent detection because of high background emission. This background emission was probably related to the polyimide coating on the FOCaps.

Chapter 4 described the chemical modification of silica capillaries to create a permanent, durable, and positively charged surface with advantages for application in capillary electrophoresis. The surface modification is based off work performed by the Rosenberg group for the extraction of metals from waste streams using modified silica particles. They have demonstrated that these chemically modified surfaces can withstand washes of acidic and basic solutions. The chemical modification was adapted for silica capillaries and an additional step was added to methylate the available amines. This

created a permanently positively charged surface that was stable to acidic and basic pH washes. The advantages of such a positively charged surface were demonstrated by the separation of small inorganic anions and cationic species.

6.2 Future Work:

The greatest limitation with the FOCap sensor described is the very high background emission. Research to overcome this problem could advance the sensor technology. Approaches to be considered include reduction of the background emission and/or a change to a fluorophore for which the background emission does not interfere. To reduce the background fluorescence materials other than polyimide should be analyzed as capillary cladding material. The polyimide material fluoresces in the same region that fluorescein does using an excitation wavelength of 485nm. At present time there is not enough fluorescein bound to the surface to overcome the background signal from the polyimide. If the cladding material does not fluoresce between 450-550nm the fluorescence signal from fluorescein should be easily detectable. Another way to improve the fluorescent signal relative to the background would be to select a pH sensitive fluorophore that fluoresces in a region different than polyimide. If the fluorophore emits between 200-450 or 600-800nm it will be in a low background region and thus will be relatively easy to detect. A very important aspect of the fluorophore is that its spectra must be pH dependant. The detection scheme of the sensor functions by the enzymatic production of acetic acid which lowers the pH and the spectrum of fluorescein changes.

Another area that should be investigated is the detection limit achievable with nerve agent mimics using either absorbance or fluorescence monitoring and whether or not the sensor is more sensitive towards any specific mimic. In this project the sensor was expected to detect the signal in fluorescence mode to obtain low detection limits. Studies to detect inhibition in the absorbance mode were considered preliminary and thus the reproducibility and specific detection limits were not determined. To determine the detection limit of nerve agent mimics new capillaries could be prepared as described in section 5.5.2 and then exposed to nerve agent mimics of decreasing concentration until the limit of detection is determined. Different nerve agent mimics could be tested to determine if the sensor has a bias to any specific agent. It would be beneficial to also study the reactivation of AChE with different nerve agents again to determine if there is a bias in the sensor.

The chemically modified capillaries for use in CE could be tested in MEKC systems and in CE-MS applications. In MEKC separations, surfactant micelles are used to create an ionic pseudo-stationary phase which has a non zero velocity. When cationic surfactants are employed, they also create a dynamic coating on the capillary surface and alter the electroosmotic flow resulting in anodic flow. By using the modified capillaries described in Chapter 4 the capillary surface would have a zeta potential determined by the modification chemistry and thus the flow could be controlled independent of the chemistry and structure of the pseudo-stationary phase.

Another promising area for the modified capillaries is use in CE-MS applications. Because of the stability of the capillaries they are an ideal candidate for use

in applications where column bleed from dynamically modified capillaries would cause severe detection interferences.

References:

[1] Dandeneau, R., Bente, P., Rooney, T., Hiskes, R., *American Laboratory* 1979, *11*, 61-62, 64, 66, 68-69.
[2] Dandeneau, R. D., Zerenner, E. H., *HRC & CC*, 1979, *2*, 351-356.
[3] Griffin, S., *LC-GC Europe* 2003, *16*, 276, 280, 282, 284, 286, 288-289.
[4] Novotny, M., *Anal. Chem.* 1978, *50*, 16A-18A, 20A, 22A, 24A, 26A, 28A, 30A, 32A.
[5] Warren, B. E., *Journal of Applied Physics* 1937, *8*, 645-654.
[6] Boksanyi, L., Liardon, O., Kovats, E. S., *Advances in Colloid and Interface Science* 1976, *6*, 95-137.
[7] Hutchins, J. R., III, Harrington, R. V., *Kirk-Othmer Encycl. Chem. Technol., 2nd Ed.* 1966, *10*, 533-604.
[8] Blomberg, L., Widmark, G., *Journal of Chromatography* 1975, *106*, 59-71.
[9] Schomburg, G., Husmann, H., Weeke, F., *Journal of Chromatography* 1974, *99*, 63-79.
[10] Grob, K., *Helvetica Chimica Acta* 1968, *51*, 718-737.
[11] Grob, K., *Chromatographia* 1974, *7*, 94-98.
[12] Franken, J. J., Trujbels, M. M. F., *Journal of Chromatography* 1974, *91*, 425-431.
[13] Aue, W. A., Hastings, C. R., Kapila, S., *Journal of Chromatography* 1973, *77*, 299-307.
[14] Hishta, C., Bomstein, J., Cooke, W. D., *(New York)* 1970, *9*, 215-242.
[15] Blomberg, L., *Journal of Chromatography* 1975, *115*, 365-372.
[16] Hair, M. L., Filbert, A. M., *Research/Development* 1969, *20*, 34-38.
[17] Hair, M. L., Filbert, A. M., *Research/Development* 1969, *20*, 30-34.
[18] Macomber, J., Stasiak, D., *LCGC North America* 2008, 63.
[19] Carman, P. C., *Transactions of the Faraday Society* 1940, *36*, 964-973.
[20] Zhuravlev, L. T., Kiselev, A. V., Naidina, V. P., Polyakov, A. L., *Journal of Physical Chemistry* 1963, *37*, 2258-2265.
[21] Davydov, V. Y., Kiselev, A. V., *Journal of Physical Chemistry* 1963, *37*, 2593-2596.
[22] Davydov, V. Y., Kiselev, A. V., Lokutsievskii, V. A., Lygin, V. I., *Journal of Physical Chemistry* 1973, *47*, 809-811.
[23] Chertov, V. M., Dzhambaeva, D. B., Plachinda, A. S., Neimark, I. E., *Journal of Physical Chemistry* 1966, *40*, 520-525.
[24] Lippincott, E. R., Schroeder, R., *Journal of Chemical Physics* 1955, *23*, 1099-1106.
[25] Pimentel, G. C., McClellan, A. L., *The Hydrogen Bond*, 1960.
[26] Davydov, V. Y., Kiselev, A. V., Zhuravlev, L. T., *Transactions of the Faraday Society* 1964, *60*, 2254-2264.
[27] Egorov, M. M., Kiselev, V. F., Krasil'nikov, K. G., *Journal of Physical Chemistry* 1961, *35*, 2234-2240.
[28] Egorov, M. M., Kiselev, V. F., Krasil'nikov, K. G., *Journal of Physical Chemistry* 1961, *35*, 2031-2038.
[29] Snyder, L. R., Ward, J. W., *Journal of Physical Chemistry* 1966, *70*, 3941-3952.
[30] Peri, J. B., *Journal of Physical Chemistry* 1966, *70*, 2937-2945.
[31] Iler, R. K., *The Colloid Chemistry of Silica and Silicates*, 1955.

[32] Stober, W., *Kolloid-Zeitschrift* 1956, *149*, 39-46.
[33] Armistead, C. G., Tyler, A. J., Hambleton, F. H., Mitchell, S. A., Hockey, J. A., *Journal of Physical Chemistry* 1969, *73*, 3947-3953.
[34] deBoer, J. H., Steggerda, J. J., *Proceedings of the Koninklijke Nederlandse Akademie van Wetenschappen, Series B: Physical Sciences* 1958, *61*, 317-323.
[35] Zhuravlev, L. T., Kiselev, A. V., *Journal of Physical Chemistry* 1965, *39*, 453-455.
[36] Basila, M. R., *Journal of Chemical Physics* 1961, *35*, 1151-1158.
[37] Hertl, W., Hair, M. L., *Journal of Physical Chemistry* 1968, *72*, 4676-4682.
[38] Aristov, B. G., Kiselev, A. V., *Journal of Physical Chemistry* 1963, *37*, 2520-2528.
[39] Babkin, I. Y., Kieselev, A. V., *Journal of Physical Chemistry* 1963, *37*, 228-232.
[40] Hair, M. L., Hertl, W., *Journal of Physical Chemistry* 1969, *73*, 4269-4276.
[41] Chiari, M., Nesi, M., Righetti, G., *Capillary Electrophoresis in Analytical Biotechnology* 1996, 1-36.
[42] Desty, D. H., Haresnape, J. N., Whyman, B. H. F., *Anal. Chem.* 1960, *32*, 302-304.
[43] Desty, D. H., *Chromatographia* 1975, *8*, 452-455.
[44] Hjerten, S., *Chromatographic reviews* 1967, *9*, 122-219.
[45] Jorgenson, J. W., Lukacs, K. D., *Anal. Chem.* 1981, *53*, 1298-1302.
[46] Grossman, P. D., Colburn, J. C., Editors, *Capillary Electrophoresis: Theory & Practice*, 1992.
[47] Guzman, N. A., Editor, *Capillary Electrophoresis Technology. [In: Chromatogr. Sci. Ser., 1993; 64]*, 1993.
[48] Jandik, P., Bonn, G., *Capillary Electrophoresis of Small Molecules and Ions*, 1993.
[49] Atkins, P. W., *Physical Chemistry*, 1978.
[50] Adamson, A. W., *Physical Chemistry of Surfaces*, 1967.
[51] Altria, K. D., Simpson, C. F., *Chromatographia* 1987, *24*, 527-532.
[52] Lukacs, K. D., Jorgenson, J. W., *HRC & CC*, 1985, *8*, 407-411.
[53] Jorgenson, J. W., Lukacs, K. D., *(Washington, DC, United States)* 1983, *222*, 266-272.
[54] Giddings, J. C., *Separation Science* 1969, *4*, 181-189.
[55] Jorgenson, J. W., DeArman Lukacs, K., *Journal of Chromatography* 1981, *218*, 209-216.
[56] Jorgenson, J. W., Lukacs, K. D., *Clinical Chemistry* 1981, *27*, 1551-1553.
[57] Rose, D. J., Jr., Jorgenson, J. W., *Anal. Chem.* 1988, *60*, 642-648.
[58] Fujiwara, S., Honda, S., *Anal. Chem.* 1987, *59*, 487-490.
[59] Huang, X., Gordon, M. J., Zare, R. N., *Anal. Chem.* 1988, *60*, 375-377.
[60] Fujiwara, S., Honda, S., *Anal. Chem.* 1987, *59*, 2773-2776.
[61] Terabe, S., Otsuka, K., Ichikawa, K., Tsuchiya, A., Ando, T., *Anal. Chem.* 1984, *56*, 111-113.
[62] Mikkers, F. E. P., Everaerts, F. M., Verheggen, T. P. E. M., *Journal of Chromatography* 1979, *169*, 1-10.
[63] Foret, F., Deml, M., Kahle, V., Bocek, P., *Electrophoresis* 1986, *7*, 430-432.
[64] Prusik, Z., Kasicka, V., Stanek, S., Kuncova, G., *et al., Journal of Chromatography* 1987, *390*, 87-96.
[65] Wang, T., Aiken, J. H., Huie, C. W., Hartwick, R. A., *Anal. Chem.* 1991, *63*, 1372-1376.

[66] Ermakov, S. V., Zhukov, M. Y., Capelli, L., Righetti, P. G., *Journal of Chromatography, A* 1995, *699*, 297-313.
[67] Towns, J. K., Regnier, F. E., *Anal. Chem.* 1991, *63*, 1126-1132.
[68] Nutku, M. S., Erim, F. B., *Journal of High Resolution Chromatography* 1998, *21*, 505-508.
[69] Timerbaev, A. R., *Electrophoresis* 2007, *28*, 3420-3435.
[70] Diress, A. G., Yassine, M. M., Lucy, C. A., *Electrophoresis* 2007, *28*, 1189-1196.
[71] Righetti, P. G., Gelfi, C., Verzola, B., Castelletti, L., *Electrophoresis* 2001, *22*, 603-611.
[72] Kasicka, V., *Electrophoresis* 2001, *22*, 4139-4162.
[73] Horvath, J., Dolnik, V., *Electrophoresis* 2001, *22*, 644-655.
[74] Schwartz, H. E., Wanders, B. J., *Chromatographic Science Series* 1998, *78*, 169-191.
[75] Schomburg, G., *Chemical Analysis* 1998, *146*, 481-523.
[76] Hardenborg, E., Zuberovic, A., Ullsten, S., Soderberg, L., *et al.*, *Journal of Chromatography, A* 2003, *1003*, 217-221.
[77] Doherty, E. A. S., Meagher, R. J., Albarghouthi, M. N., Barron, A. E., *Electrophoresis* 2003, *24*, 34-54.
[78] Spanila, M., Pazourek, J., Havel, J., *Journal of Separation Science* 2006, *29*, 2234-2240.
[79] Figeys, D., Aebersold, R., *Journal of chromatography. B, Biomedical sciences and applications* 1997, *695*, 163-168.
[80] Hjerten, S., *Journal of Chromatography* 1985, *347*, 191-198.
[81] Huang, M., Plocek, J., Novotny, M. V., *Electrophoresis* 1995, *16*, 396-401.
[82] Bruin, G. J., Huisden, R., Kraak, J. C., Poppe, H., *Journal of chromatography* 1989, *480*, 339-349.
[83] Bruin, G. J. M., Chang, J. P., Kuhlman, R. H., Zegers, K., *et al.*, *Journal of Chromatography* 1989, *471*, 429-436.
[84] Towns, J. K., Bao, J., Regnier, F. E., *Journal of Chromatography* 1992, *599*, 227-237.
[85] Smith, J. T., El Rassi, Z., *Electrophoresis* 1993, *14*, 396-406.
[86] Hofstadler, S. A., Swanek, F. D., Gale, D. C., Ewing, A. G., Smith, R. D., *Anal. Chem.* 1995, *67*, 1477-1480.
[87] Monton, M. R. N., Tomita, M., Soga, T., Ishihama, Y., *Anal. Chem.* 2007, *79*, 7838-7844.
[88] Chang, S. H., Gooding, K. M., Regnier, F. E., *Journal of Chromatography* 1976, *120*, 321-333.
[89] Bedia Erim, F., Cifuentes, A., Poppe, H., Kraak, J. C., *Journal of Chromatography, A* 1995, *708*, 356-361.
[90] Cifuentes, A., Poppe, H., Kraak, J. C., Erim, F. B., *Journal of chromatography. B, Biomedical applications* 1996, *681*, 21-27.
[91] Erim, F. B., *Journal of Chromatography, A* 1997, *768*, 161-167.
[92] Erim, F. B., *Microchemical Journal* 1997, *57*, 283-287.
[93] Kocatuerk, N., Oeztekin, N., Bedia Erim, F., *Analytical and Bioanalytical Chemistry* 2003, *377*, 1207-1211.
[94] Nutku, M. S., Berker, F. B. E., *Turkish Journal of Chemistry* 2003, *27*, 9-14.

[95] Nutku, M. S., Erim, F. B., *Journal of Microcolumn Separations* 1999, *11*, 541-543.
[96] Towns, J. K., Regnier, F. E., *Journal of Chromatography* 1990, *516*, 69-78.
[97] Guo, Y., Imahori, G. A., Colon, L. A., *Journal of Chromatography, A* 1996, *744*, 17-29.
[98] Hughes, M. A., Nielsen, D., Rosenberg, E., Gobetto, R., *et al.*, *Industrial & Engineering Chemistry Research* 2006, *45*, 6538-6547.
[99] Nielsen, D. J., 2006, p. 154 pp.
[100] Hughes, M., Miranda, P., Nielsen, D., Rosenberg, E., *et al.*, *Macromolecular Symposia* 2006, *235*, 161-178.
[101] Hughes, M. A., Rosenberg, E., *Separation Science and Technology* 2007, *42*, 261-283.
[102] Rosenberg, E., Hart, C., Hughes, M., Kailasam, V., *et al.*, *Official Proceedings - International Water Conference* 2006, *67th*.
[103] Taylor, P., Div. Pharmacology,California Univ. San Diego,La Jolla,CA,USA. 1994, p. 28 pp.
[104] Koellner, G., Kryger, G., Millard, C. B., Silman, I., *et al.*, *Journal of Molecular Biology* 2000, *296*, 713-735.
[105] Sussman, J. L., Harel, M., Raves, M., Quinn, D., Silman, I., *Jerusalem Symposia on Quantum Chemistry and Biochemistry* 1995, *27*, 455-460.
[106] Sussman, J. L., Harel, M., Raves, M., Quinn, D. M., *et al.*, *Enzymes of the Cholinesterase Family, [Proceedings of the International Meeting on Cholinesterases], 5th, Madras, Sept. 24-28, 1994* 1995, 59-65.
[107] Radic, Z., Pickering, N. A., Vellom, D. C., Camp, S., Taylor, P., *Biochemistry* 1993, *32*, 12074-12084.
[108] Bourne, Y., Taylor, P., Marchot, P., *Cell (Cambridge, Massachusetts)* 1995, *83*, 503-512.
[109] Radic, Z., Taylor, P., *Chemico-Biological Interactions* 1999, *119-120*, 111-117.
[110] Burnworth, M., Rowan, S. J., Weder, C., *Chem.--Eur. J.* 2007, *13*, 7828-7836.
[111] Silver, A., *Frontiers of Biology, Vol. 36: The Biology of Cholinesterases*, 1974.
[112] Stein, K., Schwedt, G., *Anal. Chim. Acta* 1993, *272*, 73-81.
[113] Novak, T. J., Daasch, L. W., Epstein, J., *Anal. Chem.* 1979, *51*, 1271-1275.
[114] Nieuwenhuizen, M. S., Harteveld, J. L. N., *Sens. Actuators, B* 1997, *B40*, 167-173.
[115] Steiner, W. E., Klopsch, S. J., English, W. A., Clowers, B. H., Hill, H. H., *Anal. Chem.* 2005, *77*, 4792-4799.
[116] Sohn, H., Letant, S., Sailor, M. J., Trogler, W. C., *J. Am. Chem. Soc.* 2000, *122*, 5399-5400.
[117] Anis, N. A., Valdes, J. J., Thompson, R. G., Menking, D. E., *et al.*, *Proc. SPIE-Int. Soc. Opt. Eng.* 1993, *1885*, 18-27.
[118] White, B. J., Legako, J. A., Harmon, H. J., *Biosens. Bioelectron.* 2002, *17*, 361-366.
[119] Trettnak, W., Reininger, F., Zinterl, E., Wolfbeis, O. S., *Sens. Actuators, B* 1993, *B11*, 87-93.
[120] Parvari, R., Pecht, I., Soreq, H., *Anal. Biochem.* 1983, *133*, 450-456.
[121] Andres, R. T., Narayanaswamy, R., *Talanta* 1997, *44*, 1335-1352.
[122] Bucur, B., Fournier, D., Danet, A., Marty, J.-L., *Anal. Chim. Acta* 2006, *562*, 115-121.

[123] Navas Diaz, A., Ramos Peinado, M. C., *Sens. Actuators, B* 1997, *B39*, 426-431.
[124] Weetall, H. H., Mishra, N. N., Mahfouz, A., Rogers, K. R., *Anal. Lett.* 2004, *37*, 1297-1305.
[125] Marty, J. L., Sode, K., Karube, I., *Electroanalysis (N. Y.)* 1992, *4*, 249-252.
[126] Snejdarkova, M., Svobodova, L., Evtugyn, G., Budnikov, H., *et al., Anal. Chim. Acta* 2004, *514*, 79-88.
[127] Jin, S., Xu, Z., Chen, J., Liang, X., *et al., Anal. Chim. Acta* 2004, *523*, 117-123.
[128] Vakurov, A., Simpson, C. E., Daly, C. L., Gibson, T. D., Millner, P. A., *Biosens. Bioelectron.* 2004, *20*, 1118-1125.
[129] Vakurov, A., Simpson, C. E., Daly, C. L., Gibson, T. D., Millner, P. A., *Biosens. Bioelectron.* 2005, *20*, 2324-2329.
[130] Danet, A. F., Bucur, B., Cheregi, M.-C., Badea, M., Serban, S., *Anal. Lett.* 2003, *36*, 59-73.
[131] Walker, J. P., Asher, S. A., *Anal. Chem.* 2005, *77*, 1596-1600.
[132] Ivanov, A., Evtugyn, G., Budnikov, H., Ricci, F., *et al., Anal. Bioanal. Chem.* 2003, *377*, 624-631.
[133] Mulchandani, P., Chen, W., Mulchandani, A., *Environ. Sci. Technol.* 2001, *35*, 2562-2565.
[134] Mulchandani, A., Kaneva, I., Chen, W., *Anal. Chem.* 1998, *70*, 5042-5046.
[135] Mulchandani, P., Chen, W., Mulchandani, A., Wang, J., Chen, L., *Biosens. Bioelectron.* 2001, *16*, 433-437.
[136] Schoning, M. J., Krause, R., Block, K., Musahmeh, M., *et al., Sens. Actuators, B* 2003, *B95*, 291-296.
[137] Mulchandani, A., Chen, W., Mulchandani, P., Wang, J., Rogers, K. R., *Biosens. Bioelectron.* 2001, *16*, 225-230.
[138] Heleg-Shabtai, V., Gratziany, N., Liron, Z., *Anal. Chim. Acta* 2006, *571*, 228-234.
[139] Law, K. A., Higson, S. P. J., *Biosens. Bioelectron.* 2005, *20*, 1914-1924.
[140] Simonian, A. L., Good, T. A., Wang, S. S., Wild, J. R., *Anal. Chim. Acta* 2005, *534*, 69-77.
[141] Suwansa-ard, S., Kanatharana, P., Asawatreratanakul, P., Limsakul, C., *et al., Biosens. Bioelectron.* 2005, *21*, 445-454.
[142] de Silva, A. P., Gunaratne, H. Q. N., Gunnlaugsson, T., Huxley, A. J. M., *et al., Chem. Rev. (Washington, D. C.)* 1997, *97*, 1515-1566.
[143] Rogers, K. R., Wang, Y., Mulchandani, A., Mulchandani, P., Chen, W., *Biotechnol. Prog.* 1999, *15*, 517-521.
[144] Cao, X., Mello, S. V., Leblanc, R. M., Rastogi, V. K., *et al., Colloids Surf., A* 2004, *250*, 349-356.
[145] Orbulescu, J., Constantine, C. A., Rastogi, V. K., Shah, S. S., *et al., Anal. Chem.* 2006, *78*, 7016-7021.
[146] Russell, R. J., Pishko, M. V., Simonian, A. L., Wild, J. R., *Anal. Chem.* 1999, *71*, 4909-4912.
[147] Rogers, K. R., Cao, C. J., Valdes, J. J., Eldefrawl, A. T., Eldefrawi, M. E., *Fundam. Appl. Toxicol.* 1991, *16*, 810-820.
[148] Ma Li, Y., Wang Huai, Y., Xie, H., Xu Li, X., *Spectrochim Acta A Mol Biomol Spectrosc* 2004, *60*, 1865-1872.
[149] Forster, T., *Fluoreszenz organischer Verbindungen*, 1951.

[150] Rozwadowski, M., *Acta Phys. Polon.* 1961, *20*, 1005-1017.
[151] Socka, J., *Acta Physica Polonica, A* 1973, *44*, 45-56.
[152] Martin, M. M., Lindqvist, L., *J. Lumin.* 1975, *10*, 381-390.
[153] Dave, K. I., Miller, C. E., Wild, J. R., *Chem.-Biol. Interact.* 1993, *87*, 55-68.
[154] Viveros, L., Paliwal, S., McCrae, D., Wild, J., Simonian, A., *Sens. Actuators, B* 2006, *B115*, 150-157.
[155] Wolfbeis, O. S., Posch, H. E., *Anal. Chim. Acta* 1986, *185*, 321-327.
[156] Stewart, G., Jin, W., Culshaw, B., *Sens. Actuators, B* 1997, *B38*, 42-47.
[157] Chan, K., Ito, H., Inaba, H., *J. Lightwave Technol.* 1984, *LT-2*, 234-237.
[158] Rowe-Taitt, C. A., Ligler, F. S., *Handb. Opt. Fibre Sens. Technol.* 2002, 687-704.
[159] Ferguson, J. A., Boles, T. C., Adams, C. P., Walt, D. R., *Nat. Biotechnol.* 1996, *14*, 1681-1684.
[160] Healey, B. G., Li, L., Walt, D. R., *Biosens. Bioelectron.* 1997, *12*, 521-529.
[161] Barker, S. L. R., Kopelman, R., Meyer, T. E., Cusanovich, M. A., *Anal. Chem.* 1998, *70*, 971-976.
[162] Holst, G., Mizaikoff, B., *Handb. Opt. Fibre Sens. Technol.* 2002, 729-755.
[163] Dietrich, A. M., Jensen, J. N., da Costa, W. F., *Water Environ. Res.* 1996, *68*, 391-406.
[164] Schwotzer, G., Latka, I., Lehmann, H., Willsch, R., *Sens. Actuators, B* 1997, *B38*, 150-153.
[165] Mizaikoff, B., Taga, K., Kellner, R., *Vib. Spectrosc.* 1995, *8*, 103-108.
[166] Anderson, F. P., Miller, W. G., *Clin. Chem. (Winston-Salem, N. C.)* 1988, *34*, 1417-1421.
[167] Ribeiro, A. B. L., Jackson, D. A., *Rev. Sci. Instrum.* 1993, *64*, 2974-2977.
[168] El-Sherif, M., Bansal, L., Yuan, J., *Sensors* 2007, *7*, 3100-3118.
[169] El-Sherif, M. A., Ko, F. K., *Proc. Int. Conf. Compos. Mater., 9th* 1993, *2*, 402-404.
[170] Wolfbeis, O. S., *Anal. Chem.* 2002, *74*, 2663-2677.
[171] DeGrandpre, M. D., Burgess, L. W., *Anal. Chem.* 1988, *60*, 2582-2586.
[172] Degrandpre, M. D., Burgess, L. W., *Appl. Spectrosc.* 1990, *44*, 273-279.
[173] Messica, A., Greenstein, A., Katzir, A., *Appl. Opt.* 1996, *35*, 2274-2284.
[174] Keller, B. K., DeGrandpre, M. D., Palmer, C. P., *Sens. Actuators, B* 2007, *B125*, 360-371.
[175] Tao, S., *Encycl. Sens.* 2006, *3*, 449-473.
[176] Grattan, K. T. V., Meggitt, B. T., Editors, *Optical Fiber Sensor Technology: Advanced Applications - Bragg Gratings and Distributed Sensors*, 2000.
[177] Burgess, L. W., *Sens. Actuators, B* 1995, *B29*, 10-15.
[178] Wei, L., Fujiwara, K., Fuwa, K., *Anal. Chem.* 1983, *55*, 951-955.
[179] Weigl, B. H., Wolfbeis, O. S., *Anal. Chem.* 1994, *66*, 3323-3327.
[180] Weigl, B. H., Lehmann, H., Lippitsch, M. E., *Sens. Actuators, B* 1996, *B32*, 175-179.
[181] Taitt, C. R., Anderson, G. P., Ligler, F. S., *Biosens. Bioelectron.* 2005, *20*, 2470-2487.
[182] Wolfbeis, O. S., *TrAC, Trends Anal. Chem.* 1996, *15*, 225-232.
[183] Giuliani, J. F., Wohltjen, H., Jarvis, N. L., *Opt. Lett.* 1983, *8*, 54-56.

[184] Weigl, B. H., Draxler, S., Kieslinger, D., Lehmann, H., *et al.*, *Proc. SPIE-Int. Soc. Opt. Eng.* 1995, *2508*, 199-209.
[185] George, K. M., Montgomery, M. A., Sandoval, L. E., Thompson, C. M., *Toxicology Letters* 2002, *126*, 99-105.
[186] Paprocki, E. D., Keller, B. K., Palmer, C. P., Laws, W. R., DeGrandpre, M. D., *Sens. Actuators, B* 2008, *B135*, 145-151.
[187] Keller, B. K., Shulga, O., Palmer, C. P., Degrandpre, M. D., *Sens. Transducers J.* 2008, *88*, 21-30.
[188] Ellman, G. L., Courtney, K. D., Andres, V., Jr., Featherstone, R. M., *Biochemical Pharmacology* 1961, *7*, 88-95.
[189] Fersht, A., *Enzyme Structure and Mechanism*, 1977.
[190] Scopes, R. K., *Clin. Chim. Acta* 1995, *237*, 17-23.
[191] Paprocki, E., *Mater's Thesis* 2007.
[192] Paprocki, E. D., Keller, B. K., Palmer, C. P., Laws, W. R., DeGrandpre, M. D., *Sensors and Actuators, B: Chemical* 2008, *B135*, 145-151.